Master Thesis

NTNU
Norwegian University of
Science and Technology
Faculty of Engineering
Department of Energy and Process

Student Sarawanakanth Kumarasamy

Analysis of a Stirling Engine-Based High-Temperature Heat Pump Using Helium, Nitrogen, and Argon as Working Fluids

Trondheim, 24 June 2024

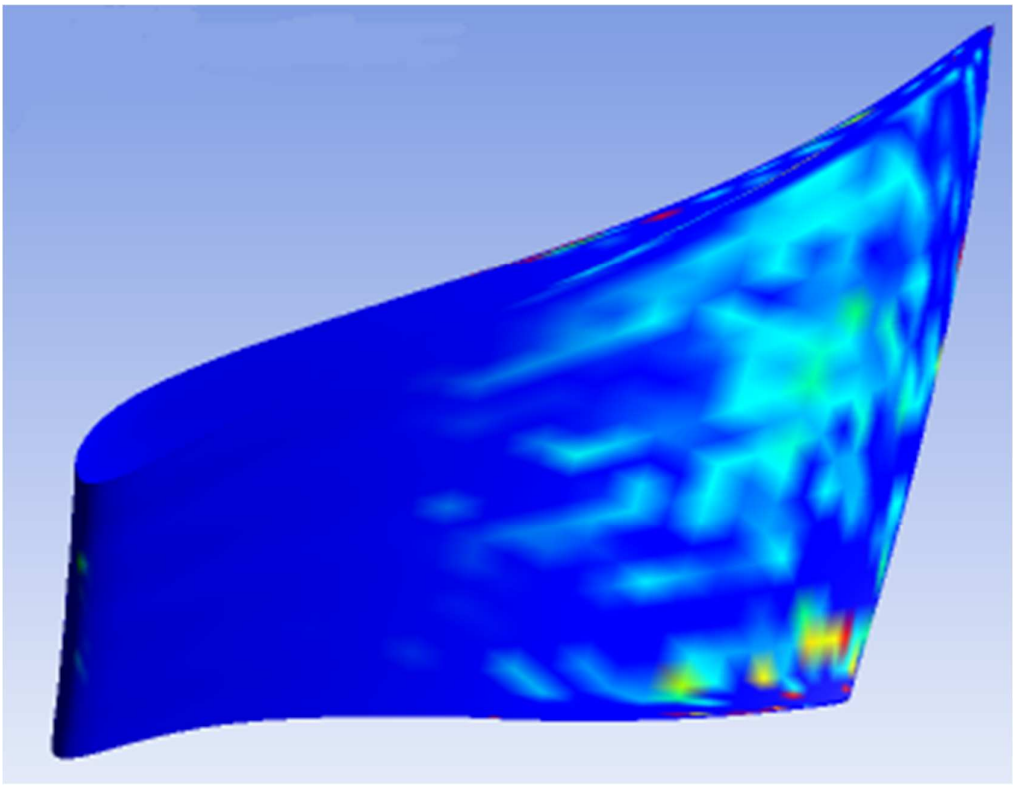

NTNU – Trondheim
Norwegian University of
Science and Technology

Abstract

This thesis investigates the performance of Stirling machine heat pump using Helium (He), Nitrogen (N2), and Argon (Ar) as working fluids, analyzing their thermodynamic properties and impacts on HP efficiency. The analysis revealed that the density of these gases increases linearly with pressure and decreases with temperature, with Helium having the lowest density and Argon the highest. Specific heat capacity (Cv) remains relatively constant across pressures and temperatures, while the Cp/Cv ratio shows minimal changes, reflecting the ideal gas behavior of these fluids. Helium exhibits the highest speed of sound and thermal conductivity due to its lower molar mass, and viscosity trends align with kinetic theory expectations, showing stability across pressures but increasing with temperature.

The study also evaluated simplified model predictions, noting a negative correlation between hot side temperature (TH) and coefficient of performance (COP), and a positive correlation between cold side temperature (TL) and COP. Optimizing TH and TL can significantly enhance COP, particularly for Argon at higher TL. Additionally, varying engine geometrical parameters such as swept volume, dead volume, and regenerator volume demonstrated that increasing swept volume improves efficiency, while increasing dead and regenerator volumes decreases it. Higher mean pressures consistently improve COP for all gases, with Helium showing the most significant enhancement.

To optimize Stirling engine performance, the study recommends selecting Helium for its superior efficiency, further investigating Argon for specific configurations, and optimizing operating conditions to balance TH, TL, mean pressures, and motor power consumption. Extended experimental studies and detailed analyses are advised to validate simulation results and refine predictive models, ultimately advancing Stirling engine technology and its applications.

Sammendrag

Denne oppgaven undersøker ytelsen til Stirling-maskinens varmepumpe ved bruk av Helium (He), Nitrogen (N2) og Argon (Ar) som arbeidsfluider, og analyserer deres termodynamiske egenskaper og innvirkning på varmepumpens effektivitet. Analysen avdekket at tettheten av disse gassene øker lineært med trykket og avtar med temperaturen, der Helium har den laveste tettheten og Argon den høyeste. Spesifikk varmekapasitet (Cv) forblir relativt konstant over trykk og temperaturer, mens Cp/Cv-forholdet viser minimale endringer, noe som reflekterer den ideelle gassoppførselen til disse fluidene. Helium utviser den høyeste lydhastigheten og termiske ledningsevnen på grunn av sin lavere molarmasse, og viskositetstrender samsvarer med forventningene fra kinetisk teori, og viser stabilitet over trykk, men øker med temperaturen.

Studien evaluerte også forenklede modellprediksjoner, og bemerket en negativ korrelasjon mellom temperatur på den varme siden (TH) og ytelseskoeffisient (COP), og en positiv korrelasjon mellom temperatur på den kalde siden (TL) og COP. Optimalisering av TH og TL kan betydelig forbedre COP, spesielt for Argon ved høyere TL. I tillegg viste variasjoner i motorens geometriske parametere, som slagvolum, dødvolum og regenerativt volum, at økning av slagvolumet forbedrer effektiviteten, mens økning av dødvolum og regenerativt volum reduserer den. Høyere middeltrykk forbedrer konsekvent COP for alle gasser, med Helium som viser den mest betydelige forbedringen.

For å optimalisere ytelsen til Stirling-motoren, anbefaler studien å velge Helium for sin overlegne effektivitet, videre undersøke Argon for spesifikke konfigurasjoner, og optimalisere driftsforholdene for å balansere TH, TL, middeltrykk og motorkraftforbruk. Utvidede eksperimentelle studier og detaljerte analyser anbefales for å validere simuleringsresultater og forbedre prediktive modeller, som til slutt fremmer Stirling-motorteknologi og dens anvendelser.

Preface

This thesis aims to provide a comprehensive investigation of Stirling machine high temperature heat pump working fluids, specifically Helium, Nitrogen, and Argon. It examines their impact on the performance of heat pumps, including the coefficient of performance (COP) and temperature lift. Additionally, this work offers an overview of the principles and applications.

Throughout this thesis work, I have attempted to balance theoretical concepts with practical insights, ensuring that readers from both academic and professional backgrounds can benefit. The study's findings highlight the potential of Stirling machine high-temperature heat pumps in advancing renewable energy technologies and improving energy efficiency.

I hope that the results of this thesis will contribute to the ongoing development of high-temperature heat pumps and inspire further research in this critical field.

Acknowledgements

I would like to express my deepest gratitude to my supervisor, Prof. Trygve M. Eikevik of NTNU, for his invaluable guidance and support throughout this thesis. His expertise and encouragement have been instrumental in the completion of this work.

I am also thankful to my co-supervisor, Kristian Løver and Arne Høeg from Enerin AS, for providing the necessary resources and funding, arranging travel for site visits, assisting with measurements, and offering their insightful feedback, guidance, and valuable discussions. Their contributions have been crucial to the success of this study.

Lastly, I am profoundly grateful to my family for their unwavering encouragement and understanding during the course of this work. Their support has been a constant source of strength and motivation.

Table of Contents

List of Figures

List of Tables

List of Abbreviations/Symbols

HP	-	Heat Pump
HTHP	-	High Temperature Heat Pump
COP	-	Coefficient of Performance
atm	-	Atmosphere
RPM	-	Revolutions per minute
kW	-	Kilowatt
TL	-	Cold Side Temperature on Stirling Machine
TH	-	Hot Side Temperature of Stirling Machine
P-V	-	Pressure vs Volume
T-S	-	Temperature vs Volume
He	-	Helium
N_2	-	Nitrogen
Ar	-	Argon

Chapter 1 Introduction

1.1 Background

The work presented in this Master's thesis builds upon my previous specialization project, titled ‘Ultra-high Temperature Heat Pumps with Helium or Hydrogen as Working Medium’. This foundational project laid the groundwork for the current thesis by exploring the feasibility and initial technical considerations of using helium and hydrogen in high-temperature heat pump applications. As such, several sections of this thesis, particularly those detailing the technical background and methodology, draw upon and expand the findings from the specialization project. This approach ensures a comprehensive understanding for the reader, providing continuity and context to the research presented here. It is important to note that while the specialization project report is not published, its significant contributions are thoroughly integrated into this thesis to enhance completeness and coherence.

Building on this foundation, the current thesis addresses the broader context of heat pumps (HPs) as a transformative solution for industrial heat requirements. The advent of heat pumps marks a significant shift in energy management strategies within the industrial sector, traditionally reliant on fossil fuels to meet high energy demands. Industries are increasingly turning to HPs due to their efficiency and potential for reducing carbon emissions. Since their inception, HPs have evolved from simple residential heating systems to robust units capable of achieving the high temperatures required for industrial processes. This transformation has been driven by advancements in technology, including improvements in compressor design and the integration of reverse Stirling mechanisms. As industries seek sustainable and cost-effective alternatives to traditional heating methods, the role of HPs has become more critical, prompting a deeper examination of their performance, economic viability, and environmental impact in industrial applications [1]

Enerin AS, a Norwegian-based company, has specialized in the development of HPs using a reversed Stirling machine mechanism since the year 2000, with a focus on high-temperature heat pumps (HTHPs) designed for industrial applications. Continuing its rigorous research and development efforts in HP technology, the company successfully launched its flagship product, the HoegTemp HP, in 2023. This advanced system is capable of generating temperatures up to 250°C, representing a significant achievement in the domain of industrial HP applications.

Their HP development is based on a patented technology that allows them to achieve high output temperatures and high coefficients of performance (COP). The company has also developed a number of other innovations in HP technology, such as its WaveClean water treatment system and its Thermonitor heat exchanger. In addition to these services, the company provides sustainable solutions such as Niprox Water Treatment, Feedwater and Production, and Advisory Services.

The development of HPs by Enerin is supported by a robust research and development infrastructure, characterized by a dedicated team of experts. Furthermore, the company actively engages in collaborative endeavors with an extensive network of partners. This network incorporates academic institutions, research institutes across Norway and the European Union, as well as industrial companies. Such collaborations are instrumental in fostering innovation, facilitating knowledge exchange, and enhancing the technological capabilities of Enerin's HP solution.

Here is a timeline of Enerin's HP development:

2000: It is founded and begins developing HPs based on Stirling machine for industrial applications. Lab engine for Sigma Bektroteknisk, heat pumping from (-165)°C to 650°C, 2000 hours service interval, qualified at Statoil Tjeldbergodden, one prototype still in operation at HVL (Western Norway University of Applied Sciences)

2003: CE certified Stirling engine for Disenco PLC, fleet tested in the UK.

2011: First high-temperature lift HP for Single-Phase Power, 400 kW at 120°C, more than 30000 hours of operation at TINE Byrkjelo, TINE Frya and Lerum.

2018: R&D project started for the new HoegTemp ultra HTHP.

2019: Patent granted for improved helium sealing technology, that reduces cost of operation.

2020: Patent granted for new heat pump lay-out, that improves high-temperature performance, reduces cost, and improves efficiency and COP.

2021: Patent granted for improved heat exchanger technology, that improves efficiency and COP.

2023: First Hoeg Temp installation at IVAR biogas facility (CO_2 capture).

2024: Hoeg Temp installations at GE Healthcare (pharmaceutical plant) and Pelagia (fishmeal plant).

Enerin begins working with Pelagia, Slakteriet AS, Optimar, NTNU, and the Institute for Energy Technology to develop a concept for using industrial HPSs to deep-freeze fish for better quality and energy efficiency. Also, high lift high temperature HPs for steam generator for energy efficiency.

It begins working on the SUSHEAT project, an EU-funded project to develop innovative technological solutions for the decarbonization of the industrial sector.[2]

The development of HPs continues actively, with the company dedicated to enhancing product efficiency and reliability. It aims to offer customers top-tier, efficient HPs. The HoegTemp high lift HP, notable for its pilot installation at the IVAR biogas facility near Stavanger, Norway, exemplifies this commitment. This pilot installation is illustrated in *Figure 1*

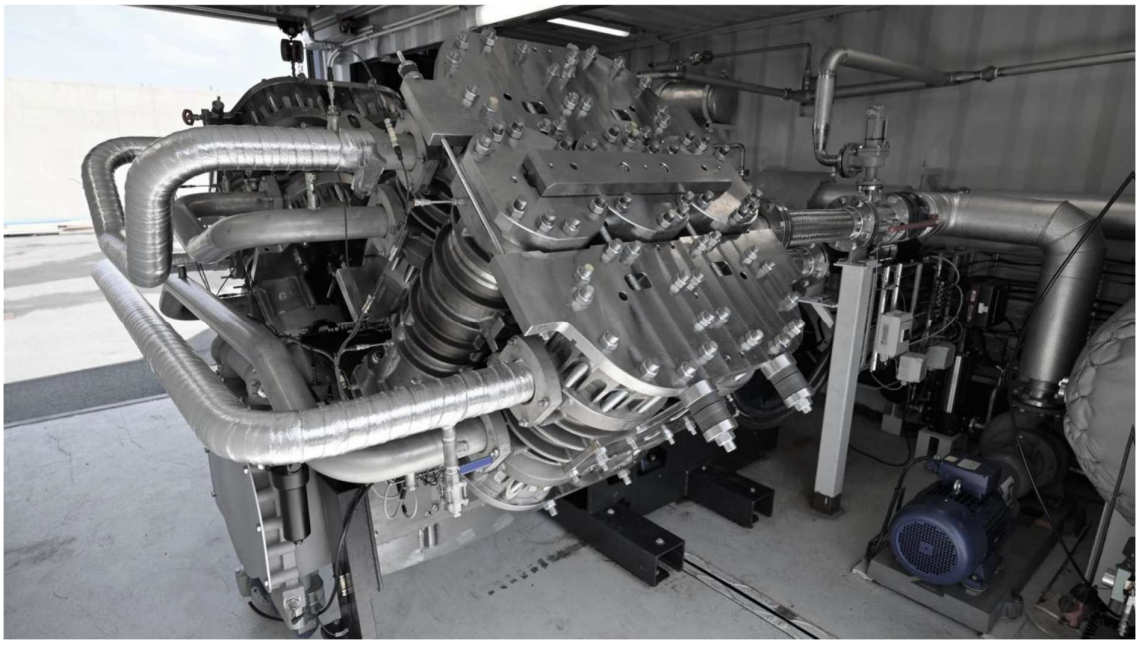

Figure 1 The pilot HoegTemp heat pump installation.

1.2 Development of the Stirling Cycle

Robert Stirling in 1816, invented the Stirling engine in Scotland, performed significant commercial success until the early 1900s, preceding the diesel engine by about 80 years. Operating on a closed regenerative thermodynamic cycle, the Stirling cycle machine involves compression and expansion of the working fluid at different temperature levels, with flow controlled by volume changes, resulting in a net heat conversion to work or vice versa. Commonly referred to as hot-air or hot-gas engines, Stirling engines faced limitations in the 19th century due to the quick development of internal combustion engines and electrical machinery.

Stirling engines known for high heat efficiency, low noise operation, and fuel versatility, address the demand for effective energy use and environmental security. They are considered optimal for low-power range solar thermal conversion units. Ongoing worldwide development of simulation codes aims to analyze and enhance the performance of key subsystems: the solar receiver, thermodynamic gas circuit, and drive mechanism.

The 1980 fuel crises marked a turning point, making Stirling engines viable with advances in material technology, representing the second stage of their transformation. This report presents a literature review on Stirling engine technological development, aiming to explore feasible solutions for a preliminary conceptual design [2].

Today, Stirling-cycle based systems are used commercially as efficient and environmentally friendly power sources with the current technology, the Stirling engine can achieve 65-70 % of the Carnot cycle efficiency.

The main irreversibilities in a Stirling engine are:

- **Regenerator holdup:** The regenerator is kind of a heat exchanger which transfer heat from the hot working fluid to the cold working fluid. It is made up of a matrix of material that has a high thermal conductivity. The regenerator is used to improve the efficiency of the Stirling engine by reducing the amount of heat that is lost to the surroundings. However, the regenerator is not perfect, and some of the heat that is transferred to the cold working fluid is not recovered. This is called regenerator holdup. Regenerator holdup is a major source of irreversibility in Stirling engines.

- **Heat Exchanger Irreversibility:** The heat exchangers are used to transfer heat between the working fluid and the hot and cold reservoirs. The heat exchangers are not perfect, and some of the heat that is transferred is lost to the surroundings. This is called heat exchanger irreversibility. Heat exchanger irreversibility is a major source of irreversibility in Stirling engines.
- **Fluid friction:** Fluid friction is a type of irreversibility that occurs when the working fluid flows through the engine. Fluid friction is caused by the interaction between the working fluid and the walls of the engine. Fluid friction reduces the efficiency of the engine by dissipating energy as heat.

Any substance with a high specific heat capacity can be utilized in a Stirling cycle engine. During the 19th century, air was predominantly employed as the working fluid in these engines, operating at or near atmospheric pressure due to its affordability and widespread availability. The working fluid selected for a Stirling engine should possess specific thermodynamic, heat transfer, and gas dynamic characteristics:

- High thermal conductivity
- High specific heat capacity
- Low viscosity
- Low density

In addition to the above-mentioned properties, considerations such as ease of availability, cost, safe operation, and storage requirements play a crucial role in enhancing overall system performance [2]. Today, predominant working fluids are hydrogen and helium, but new composite working fluids are under investigation [3]. Helium has a practical advantage over hydrogen, as helium is an inert gas while hydrogen is a highly reactive gas. However, Stirling engines with hydrogen as working fluid has a better efficiency and performance than helium. Both hydrogen and helium have low molecular weights and can be difficult to operate in a pressurized system because of the leakage hazard [4].

The major development steps of Stirling engine development [5]

1- 1807: Sir G. Caley Hot air engine (Alpha design)

2- 1816: R. Stirling closed regenerative cycle gas engine patent (Beta design)

3- 1827: Stirling brothers Gamma design

4- 1872: First solar-Stirling system by J. Ericsson

5- 1876: Alpha design by A. K. Rider

6- 1905: Ringbom design

7- 1938: Philips new interest for Stirling engines

8- 1964: W. Beale Free Piston Stirling engine

9- 1978: End of Philips development of Stirling engines

10- Beginning of 1990's: New interest in Stirling engine

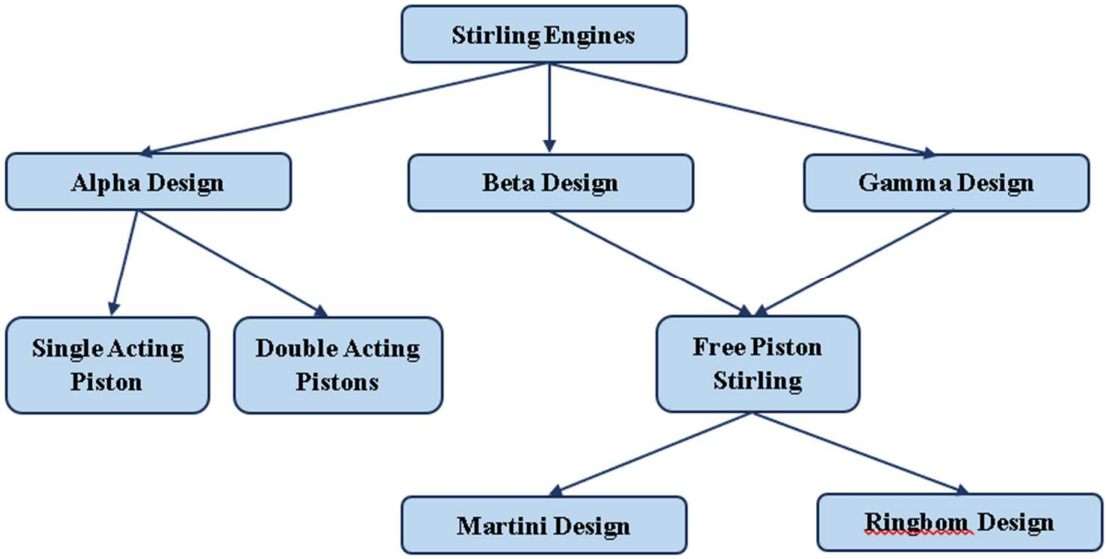

Figure 2 Stirling engine technology tree[5]

The Stirling engine operates on a closed regenerative thermodynamic cycle, with cyclic compression and expansion of the working fluid at different temperature levels. The flow is controlled by volume changes so that there is a net conversion of heat to work or vice versa. The Stirling engine is composed of two compartments at different temperatures connected to each other through two heat exchangers and a regenerator. The ideal Stirling engine's main operation processes are described as follow [6]:

1. **Isothermal compression process 1–2:** The working fluid is compressed isothermally while space discharges the heat to the heat sink. Therefore, the temperature of the heat sink is increased.
2. **Constant volume heat rejection process 2–3:** Isochoric regeneration (heat addition): Heating occurs at the regenerator under constant volume. The temperature of the working fluid increases from TL to TH.
3. **Isothermal expansion process 3–4:** Isothermal expansion: The working fluid expands isothermally while space is heated externally by the heat source. At this stage, the engine produces useful work.

4. **Constant volume heat addition process 4-1:** Isobaric regeneration (heat rejection): Cooling occurs at regeneration component at constant volume. Regenerator absorbs heat from the working fluid. The temperature of the working fluid reduces from TH to TL.

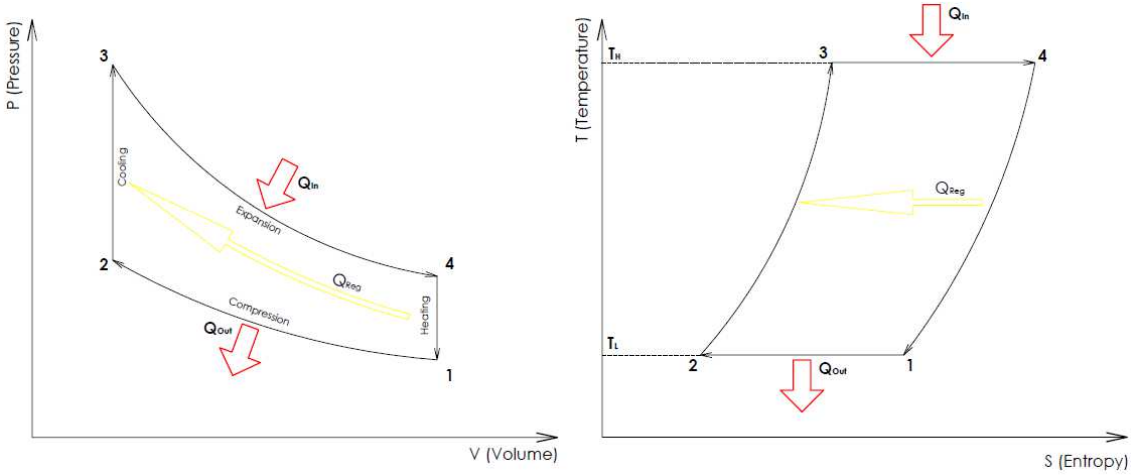

Figure 3 P-V & T-S diagram of Ideal Stirling Engine

In a more practical way, different designs of Stirling engine exist, which follows all the same basic cycle presented before. As can be seen in following *Figure 4*, which corresponds to a particular design (alpha design, see the part on the different Stirling engine designs for more details), a Stirling engine can be modeled by the combination of compression (cooling) and expansion (heating) spaces and a regenerator which is a device, usually a metal mesh, used to recover passively heat during the cycle [2].

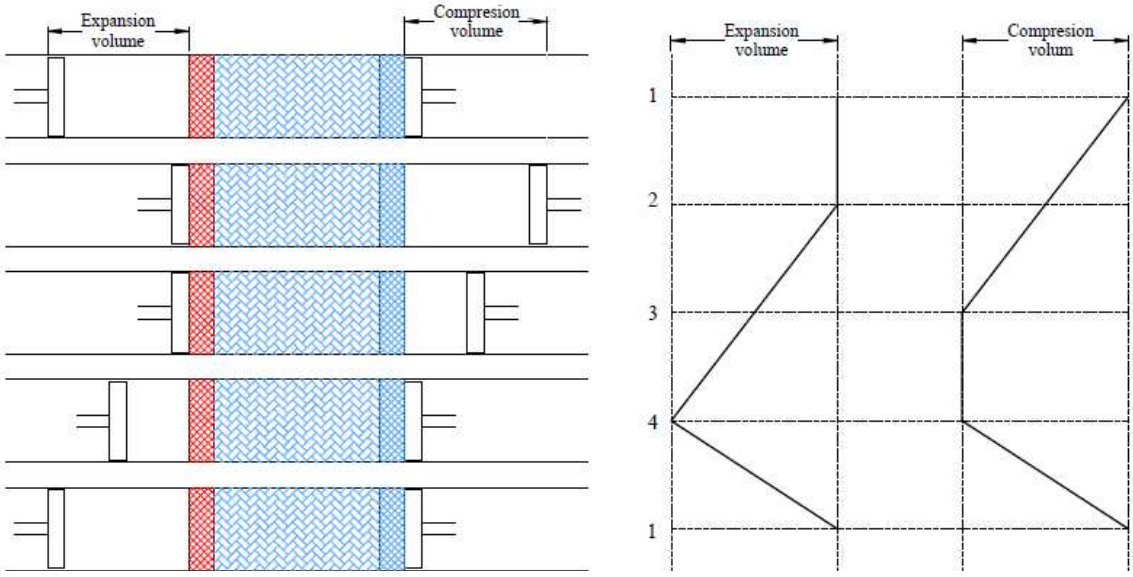

Figure 4 Simple Mechanical Model of Main Processes 1-4 of Stirling Cycle

1.2.1 Alpha design Stirling engine

The Alpha Stirling engine features two separate cylinders: one hot and one cold by the fact that the expansion and compression spaces. Each cylinder contains its own piston as shown in *Figure 5*. This configuration corresponds to a single acting piston configuration: one of the pistons is the compression piston (cold side in blue) compressing the gas and pushing it in the hot side during the cycle and the other one is the expansion piston (hot side in red) which generates work during the expansion part of the cycle [7].

This configuration can achieve higher power outputs and efficiencies due to the greater temperature difference between the hot and cold ends. However, it is more complex and expensive to manufacture due to its dual-cylinder setup.

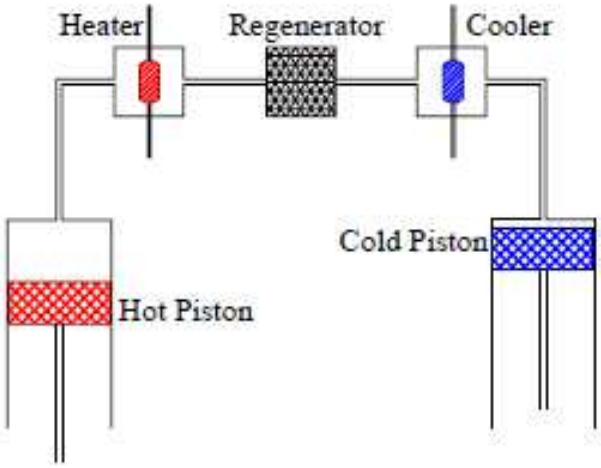

Figure 5 An Alpha design of a Stirling engine

1.2.2 Beta design Stirling engine

In this design, two pistons are in a same cylinder: the displacer piston (in red color shown in the *Figure 6*) which is not sealed and makes the gas circulate in the cylinder between compression and expansion space of the engine and the power piston (in blue color shown in the *Figure 6*) which is sealed and which generates the work during the cycle.

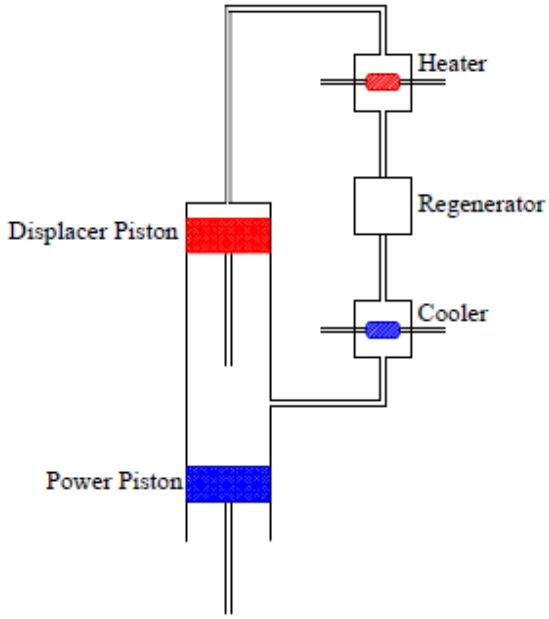

Figure 6 A Beta design of a Stirling engine

1.2.3 Gamma design Stirling engine

For this design as for Beta design, there is a displacer and a power piston but in this particular case, the two pistons are in different cylinders as shown in the *Figure 7*.

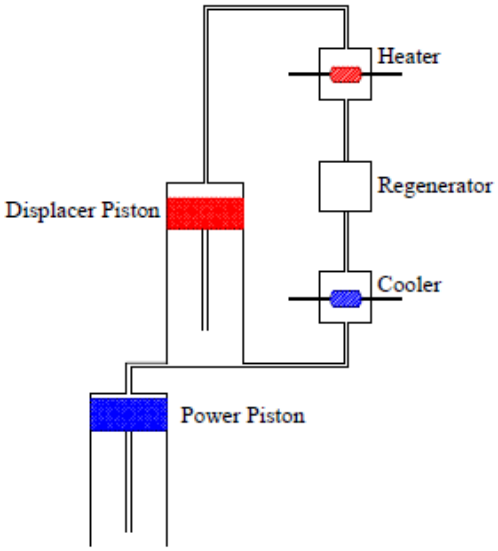

Figure 7 A Gamma design of a Stirling engine

In this *Figure 7*, the power generation is done using a linear alternator, the power piston being or containing a permanent magnet which creates a magnetic field. In some other cases, the power is generated by connecting an alternator (rotating) to the power piston wheel. In this case, the power piston does not have to create a magnetic field.

1.3 Objective of the Study

The primary objective of this thesis is to conduct an in-depth investigation into the effects of various working fluids, namely nitrogen, helium, and argon, on the performance and efficiency of Stirling machine HPs. This research aims to enhance our understanding of the way in which the basic thermodynamic properties of these working fluids interact with the Stirling cycle and the geometry of the machine, thereby influencing the overall performance of the system.

Specifically, the studies seek to:

- Evaluate the Relationship Between Working Fluid Properties and Stirling Cycle Performance: Analyze how the density, conductivity, specific heat capacity (C_p/C_v), and heat capacity ratio of nitrogen, helium, and argon impact the efficiency and effectiveness of the Stirling cycle. This involves developing a simplified theoretical model to predict performance outcomes based on fluid properties and machine design.
- Correlate Theoretical Predictions with Experimental Data: Utilize experimental data from IVAR to test the relationships and performance predictions made by the simplified Stirling cycle model. This includes assessing the accuracy of the model and identifying any discrepancies between theoretical predictions and observed outcomes.
- Investigate the Impact of Higher Compression: Extend the analysis to consider the effects of operating the Stirling machine under conditions of higher compression, examining how this variable influences the performance of the system with each of the selected working fluids.
- Optimize Stirling Machine Design and Operation: Based on the insights gained from theoretical and empirical analyses, offer recommendations for optimizing the design and operational parameters of Stirling machine HPs. This includes identifying the most effective working fluid and machine configurations for different application scenarios.

Through these objectives, the thesis will contribute valuable knowledge to the field of thermal engineering, specifically in optimizing Stirling machine HPs for enhanced performance and efficiency. The research outcomes are expected to guide future design and operational decisions, facilitating the broader adoption and application of Stirling technology in sustainable energy systems.

1.4 Scope of the Thesis

This thesis is dedicated to investigating the impact of different working fluids on the performance and efficiency of Stirling machine HPs, with a particular focus on nitrogen, helium, and argon. Given the complexity and broad potential of the topic, the scope has been carefully defined to ensure a focused and in-depth analysis. The research encompasses several key areas:

Working Fluids Analysis: The study is limited to three working fluids (nitrogen, helium, and argon) due to their practical relevance and distinct physical properties that potentially affect Stirling cycle performance. The choice allows for a comparative analysis under similar operational conditions.

Theoretical Modeling and Empirical Testing: The thesis will employ a dual approach combining theoretical modeling with empirical testing. The scope includes the development of a simplified Stirling cycle model to understand the fundamental interactions between working fluid properties and cycle performance. Experimental data from IVAR will be used to validate the model, with the analysis focusing on how accurately the model predicts real-world performance.

Compression Ratio Variations: While acknowledging the significance of compression ratio in Stirling machine operation, the study will specifically explore the effects of higher compression settings. This aspect aims to understand the operational limits and efficiency gains possible with each working fluid under increased compression.

Comparison with Advanced Models: The research will incorporate a comparison with advanced polynomial/correlation models provided by Enerin AS. The scope here is to assess the simplified model's validity and to refine its accuracy based on advanced simulations, focusing specifically on the behavior of the selected working fluids.

Design and Operational Recommendations: Based on the findings, the thesis will offer recommendations for optimizing Stirling machine design and operation. However, the recommendations will be confined to the implications of working fluid selection and the specific case studies examined. Broader design considerations outside the immediate findings related to working fluids and compression ratios will not be covered in detail.

Geographical and Practical Constraints: While the research aims to contribute broadly to the field, the experimental data and case studies are primarily sourced from IVAR. Therefore, the findings are contextualized within the operational environments and constraints specific to IVAR's implementation of Stirling machines.

Literature and Previous Studies: The review and analysis of existing literature will be extensive but not exhaustive. The focus will be on studies directly relevant to the working fluids in question, Stirling cycle performance, and machine design considerations pertinent to the thesis objectives.

By defining this scope, the thesis aims to provide a focused and detailed exploration of how nitrogen, helium, and argon, as working fluids, influence the performance and efficiency of Stirling machine HPs. The research is designed to yield insights that are both scientifically rigorous and practically applicable, contributing to the optimization of Stirling machines for enhanced sustainability and efficiency in energy systems.

1.5 Structure of the Thesis

This thesis is structured into seven main chapters, each designed to systematically explore the investigation into different working fluids in a Stirling machine HP, focusing on nitrogen, helium, and argon as practical candidates. Below is a brief overview of each chapter's content and purpose:

Chapter 1: Introduction
This opening chapter sets the stage for the research, providing background information on the significance of the study. It outlines the objectives, scope, and the overall structure of the thesis, offering readers a clear understanding of the research context and its contributions.

Chapter 2: Literature Review
Chapter 2 explores into existing research and developments in the field of Stirling machines and working fluids used within them. It critically reviews the properties of nitrogen, helium, and argon, and their implications for HP performance, identifying gaps in current knowledge that this study aims to address.

Chapter 3: Theoretical Framework
The third chapter introduces the simplified Stirling cycle model used in this study, including the assumptions made and the mathematical formulations applied. It discusses how different

working fluid properties and machine geometries are expected to influence Stirling cycle performance.

Chapter 4: Methodology

This chapter describes the experimental setup at IVAR, detailing the procedures for data collection, analysis methods, and model validation. It also explains the testing procedure for evaluating the effect of higher compression on system performance.

Chapter 5: Results

Chapter 5 presents the findings from both the theoretical model and experimental data. It compares the effects of working fluid properties on cycle performance, the influence of machine geometry, and the impact of higher compression settings.

Chapter 6: Discussion

The discussion chapter analyzes the results in the context of the theoretical framework and existing literature. It evaluates the accuracy of the simplified model, the insights gained from higher compression tests, and the comparison with advanced model predictions provided by Enerin AS.

Chapter 7: Conclusion and Recommendations

In this chapter, the key findings of the research are summarized, along with their practical implications. Limitations of the current study are acknowledged, and directions for future research are suggested. The chapter concludes with final remarks on the study's contributions to the field

References

This chapter lists all the bibliographic references cited throughout the thesis, providing a comprehensive resource for readers interested in further exploration of the topics discussed.

Appendices

The appendices provide supplementary material to support the thesis's main text, including detailed information about the experimental setup, data analysis code, models, and additional tables and figures not included in the main chapters.

Chapter 2 Literature Review

2.1 Introduction to heat pump

Heat pumps are devices that efficiently transfer heat from one location to another by harnessing a small amount of external energy through the thermodynamic cycle. These versatile systems utilize either the vapor-compression or absorption refrigeration cycle to effectively move thermal energy against its natural direction, making them suitable for both heating and cooling applications in residential and commercial environments. Their functionality is comparable to a refrigerator, employing a refrigerant that absorbs heat at a low temperature and releases it at a higher temperature through a cycle involving an evaporator, compressor, condenser, and expansion valve. The performance of HPs is commonly evaluated by the coefficient of performance (COP), which is the ratio of heat output to the electrical energy input, highlighting their role in reducing heating costs and environmental impact compared to conventional methods.

2.1.1 High-temperature heat pump

High-temperature heat pumps (HTHPs) are an advanced type of HP capable of reaching output temperatures up to 160°C, which can significantly benefit industrial processes such as drying, pasteurization, and other heat-intensive applications. The latest developments in HTHPs involve integrating hybrid systems that combine absorption and compression cycles to enhance temperature lifts and expand operational ranges, making them highly effective for recovering and upgrading low-grade heat to higher temperatures. Innovations in compressor technology and the use of non-traditional working fluids are key to achieving these higher temperatures and improving the overall efficiency of the systems.[8]

In addition, the development of alternative technologies for HPs is progressing, notably the Stirling machine-based HP. This technology is one of the oldest yet still evolving within the industry, holds substantial potential for innovation and efficiency improvements in thermal management applications. These high-temperature HPs have emerged as critical technological solutions for industrial applications, offering efficient and sustainable thermal energy management in environments that exceed the capabilities of conventional HPs. Unlike traditional HPs which are designed for moderate temperature differentials, these systems cater to extreme heat requirements, capable of reaching temperatures of 200°C and above.

The development and utilization of HTHPs have garnered significant interest due to their potential to meet the energy demands of various industrial sectors.[9]

2.1.2 The Need for High-Temperature Heat Pumps.

In various industries such as chemical processing, food and beverages, and paper production, there is a significant demand for high-temperature heat, which traditional heating methods struggle to provide efficiently, often resulting in higher carbon emissions. HTHPs address this challenge by efficiently extracting heat from lower-temperature sources and elevating it to the required levels for industrial processes, also can achieve temperatures above 200°C to meet the high temperature demand in the industries. These systems not only facilitate substantial energy savings and reduce reliance on oil and gas, but also support environmental goals by replacing fossil fuel-dependent industrial boilers. As such, HTHPs are instrumental in enabling sectors like chemical manufacturing and power generation to achieve decarbonization targets and advance towards climate neutrality, reflecting their critical role in modern industrial applications.[10]

In various industries, including chemical processing, food and beverages, and paper production, there is a significant demand for high-temperature heat, which traditional heating methods struggle to provide efficiently. Traditional methods, often fossil fuel-based, are not only less efficient but also contribute significantly to carbon emissions. HTHPs offer a promising solution by extracting heat from lower-temperature sources and elevating it to the levels required for these industrial processes. The ability of HTHPs to achieve temperatures above 200°C makes them particularly suitable for meeting the rigorous demands of these sectors.[10]

HTHPs not only facilitate substantial energy savings but also reduce reliance on conventional oil and gas heating methods. The replacing industrial boilers with HTHPs can decrease energy consumption by up to 40% in high-temperature applications. This transition supports environmental goals by significantly reducing the carbon footprint associated with industrial heating. Moreover, the integration of renewable energy sources with HTHP systems further enhances their environmental benefits, positioning them as a cornerstone of sustainable industrial practices.[1]

The role of HTHPs extends beyond mere energy efficiency; they are instrumental in enabling sectors like chemical manufacturing and power generation to meet decarbonization targets.

The industries incorporating HTHPs have seen a reduction in greenhouse gas emissions by approximately 30% advancing towards climate neutrality. This capability reflects the critical role of HTHPs in modern industrial applications and their potential in shaping a sustainable future. As such, the development and integration of high-temperature HP technology are crucial for achieving global environmental goals and promoting a shift towards more sustainable industrial processes.

2.1.3 Working Principles and Challenges.

The operational mechanism of vapor-compression HTHPs is based on the principle of reversing the natural heat flow, transferring heat from a cooler source to a warmer one. This process is facilitated by the refrigeration cycle, which involves evaporation, compression, condensation, and expansion of a refrigerant. The efficiency of this cycle in HTHPs is critical as it directly influences their ability to achieve higher temperature differentials. Advanced compressors and exchangers are therefore integral to the design of effective HTHPs, allowing them to reach temperatures above 200°C, which are requisite in many industrial applications. The engineering of these components must address the thermal and mechanical stresses encountered at these elevated temperatures.

However, the design and operation of HTHPs are not without challenges. One of the primary difficulties lies in handling the increased thermal differentials and the higher pressures that result from the compression of refrigerants at high temperatures. These conditions demand robust system components that can resist wear and deformation over time, which not only affects the durability but also the safety and reliability of the HPs. Moreover, the selection of suitable working fluids is another critical factor. These fluids must not only be effective in heat transfer but also stable and environmentally friend at high temperatures. The development of new refrigerants aims to meet these needs while minimizing environmental impact.

To address these challenges, ongoing research and development in the field of HTHPs focus on innovating more resilient materials and efficient system designs. For instance, recent studies have explored the use of nanotechnology to enhance the thermal conductivity and stability of refrigerants under extreme conditions. Furthermore, there is a concerted effort to integrate smart control systems that optimize the operation of HTHPs, thereby improving their efficiency and adaptability in diverse industrial settings. These advancements are crucial as they not only enhance the performance of HTHPs but also contribute to their scalability and economic viability in the market.

The Stirling machine HPs, a variant within the broader category of HPs, operates on the Stirling cycle which is renowned for its potential in achieving high-efficiency heat transfer across significant temperature gradients. Unlike traditional vapor-compression HPs, the Stirling machine operates on a closed-loop regenerative thermodynamic cycle that utilizes a constant volume of working fluid, typically a gas that is permanently enclosed within the system. This cycle involves sequential heating and cooling of the gas at different positions in its cycle, enabling heat transfer from a lower to a higher temperature reservoir without requiring the gas to change phases. This characteristic allows the Stirling HP to achieve high efficiencies even at very high temperatures, which is particularly advantageous for industrial applications that require durable and robust heating solutions. The challenges associated with Stirling HPs include their complexity in design and higher initial costs. Additionally, the precision needed in manufacturing components such as the heat exchangers and the displacer must be addressed to optimize performance and reliability.

2.1.4 Role of Stirling Process in High-Temperature Applications

The Stirling process plays a pivotal role in high-temperature applications primarily due to its inherent operational efficiency and adaptability in thermal management. Unlike conventional HP systems, the Stirling engine operates on a closed-cycle process that utilizes a regenerative heat exchange mechanism enabling it to efficiently manage high thermal differentials without the need for phase transitions of the working fluid. This capability makes it exceptionally suitable for industries where stable and high-temperature heat is crucial such as in metal refining and ceramic production. The efficiency of the Stirling process is further underscored by its ability to convert thermal energy into mechanical power with minimal energy loss which is a significant advantage in reducing operational costs and enhancing energy sustainability in industrial practices.

Moreover, the integration of the Stirling process in high-temperature applications presents unique challenges, including the need for precise material selection and advanced engineering designs to withstand extreme operating conditions. The materials used in constructing Stirling engines must exhibit high thermal resistance and durability to maintain performance over prolonged periods under high temperatures. The development of high-grade alloys and composite materials that can endure the rigidities of the Stirling cycle while maintaining efficiency.

Additionally, the Stirling process requires meticulous calibration of mechanical components to optimize the phase displacement and heat transfer rates, necessitating ongoing technological innovations to overcome these engineering challenges.

One notable approach to achieving high-temperature heat pumping involves the use of the Stirling process. This system renowned for its high efficiency and adaptability to various temperature ranges has gained attention as a promising technology for these demanding applications. By leveraging the Stirling process, it becomes feasible to harness the potential of working mediums like helium or hydrogen to transfer heat effectively in high-temperature environments.

2.2 Stirling Machine Heat Pump Fundamentals

The Stirling machine HP functions based on the reversed Stirling cycle, a thermodynamic process essential to the operation of Stirling cycle HPs and refrigeration units. Unlike the traditional Stirling cycle which is designed to convert thermal energy into mechanical work, the reversed Stirling cycle uses mechanical work to transfer heat from a cooler to a warmer environment and vice versa, through the compression and expansion of a working fluid at different temperature levels. This reversal of function makes it highly effective for cooling and heating applications.[12]

This cycle is characterized by its use of a regenerator, a key component that differentiates it from other thermodynamic cycles. The regenerator is a type of heat exchanger that stores heat from the working fluid during the hot part of the cycle and returns it during the cold part, thereby enhancing the overall efficiency of the cycle. The cycle consists of four main processes: isothermal expansion, isochoric (constant volume) heat removal, isothermal compression, and isochoric heat addition. Additionally, the mechanical components of the Reversed Stirling Cycle HP system, including the compression and expansion processes, are typically driven by an external motor or some form of mechanical drive. This motor provides the necessary energy to move the working fluid through the various phases of compression, heat rejection, expansion, and heat absorption, enabling the HP to effectively transfer heat between different temperature environments.[13]

Process 1–2, Isothermal compression – The compression piston does work to the gas and compresses it isothermally at hot end temperature, hence rejecting heat to the hot space (via the heat rejecting heat-exchanger). Because the gas is at high pressure, more work is required for compression than was obtained from the gas during expansion (in 3-4).

Process 2–3, Constant volume regenerative transfer process – In this process the displacer piston moves to transfer all the working gas isochorically through the regenerator to the cold end of the machine. Heat is absorbed from the gas as it passes through the regenerator, thus lowering the temperature of the gas to that of the cold space. As the temperature reduces the gas pressure drops significantly.

Process 3–4, isothermal expansion process – In this process, low-pressure working gas expands isothermally at cold end temperature, hence absorbing heat from the cold space (via the heat absorbing heat-exchanger) and doing work to the expansion piston. As the expansion proceeds, the pressure decreases as volume increases. The temperature maintained constant by adding heat to the system from external source. There is no change in the internal energy but an increase in the entropy of the working fluid.

Process 4–1, Constant volume regenerative transfer process – In this process the displacer piston moves to transfer all the working gas isochorically through the regenerator to the hot end of the machine. Heat is delivered to the gas as it passes through the regenerator, thus raising the temperature of the gas to that of the hot space. As the temperature rises the gas pressure increases significantly.

Stirling cycle HPs cyclic process utilize the regenerative thermodynamic cycle to move heat from a low-temperature source to a high-temperature sink. This is achieved through the cyclic compression and expansion of the working fluid which is typically a gas such as helium, hydrogen, or air. The choice of working fluid significantly impacts the system's efficiency and performance as it influences the thermal conductivity, viscosity, and specific heat capacity of the cycle.

The efficiency of a Stirling cycle HP is often measured by its coefficient of performance (COP) which is the ratio of the heat output to the work input. Factors that affect the COP include the temperature differential between the heat source and sink, the properties of the working fluid, and the effectiveness of the regenerator.

Stirling cycle HPs are renowned for their versatility and efficiency, finding applications in residential heating and cooling, industrial processes, and even in space exploration for thermal management. Recent advancements in materials science and engineering have led to improvements in the design and performance of Stirling cycle machines including enhanced regenerators, optimized heat exchangers, and the use of alternative working fluids.

2.3 Overview of Stirling Machines

Stirling machines, encompassing both engines and coolers operate on the Stirling cycle, a thermodynamic cycle that describes the conversion of heat energy into mechanical power through compression and expansion of a working fluid, typically gas. This cycle conceived by Robert Stirling in 1816 offers a highly efficient and environmentally friendly alternative to traditional internal combustion engines.

2.3.1 Principles of Operation

The fundamental principle behind Stirling machines is the cyclic compression and expansion of the working fluid at different temperature levels leading to the conversion of thermal energy into mechanical work. The cycle consists of four main phases: isothermal expansion, isochoric (constant-volume) cooling, isothermal compression, and isochoric heating. These phases are facilitated by the movement of the working fluid between hot and cold heat exchangers within the machine.

2.3.2 Types of Stirling Machines

Stirling machines are broadly categorized into two types: engines and coolers/HPs.

- Stirling Engines: These convert heat energy into mechanical work which can then be transformed into electricity. They are known for their high efficiency, quiet operation, and ability to utilize various heat sources, including solar energy, biomass, and waste heat.
- Stirling Coolers/HPs: Operating on the reverse Stirling cycle, these machines use mechanical work to drive a refrigeration process, achieving temperatures below ambient and even approaching absolute zero in some applications. They are used in precision cooling such as in cryogenics and electronic equipment.

2.3.3 Design Variations

The design of Stirling machines varies to cater to different applications with the most common configurations being the alpha, beta, and gamma types. Each design varies in its arrangement of pistons and cylinders, affecting power output, efficiency, and suitability for specific tasks. The same was discussed details in chapter 1.2.

2.3.4 Applications and Future Prospects

Stirling machines find applications in a wide range of fields from small-scale power generation and solar power plants to cooling systems for electronic devices and cryogenic applications. Their ability to utilize renewable energy sources and waste heat makes them particularly appealing for sustainable development projects. For instance, in the automotive industry, Stirling engines are being explored for their potential to reduce emissions and improve fuel efficiency, providing a viable alternative to traditional internal combustion engines. Additionally, Stirling engines are effective in HP systems, contributing to efficient building heating and cooling. In the field of electricity generation, they are particularly valuable in remote locations where reliability and low maintenance are crucial. The engines' high efficiency and low noise also make them suitable for urban environments and various industrial applications.[14]

The future prospects for Stirling machines are promising with potential improvements in materials and design poised to enhance their efficiency and reduce costs, facilitating broader adoption in both developing and developed countries. Advances in heat source technology and integration with renewable energy systems present exciting opportunities for the wider use of Stirling technology. For example, solar-powered Stirling engines are expected to become more prevalent as the cost of solar technology decreases and efficiency improves. The development of compact and high-efficiency radiators for automotive Stirling engines will enhance their viability in the transportation sector. As global concerns regarding energy and the environment intensify, Stirling engines offer a compelling pathway to improved energy efficiency, reduced emissions, and a more diversified energy landscape, driving innovation across various sectors.[15]

2.4 Working Fluids in Stirling Machines

The selection of working fluids is crucial for the efficiency and functionality of Stirling machines, impacting their performance, durability, and applicability across various domains. Working fluids are the media through which heat is converted into mechanical work in Stirling engines, or vice versa in Stirling coolers/HPs. The ideal characteristics of these fluids include high thermal capacity, low viscosity, low density stability under high temperatures, and environmental friendliness.**Error! Reference source not found.** [5]

2.4.1 Criteria for Selection of working fluids

When selecting a working fluid, several criteria are considered to optimize the Stirling machine's performance: [4],[17]

- Thermal Efficiency: The fluid should have a high specific heat capacity to carry significant amounts of heat with minimal temperature change.
- Viscosity: Lower viscosity fluids reduce friction losses and improve the mechanical efficiency of the machine.
- Density: Lower density fluids enable the Stirling machine to achieve higher speeds and efficiencies by reducing the mass of the working fluid that must be accelerated and decelerated during each cycle. This reduction in mass leads to less inertia and smoother operation, thereby improving overall engine performance.
- Thermal Stability: The fluid must remain stable (not decompose or react chemically) at the operating temperatures of the Stirling machine.
- Environmental Impact: Ideally, the working fluid should have low global warming potential (GWP) and zero ozone depletion potential (ODP).

Additionally, the fluid should have a high specific heat capacity to efficiently transfer heat. Safety and chemical stability are also important considerations, as certain gases like hydrogen, while efficient, pose significant risks due to flammability.

2.4.2 Common Working Fluids

Stirling engines can utilize a variety of working fluids each with distinct properties that influence the engine's performance. Air is one of the most common working fluids due to its availability and ease of handling, though it offers lower efficiency compared to other gases. Helium is highly preferred in Stirling engines for its excellent thermal conductivity and low viscosity, which enhance engine efficiency and power output. Nitrogen, while safer and non-flammable, has a lower thermal conductivity, making it less efficient than helium and hydrogen but still a viable option in experimental setups. Argon, another noble gas, is inert and safe to use but has a higher molar mass, resulting in lower performance compared to helium and hydrogen. Hydrogen offers the highest thermal conductivity and efficiency, significantly boosting engine performance. However, its flammability poses significant safety risks, requiring careful handling and robust safety measures. These fluids are chosen based on a balance of thermal properties, safety, and application requirements, with each bringing its own advantages and trade-offs to the operation of Stirling engines.[16],[17],[18]

Nitrogen

Nitrogen is a highly abundant, inert gas that poses minimal risk in terms of flammability and toxicity, making it a safe choice for Stirling machines. It operates under a wide range of temperatures without significant degradation or reactivity, ensuring the durability and reliability of the system. While nitrogen is a cost-effective and safe option due to its non-reactive nature and abundant availability, its thermal conductivity and specific heat capacity are lower than those of helium and hydrogen resulting in modest efficiency gains.[16]

Advantages:

- Safety and Abundance: Its non-reactive nature and abundant availability make it a cost-effective and safe option.
- Thermal Stability: Nitrogen maintains its chemical stability across the operational temperature range of most Stirling machines.

Limitations:

- Performance: While safer and more stable, nitrogen's thermal conductivity and specific heat capacity are lower than helium and hydrogen, resulting in modest efficiency gains.

Helium

Helium, a noble gas is preferred for its superior thermal conductivity and low density, which significantly enhance the efficiency of Stirling machines. Its inertness contributes to the system's overall safety and durability, making it a highly desirable working fluid despite its higher cost. The excellent thermal properties of helium allow for greater heat transfer efficiency and faster system response, while its low viscosity reduces frictional losses within the machine.[16][17]

Advantages:

- High Efficiency: The excellent thermal properties of helium allow for greater heat transfer efficiency and faster system response.
- Low Viscosity: Its low viscosity reduces frictional losses within the machine, further enhancing efficiency.

Limitations:

- Cost and Availability: The scarcity and resulting cost of helium can be prohibitive, and the requirement for tight seals to prevent leakage adds to the operational complexity.

Argon

Argon, another noble gas strikes a balance between performance and cost-effectiveness in Stirling machines. While it does not offer the same level of efficiency improvement as helium, its better availability and moderate price make it an attractive alternative for applications where budget constraints are a significant consideration. Argon provides better thermal conductivity than nitrogen, leading to improved efficiency over nitrogen-based systems.[17]

Advantages:

- Moderate Efficiency: Argon provides better thermal conductivity than nitrogen leading to improved efficiency over nitrogen-based systems.
- Safety and Stability: As an inert gas, argon is safe to use and does not react with other materials, ensuring the longevity of the engine components.

Limitations:

- Efficiency vs. Cost: Although more efficient than nitrogen, argon's performance does not match that of helium. Its advantage lies in its cost-effectiveness compared to helium.

By understanding the properties and trade-offs of each working fluid, Stirling machine designers can select the most suitable gas to optimize the performance and applicability of Stirling machines.

2.5 Working Fluid Properties and Their Impact

The performance of a Stirling cycle-based HP is heavily influenced by the thermophysical properties of the working fluid used. The choice of working fluid can affect various aspects of the HP's operation, such as heat transfer rates, efficiency, and overall stability. In the context of your analysis which considers argon (Ar), helium (He), nitrogen (N_2), and air, it is essential to understand how the properties of these gases namely density, thermal conductivity, specific heat capacity, and heat capacity ratio C_P/C_V impact the Stirling cycle's performance.

Table 1 Properties of Gases at Standard Condition (0 °C & 1 atm) [25]

Gas	M	ρ	k	C_P	C_V	R
He	4	0.1786	0.1513	5.19	3.11	2.08
N_2	28	1.2506	0.024	1.04	0.74	0.297
Ar	40	1.784	0.0177	0.52	0.31	0.208
Air	29	1.225	0.0257	1.01	0.72	0.287

Where, M – molar mass(kg/kmol), ρ – density(kg/m^3), k - thermal conductivity (W/(m·K)), Cp – Specific heat capacity at constant pressure (kJ/kg·K), Cv – Specific heat capacity at constant volume (kJ/kg·K), & R – Gas constant (kJ/kg·K)

2.5.1 Density

Density is a critical factor because it influences the mass flow rate of the gas within the system, which in turn affects the pressure and volume changes during the Stirling cycle. Gases like helium have a significantly lower density compared to argon and nitrogen, which can lead to faster movement of the gas through the system, affecting both the regenerative heat exchange and the compression/expansion processes. Lower density gases typically require tighter sealing and more precise control mechanisms to maintain efficiency.

2.5.2 Thermal Conductivity

Thermal conductivity is another key property, as it affects the heat transfer capabilities of the working fluid. Helium has a higher thermal conductivity than argon, nitrogen, and air, which makes it more effective in transferring heat quickly between the hot and cold regions of the HP. This can enhance the efficiency of the cycle, particularly in applications requiring rapid heat exchange. Conversely, gases with lower conductivity like argon may lead to slower response times but can be beneficial in applications where a slower rate of heat transfer is desired for stability.

2.5.3 Specific Heat Capacity

Specific heat capacity (C_P and C_V) determines the amount of heat the gas can store per unit mass per degree temperature change, impacting the thermal efficiency of the cycle. Helium's higher specific heat capacities allow it to absorb and relinquish more heat during the HP's operation, potentially leading to better performance in temperature control applications. In contrast, argon's lower specific heat capacities may make it less efficient in terms of energy storage but could be advantageous in systems where minimal temperature fluctuation is needed.

2.5.4 Heat Capacity Ratio (C_P/C_V)

The heat capacity ratio, also known as the gamma (γ), influences the thermodynamic efficiency of the cycle. Gases with a higher C_P/C_V ratio, like helium, can achieve higher efficiency in ideal thermodynamic cycles because they are capable of more substantial pressure changes during adiabatic processes. This property is crucial in optimizing the power output and efficiency of the Stirling engine cycle.

2.6 Advances in Working Fluids

Recent research into Stirling engines has concentrated on enhancing performance through the use of advanced working fluids, including gas mixtures and nanofluids. Studies have explored helium-xenon mixtures, leveraging their potential to balance thermal conductivity with operational safety. Additionally, the incorporation of nanoparticles, such as ZnO, into working fluids has demonstrated significant improvements in heat transfer and overall engine efficiency. Further investigation into alternative working fluids has also considered binary and ternary gas mixtures, aiming to combine gases to achieve optimal thermodynamic properties while balancing cost, efficiency, and safety. Phase-change liquids represent another promising area of research, where fluids undergoing phase transitions within the cycle may boost the efficiency of the energy conversion process. These advancements suggest a multifaceted approach to overcoming the limitations of traditional gases in Stirling engines, paving the way for more efficient and safer energy solutions. [4]

2.6.1 Future Directions

Future advancements in Stirling machine working fluids are focused on enhancing efficiency, safety, and environmental sustainability. Research is increasingly exploring the use of gas mixtures and chemically reactive gases to optimize thermodynamic properties and performance under various operational conditions. For instance, mixtures like helium-xenon are being investigated for their ability to balance thermal conductivity and safety. Additionally, nanofluid technologies, which incorporate nanoparticles into traditional working fluids, are being developed to improve heat transfer rates and overall engine efficiency. Furthermore, the exploration of low-temperature Stirling engines pressurized with real gas effects offers potential for increased power and efficiency in applications with relatively lower operating temperatures. These innovations aim to overcome current limitations and make Stirling engines more viable for diverse and renewable energy applications.[20]

Chapter 3 Theoretical Framework

3.1 Simplified Stirling Cycle Model

The Reversed Stirling Cycle is a thermodynamic process that operates in a closed loop using a working fluid (typically a gas like helium or hydrogen) to achieve energy conversion. The cycle essentially reverses the processes of a traditional Stirling engine enabling it to function as a HP or refrigerator. [22]

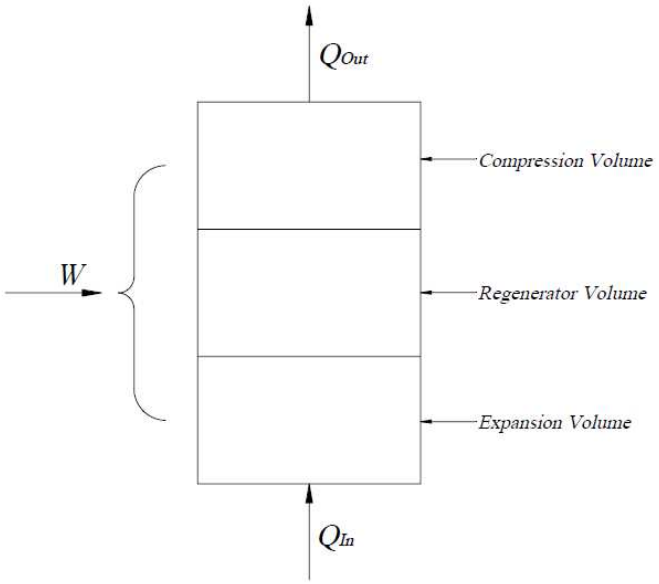

Figure 8 Reversed Stirling Cycle Concept

Basic principles of the Reversed Stirling Cycle include;

- *Closed-Cycle Regeneration:* The Stirling process is considered by a constant volume of working fluid, which is cyclically compressed and expanded in a closed system. The efficiency of the cycle is enhanced by the regenerative heat exchange, where a regenerator, typically a porous material, temporarily stores heat from the hot portion of the cycle and returns it in the cold portion.
- *Isothermal Processes:* Ideally, the Stirling cycle comprises two isothermal processes: isothermal expansion at a high temperature and isothermal compression at a low temperature. Conversely, in the reversed Stirling cycle, it involves isothermal compression at a high temperature and isothermal expansion at a low temperature. During these phases, heat is transferred to and from the working fluid while it maintains a constant temperature.

- *Displacer and Piston Mechanism:* The Stirling engine typically uses a displacer to move the working fluid between the hot and cold heat exchangers and a power piston to compress and expand the working fluid. The phase difference between the displacer and power piston movements is crucial for the efficiency of the cycle.

In the analysis of Stirling engines, three primary methods are employed, each with varying degrees of complexity and accuracy:

1st-Order Methods: These analyses use experimental values and engine dimensions, or ideal analysis models to estimate performance. Examples include the Beale Number, Schmidt model, and ideal adiabatic model.

2nd-Order Methods: These analyses take into account various types of losses building upon the results of ideal analyses. Examples include the isothermal model and adiabatic model which incorporate real-world inefficiencies.

3rd-Order Methods: These analyses solve complex equations related to fluid flow and different types of losses, providing a detailed understanding of the interactions between losses. An example is the quasi-steady flow model which offers a comprehensive analysis of the engine's performance.

However, the primary focus of this thesis is on 1st-Order Methods which utilize experimental data and simplified theoretical models to estimate the performance of the Stirling engine. Specifically, this analysis is grounded in Schmidt's Theory which provides a foundational framework for understanding the idealized behavior of the machine under various conditions. By employing experimental techniques, this approach aims to bridge the gap between theoretical predictions and practical performance offering insights into the efficiency and operational characteristics of the Stirling machine. This method not only simplifies the complex dynamics of the machine but also facilitates a more straightforward evaluation.

3.2 Ideal Stirling Cycle analysis.

The ideal Stirling cycle calculations can be approached with the basic thermodynamic equations to calculate the heat transfer & work. This procedure used for initial estimations purposes, and also academic works. This analysis uses the four process of ideal Stirling cycle, i.e. isothermal expansion, isochoric cooling, isothermal compression, isochoric heating.

3.2.1 Mathematical formulation of ideal cycle

The Ideal Reversed Stirling Cycle involves four main thermodynamic processes:[23]

- **Process 1-2**: Isothermal compression,

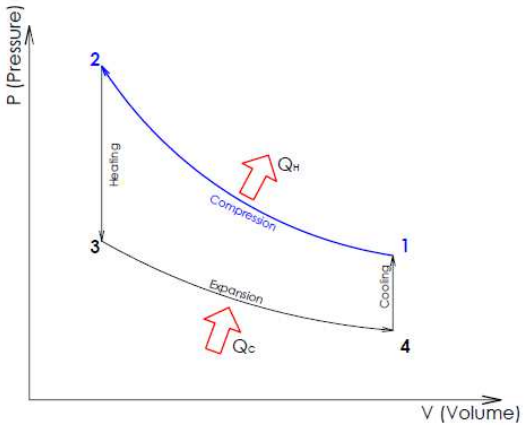

$$P_1V_1 = P_2V_2$$

$$T_1 = T_2 = T_H$$

$$\int dQ|_H = Q_H = -RT_H \, ln\left[\frac{V_2}{V_1}\right] \quad (1)$$

Figure 9 Process 1-2 Isothermal Compression

- **Process 2-3:** Constant Volume heat rejection,

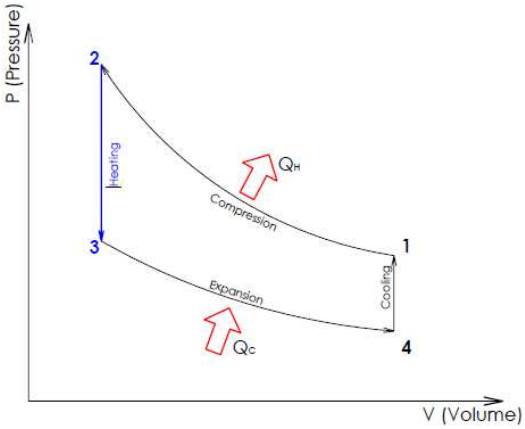

$$V_2 = V_3$$

$$T_2 = T_H \;\&\; T_3 = T_L$$

$$Q_{2-3} = +C_v(T_L - T_H) \quad (2)$$

Figure 10 Process 2-3 Constant Volume Heat Rejection

- **Process 3-4:** Isothermal expansion,

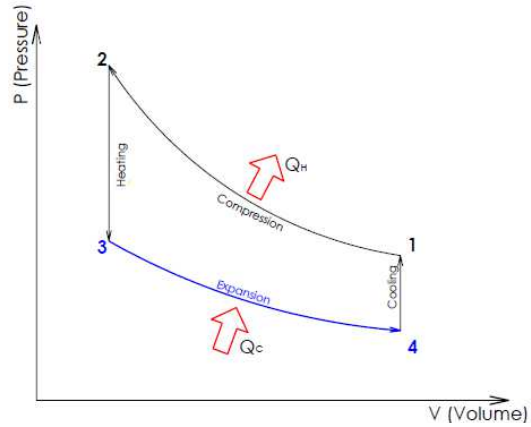

$$P_3V_3 = P_4V_4$$

$$T_3 = T_4 = T_L$$

$$\int dQ|_L = Q_L = -RT_L \, ln\left[\frac{V_4}{V_3}\right] \quad (3)$$

Figure 11 Process 3-4 Isothermal Expansion

- **Process 4-1:** Constant Volume heat absorption,

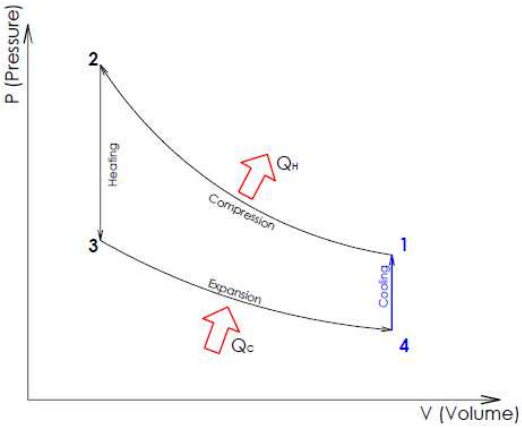

$$V_4 = V_1$$

$$T_1 = T_H \;\&\; T_4 = T_L$$

$$Q_{4-1} = -C_v(T_H - T_L) \tag{4}$$

Figure 12 Process 4-1 Constant Volume Heat Absorption

Say,

$$\frac{V_2}{V_1} = \frac{V_4}{V_3} = v$$

For the thermodynamic cycle 1-2-3-4-1, principle of energy conservation results,

$$W_{Net} = Q_{Net} = Q_H - Q_L = mR\, ln\, v\, (T_H - T_L) \tag{5}$$

Coefficient of performance of the Cycle $(COP)_{HP}$,

$$COP_{HP} = \frac{Q_H}{W_{Net}} = \frac{Q_H}{(Q_H - Q_L)} = \frac{-RT_H\, ln\left[\frac{V_2}{V_1}\right]}{-RT_H\, ln\left[\frac{V_2}{V_1}\right] - RT_L\, ln\left[\frac{V_4}{V_3}\right]} = \frac{T_H}{(T_H - T_L)} \tag{6}$$

The average net power for one cycle can be found by dividing the net cycle work by the time for one cycle t. This approach yields the following equation for the net cycle power:

$$P = \frac{W_{net}}{t} = \frac{mR\, ln\, v\, (T_H - T_L)}{t} \tag{7}$$

The total cycle time is the sum of the individual process times,

$$t = t_{1-2} + t_{2-3} + t_{3-4} + t_{4-1} \tag{8}$$

The average rates of external heat transfer into and out of the cycle can be quantified by using thermodynamic theory as, $(Q_{in} = Q_L \;\&\; Q_{out} = Q_H)$

$$\dot{Q}_{in} = \frac{Q_{in}}{t_{3-4}} = \frac{mRT_L\, ln\, v}{t_{3-4}} \tag{9}$$

$$\dot{Q}_{out} = \frac{Q_{out}}{t_{1-2}} = \frac{mRT_H \ln v}{t_{1-2}} \quad (10)$$

The rates of external heat transfer into and out of the engine may also be quantified from heat transfer theory as being proportional to the temperature difference between the respective thermal reservoirs and the constant-temperature states of the working fluid during each process.

$$\dot{Q}_{in} = U_L A_L LMTD_L \quad (11)$$

$$\dot{Q}_{out} = U_H A_H LMTD_H \quad (12)$$

$$t_{3-4} = \frac{mRT_L \ln v}{U_L A_L LMTD_L} \quad (13)$$

$$t_{1-2} = \frac{mRT_H \ln v}{U_H A_H LMTD_H} \quad (14)$$

The times associated with the regenerative heat transfer processes can be expressed as

$$t_{2-3} = t_{4-1} = \frac{mC_V(T_H - T_L)}{U_{reg} A_{reg} LMTD_{reg}} \quad (15)$$

$$t = \frac{mRT_H \ln v}{U_H A_H LMTD_H} + \frac{mRT_L \ln v}{U_L A_L LMTD_L} + \frac{2mC_V(T_H - T_L)}{U_{reg} A_{reg} LMTD_{reg}} \quad (16)$$

3.3 Schmidt's Theory Analysis

The Schmidt Analysis stands out as a pivotal methodology. It is the simplest method and very useful during Stirling engine development. Schmidt Analysis, named after Gustav Schmidt who introduced it in the late 19th century, this theoretical approach extends beyond the basic thermodynamic equations of the ideal Stirling cycle by incorporating key aspects of the engine's physical characteristics, such as phase difference between the power piston and the displacer piston, and the varying volumes within different sections of the engine.

The Schmidt formula, which integrates the effects of compression ratio, dead volume, and drive mechanism. However, this does not account for all the losses and complexities characteristic in a practical engine. Such as losses due to fluid friction, regenerator inefficiency, or non-ideal gas properties and etc. Schmidt Analysis remains a foundation stone in Stirling engine design and optimization, offering a valuable tool for engine designers and researchers.

3.3.1 Assumptions

The performance of the engine can be calculated from a Pressure-Volume diagram. The engine volume can be easily calculated through its internal geometry. When the volume, mass of the working fluid and the temperature is decided, the pressure is calculated using an ideal fluid approach, [20],[24]

The engine pressure can be calculated under following assumptions:

a. There is no pressure loss in the heat exchangers and there are no internal pressure differences.
b. The expansion process and the compression process change isothermal.
c. Conditions of the working gas are changed as an ideal gas.
d. There is a perfect regeneration.
e. The expansion dead space maintains the expansion gas temperature - T_E, the compression dead space maintains the compression gas temperature - T_C during the cycle.
f. The regenerator gas temperature is an average of the expansion gas temperature - T_E and the compression gas temperature - T_C.
g. The expansion space - V_E and the compression space - V_C changes according sine curves.

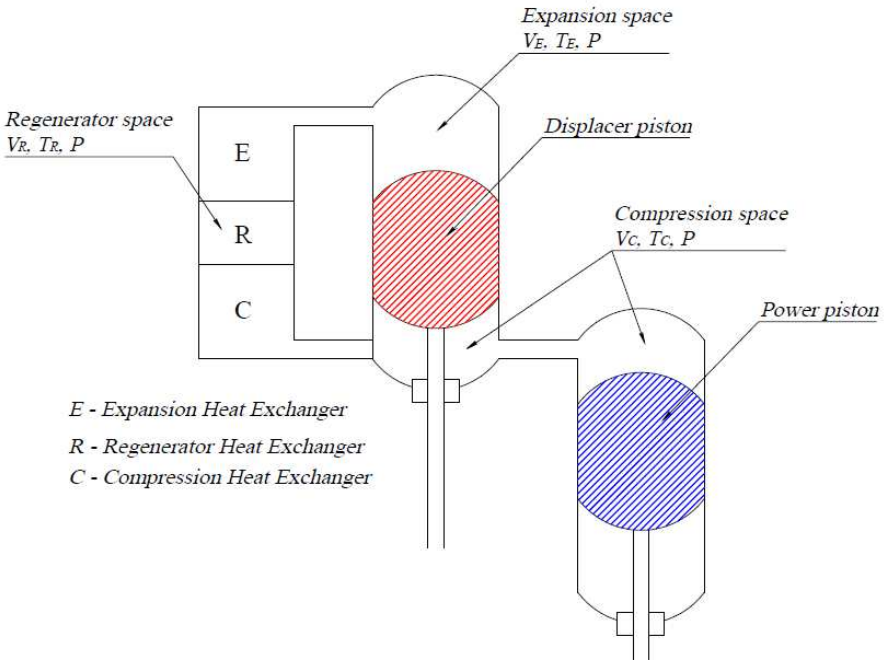

Figure 13 Gamma-type Stirling Engine

3.3.2 Mathematical Formulation

Table 2 Schmidt Theory notation and symbols

Name	**Symbol**	**Unit**
Engine pressure	P	Pa
Engine mean pressure	P_{Mean}	Pa
Engine maximum pressure	P_{Max}	Pa
Engine minimum pressure	P_{Min}	Pa
Swept volume of expansion piston or displacer piston	V_{SE}	m^3
Swept volume of compression piston or power piston	V_{SC}	m^3
Dead volume of expansion space	V_{DE}	m^3
Regenerator volume	V_R	m^3
Dead volume of compression space	V_{DC}	m^3
Expansion space momental volume	V_E	m^3
Compression space momental volume	V_C	m^3
Total momental volume	V	m^3
Total mass of working gas	m	kg
Gas constant	R	J/kgK
Expansion space gas temperature	T_E	K
Compression space gas temperature	T_C	K
Regenerator space gas temperature	T_R	K
Phase angle	dx	deg
crank angle	x	deg
Temperature ratio	t	
Swept volume ratio	v	
Dead volume ratio	X	
Engine speed	n	Hz
Indicated expansion energy	W_E	J
Indicated compression energy	W_C	J
Indicated energy	W_i	J
Indicated expansion power	L_E	W
Indicated compression power	L_C	W
Indicated power	L_i	W
Indicated efficiency	η	

The volumes of the expansion- and compression cylinder at a given crank angle x are determined at first. The momental volumes is described with a crank angle. This crank angle is defined as $x = 0$ when the expansion piston is located the most top position or top dead position. The momental expansion volume - V_E is formulated in equation (17) with a swept volume of the expansion piston - V_{SE}, an expansion dead volume - V_{DE} based on the condition of assumption (g).

$$V_E = \frac{V_{SE}}{2}(1 - cosx) + V_{DE} \quad (17)$$

The momental compression volume - V_C is formulated in equation (3) with a swept volume of the compression piston - V_{SC}, a compression dead volume - V_{DE} and a phase angle - dx

$$V_C = \frac{V_{SE}}{2}\{1 + \cos(x)\} + \frac{V_{SC}}{2}\{1 - \cos(x - dx)\} + V_{DC} \quad (18)$$

The total momental volume of the engine is formulated in equation (19)

$$V = V_E + V_R + V_C \quad (19)$$

Based on the assumptions (a), (b) & (c), the total fluid mass in the engine - m is formulated using the engine pressure - P, each temperature - T, each volume - V and the gas constant - R.

$$PV = mRT \quad (20)$$

$$m = \frac{PV_E}{RT_E} + \frac{PV_R}{RT_R} + \frac{PV_C}{RT_C} \quad (21)$$

The temperature ratio t,

$$t = \frac{T_C}{T_E} \quad (22)$$

The swept volume ratio v,

$$v = \frac{V_{SC}}{V_{SE}} \quad (23)$$

Similarly other dead volume ratio,

$$X_{DE} = \frac{V_{DE}}{V_{SE}} \quad (24)$$

$$X_{DC} = \frac{V_{DC}}{V_{SC}} \quad (25)$$

$$X_R = \frac{V_R}{V_{SE}} \quad (26)$$

The regenerator temperature - T_R is formulated in equation (27), based on the assumption (f).

$$T_R = \frac{T_E + T_C}{2} \quad (27)$$

The equation (21) is modified to become equation (28), with substitutions from equations (22) to (26), the total fluid mass m is described in the next equation,

$$m = \frac{P}{RT_C}\left(tV_E + \frac{2tV_R}{(1+t)} + V_C\right) \tag{28}$$

The equation (28) is modified to become equation (29), with substitutions from equations (17) and (18),

$$m = \frac{PV_{SE}}{2RT_C}\{S - B \cdot cos(x-a)\} \tag{29}$$

Now,

$$a = tan^{-1}\left(\frac{v \cdot sin\, dx}{t + cos\, dx + 1}\right) \tag{30}$$

$$S = t + 2 \cdot t \cdot X_{DE} + \left(\frac{4 \cdot t \cdot V_r}{1+t}\right) + v + 2 \cdot X_{DC} + 1 \tag{31}$$

$$B = \sqrt{t^2 + 2 \cdot (t-1) \cdot v \cdot cos\, dx + v^2 - 2 \cdot t + 1} \tag{32}$$

The engine pressure - P is redefined from equation (33),

$$P = \frac{2mRT_c}{V_{SE}\{S - B\, cos(x-a)\}} \tag{33}$$

The mean pressure of the engine P_{Mean} can be formulated as in the equation (34),

$$P_{Mean} = \frac{1}{2\pi}\oint P dx = \frac{2mRT_c}{V_{SE}\sqrt{S^2 - B^2}} \tag{34}$$

Accordingly, c is defined as in the next equation.

$$c = \frac{B}{S} \tag{35}$$

The engine pressure - P redefined based on the mean pressure P_{Mean}, the minimum pressure P_{Min} and the maximum pressure P_{Max} are formulated in the equations (36).

$$P = \frac{P_{Mean} \cdot \sqrt{1-c^2}}{1 - c \cdot cos(x-a)} = \frac{P_{Min} \cdot (1+c)}{1 - c \cdot cos(x-a)} = \frac{P_{Max} \cdot (1-c)}{1 - c \cdot cos(x-a)} \tag{36}$$

The indicated energy (*area of the P-V diagram*) in the expansion and compression space can be calculated as an analytical solution with use of the above coefficients. The indicated energy in the expansion space (indicated expansion energy) - $W_E(J)$, based on the mean pressure P_{Mean}, the minimum pressure P_{Min} and the maximum pressure P_{Max} are described in the following equations.

$$W_E = \oint P \cdot dV_E = \frac{P_{Mean} \cdot V_{SE} \cdot \pi c \cdot sin(a)}{1 + \sqrt{1 - c^2}} = \frac{P_{Min} \cdot V_{SE} \cdot \pi c \cdot sin(a)}{1 + \sqrt{1 - c^2}} \cdot \sqrt{\frac{1 - c}{1 + c}}$$

$$= \frac{P_{Max} \cdot V_{SE} \cdot \pi c \cdot sin(a)}{1 + \sqrt{1 - c^2}} \cdot \sqrt{\frac{1 + c}{1 - c}} \quad (37)$$

The indicated energy in the compression space (indicated compression energy) $W_C(J)$ are formulated in the next equations

$$W_C = \oint P \cdot dV_C = -\frac{P_{Mean} \cdot V_{SE} \cdot \pi ct \cdot sin(a)}{1 + \sqrt{1 - c^2}} = -\frac{P_{Min} \cdot V_{SE} \cdot \pi ct \cdot sin(a)}{1 + \sqrt{1 - c^2}} \cdot \sqrt{\frac{1 - c}{1 + c}}$$

$$= -\frac{P_{Max} \cdot V_{SE} \cdot \pi ct \cdot sin(a)}{1 + \sqrt{1 - c^2}} \cdot \sqrt{\frac{1 + c}{1 - c}} \quad (38)$$

The indicated energy per one cycle of this engine $W_i(J)$ is demanded in the next equations.

$$W_i = W_E + W_C \quad (39)$$

$$W_i = \frac{P_{Mean} \cdot V_{SE} \cdot \pi c \cdot (1 - t) \cdot sin(a)}{1 + \sqrt{1 - c^2}} = \frac{P_{Min} \cdot V_{SE} \cdot \pi c \cdot (1 - t) \cdot sin(a)}{1 + \sqrt{1 - c^2}} \cdot \sqrt{\frac{1 - c}{1 + c}}$$

$$= \frac{P_{Max} \cdot V_{SE} \cdot \pi c \cdot (1 - t) \cdot sin(a)}{1 + \sqrt{1 - c^2}} \cdot \sqrt{\frac{1 + c}{1 - c}} \quad (40)$$

Relations between P_{mean}, P_{min} and P_{max} are determined in the following equations

$$P_{Mean} = \sqrt{P_{Min} \cdot P_{Max}} \quad (41)$$

$$\frac{P_{Min}}{P_{Mean}} = \sqrt{\frac{1 - c}{1 + c}} \quad (42)$$

$$\frac{P_{Max}}{P_{Mean}} = \sqrt{\frac{1 + c}{1 - c}} \quad (43)$$

The indicated expansion power $L_E(W)$, the indicated compression power $L_C(W)$, and the indicated power of this engine $L_i(W)$, are defined in the following equations, using the engine speed per second, *n (rps, Hz).*

$$L_E = W_E \cdot n \quad (44)$$

$$L_C = W_C \cdot n \quad (45)$$

$$L_i = W_i \cdot n \quad (46)$$

The indicated expansion energy - W_E found equation (37) means an input heat from a heat source to the engine. The indicated compression energy -W_C calculated by equation (38) means a reject heat from the engine to cooling water or air. Then the thermal efficiency of the engine - η is calculated in the next equation.

$$\eta = \frac{W_i}{W_E} = 1 - t = 1 - \frac{T_C}{T_E} \tag{47}$$

This efficiency equals that of a Carnot cycle that is the highest efficiency in ever thermal engines.

3.4 Machine Geometry and Its Influence on Performance

The geometry of a machine, particularly in complex mechanical systems like Stirling engines or HPs, plays a pivotal role in determining its efficiency and overall performance. In the context of Stirling-based systems, the design of components such as the displacer, piston, regenerator, and heat exchangers are crucial. These components' dimensions and spatial arrangements directly affect the fluid dynamics, heat transfer capabilities, and ultimately the thermodynamic efficiency of the machine.

Displacer and Piston Design

The dimensions and stroke length of the displacer and piston in a Stirling engine significantly influence the compression ratio and the phase angle between the displacer and piston movements. These parameters are critical as they determine the timing and extent of heat transfer between the working fluid and the heat exchangers. Optimizing the displacer's diameter and stroke can lead to more effective compression and expansion cycles, enhancing the machine's output power and efficiency.

Regenerator Effectiveness

The geometry of the regenerator, including its volume, shape, and the material used for the matrix, affects its ability to store and transfer heat. A well-designed regenerator minimizes dead volume while maximizing surface area, thus enhancing heat transfer between the hot and cold gases. The positioning of the regenerator between the hot and cold heat exchangers also impacts its effectiveness, influencing the overall thermal efficiency of the system.

Heat Exchanger Configuration

The configuration and sizing of the heat exchangers directly impact the heat transfer rates necessary for the Stirling cycle. The surface area, flow configuration, and fin design on the heat exchangers can be optimized to enhance the convective heat transfer, facilitating more rapid and efficient heat exchange. For instance, increasing the surface area or improving the flow paths within the heat exchangers can significantly reduce thermal resistance and improve the system's performance.

Integration and Compactness

The overall layout and compactness of the machine influence not only the efficiency but also the practical application and scalability of the technology. A compact design reduces material usage and heat losses but must be balanced against the risk of increased internal friction and reduced heat transfer efficiency due to closer component spacing.

3.4.1 Heat transport mechanisms and challenges at elevated temperatures

Heat transfer at high temperatures is a critical aspect of thermal management. There are three primary mechanisms, conduction, convection, and radiation. When temperatures get really high, how well each of these methods works can change a lot. Conduction, the transfer of heat through a medium without the movement of the material itself, becomes increasingly challenging to manage as materials tend to expand and change properties at high temperatures, affecting their thermal conductivity. Convection is different – it's about heat moving with a fluid motion. This method works better at high temperatures because the heat makes the fluid move faster. But to get the most out of convection, you need a good design that makes sure optimized fluid flows and maximize heat exchange.

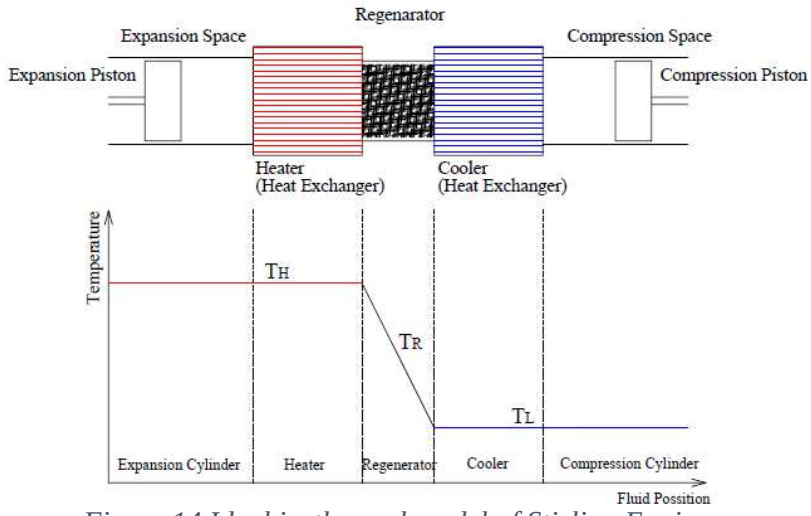

Figure 14 Ideal isothermal model of Stirling Engine

3.4.2 Heat Exchanger Geometry

The reversed Stirling cycle, which is highly efficient in managing heat, shows great potential for improving thermal management systems. Recent research has pointed out its usefulness in situations where a lot of heat needs to be moved with little energy used. This cycle works by absorbing and releasing heat in a repeating pattern, which greatly lowers the amount of heat that is lost. This cycle differs from standard approaches, as it uses a regenerator to store heat energy when heating and then release it during cooling. This leads to better heat transfer, making it more efficient than usual heat exchangers.

The key features of the heat exchanger are the number of tubes, the diameter of the tubes, the thickness of the tubes, and the length of the compression and expansion areas. These parameters will help in designing efficient and optimized heat exchangers for Stirling machines under different temperature conditions.

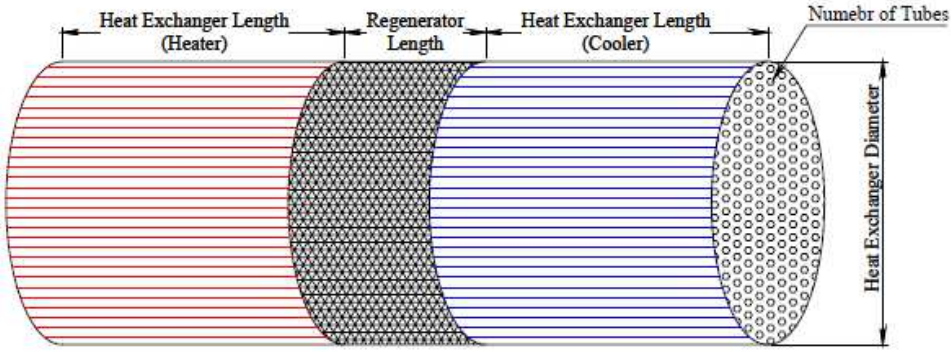

Figure 15 Geometry of the heat exchanger

3.4.3 Regenerator Geometry

The regenerator is a type of heat exchanger that temporarily stores heat from a hot fluid and then transfers it to a cooler fluid. This process is fundamental in various applications and industrial waste heat recovery systems. The geometry of a regenerator, encompassing aspects like shape, size, and the arrangement of its internal components, directly impacts its ability to store and transfer heat.

The key factors of the regenerator, an important part of the Stirling machine, include the diameter of the threads used inside it, the overall diameter of the regenerator itself, and the porosity of the regenerator.

Thread Diameter: This refers to the thickness of the threads or fibers used in the regenerator. The size of these threads affects how well the regenerator can transfer heat.

Regenerator Diameter: This is about how wide the entire regenerator is. The size can impact the total area available for heat exchange and how the machine handles different temperatures.

Porosity: This tells us how much open space is in the regenerator. A higher porosity means there are more spaces for fluid to flow through, which can influence the efficiency of heat transfer.

The Heat exchanger unit optimization, these parameters influence to maximize efficiency and performance of the Stirling machine. Also, to manage how well it operates the cycle at different temperature lift conditions.

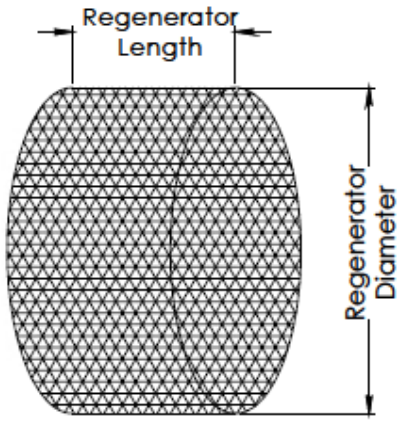

Figure 16 Geometry of the regenerator

3.4.4 Heat Transfer Analysis

In the Stirling machine, the primary medium for heat transfer is the working fluid. For the machine's efficiency, it is important that this working medium can transfer a large amount of heat. The rate of heat transfer, denoted as, $\dot{Q}$, between the fluid and the tube is:

$$\dot{Q} = hA\Delta T \tag{48}$$

with h representing the heat transfer coefficient, A the area for heat transfer and ΔT is the temperature difference between wall and fluid. It was assumed the flow inside a Stirling engine is turbulent however by theoretical calculation it was proven that the flow is turbulence. This benefit to introduce a dimensionless parameter called the Nusselt number;

$$Nu = f(x, Re_L, Pr) \tag{49}$$

The Nusselt number is a function of the spatial variable x, and the dimensionless Reynolds number and Prandtl number. Assuming turbulent flow, the Nusselt number is given by following equation.[25]

The corresponding relation for turbulent flow is

$$Nu = 0,023Re^{0.8}Pr^{0.33} \quad (50)$$

Where, $0.6 \leq Pr \leq 60$ & $5 \times 10^5 \leq Re \leq 10^7$

The Nusselt number is the ratio of convection to pure conduction heat transfer,

$$Nu = \frac{hD}{k} \quad (51)$$

Where, h convection coefficient, k is the thermal conductivity of the fluid and D (L_C) is the characteristic length.

The Reynolds number is the ratio of the inertia and viscous forces.

$$Re = \frac{\rho DV}{\mu} \quad (52)$$

Where, ρ density of the fluid, D characteristic length, V velocity of the fluid, and μ dynamic viscosity of the fluid

The Prandtl number is the ratio of the momentum and thermal diffusivities,

$$Pr = \frac{C_p\mu}{k} \quad (53)$$

Where C_p Heat capacity, μ is the Viscosity of the fluid and k is the thermal conductivity of the fluid.

Redefining above equations:

$$\frac{hD}{k} = 0.023 \cdot \left(\frac{\rho DV}{\mu}\right)^{0..8} \cdot \left(\frac{C_p\mu}{k}\right)^{0.33} \quad (54)$$

$$h = 0.023 \cdot \frac{k}{D} \cdot \left(\frac{\rho DV}{\mu}\right)^{0..8} \cdot \left(\frac{C_p\mu}{k}\right)^{0.33} \quad (55)$$

Similarly, from equation (49),

$$\dot{Q} = 0.023 \cdot \frac{k}{D} \cdot \left(\frac{\rho DV}{\mu}\right)^{0..8} \cdot \left(\frac{C_p\mu}{k}\right)^{0.33} \cdot A \cdot \Delta T \quad (56)$$

3.4.5 Beale Number

The Beale number is a dimensionless number that provides a measure of the potential power output of a Stirling engine relative to its displacement volume and the temperature difference between its hot and cold sides. It is defined by the formula:[27]

$$B_n = \frac{W}{V_s \cdot \Delta T} \tag{57}$$

Where W is the work output per cycle, $V_s$is the swept volume of the engine, and ΔT is the temperature difference between the hot and cold heat exchangers.

Performance Prediction: The Beale number allows for the prediction of a Stirling engine's performance without the need for detailed thermodynamic cycle analysis. It provides a quick estimation tool for comparing the theoretical and actual performance of different Stirling engines or design configurations.

Design Optimization: By analyzing the Beale number, engineers can optimize Stirling engine designs for maximum efficiency and power output. This analysis aids in making informed decisions regarding the size, materials, and configuration of engine components to achieve desired performance characteristics.

Comparative Analysis: The Beale number facilitates the comparison of engines of different sizes and operating conditions on a common basis. This is particularly useful in research and development when assessing the impact of various design changes or operational improvements.

3.4.6 Sound Speed

The speed of sound in the working fluid of a Stirling engine is a critical factor in determining the engine's operating frequency and overall efficiency. The speed of sound is influenced by the properties of the working fluid and affects the pressure wave propagation within the engine.

The analyze of Stirling engines and their performance with respect to the speed of sound, several key equations and principles come into play. The speed of sound a in a medium is fundamentally given by the equation:

$$a = \sqrt{\frac{\gamma \cdot P}{\rho}} \tag{58}$$

Where, a is the speed of sound, γ (gamma) is the adiabatic index (or specific heat ratio) of the gas, which is the ratio of the specific heat at constant pressure C_p to the specific heat at constant volume C_v, i.e $\gamma = C_P/C_V$, P is the pressure of the gas, and ρ is the density of the gas.

- Resonance and Operating Frequency: The speed of sound in the working fluid sets a limit on the engine's operating frequency, especially in thermoacoustic Stirling engines, where the engine's efficiency is maximized at resonant frequencies. Operating the engine close to the speed of sound can enhance efficiency but requires careful design to avoid destructive resonances.
- Pressure Drop and Flow Characteristics: Understanding the sound speed is essential for minimizing pressure drops and optimizing the flow characteristics within the engine. It helps in the design of the engine's heat exchangers, regenerators, and other components to ensure that fluid dynamics do not adversely affect performance.
- Material selection and design: The speed of sound in the working fluid impacts material selection and design decisions, especially for components like the regenerator, where the flow speed relative to the speed of sound can influence heat transfer and pressure loss characteristics.

These equations are fundamental for understanding the propagation of sound waves within the engine and for designing the engine components to optimize performance. For Stirling engines, in particular, a few specific applications of sound speed include:

- Designing for Resonance: By matching the engine's operating frequency with the natural acoustic frequency of the system (which depends on the speed of sound within the engine), designers can reduce energy losses and increase efficiency. This involves calculating the natural frequencies of the engine's components and spaces, which depend on the geometry and the speed of sound in the working fluid.
- Regenerator Effectiveness: The design of the regenerator, a core component of Stirling engines, can be optimized by understanding how sound waves propagate through the regenerator material. This involves complex calculations of heat transfer and fluid dynamics, where the speed of sound plays a role in determining the flow characteristics and thermal gradients.
- Pressure Wave Dynamics: The analysis of pressure waves and their reflection and absorption in different parts of the engine is crucial for minimizing energy losses and enhancing power output. The speed of sound in the working fluid directly affects the

wavelength and propagation speed of these waves, influencing the design of components like heat exchangers and expansion/compression spaces.

- Thermodynamic Analysis: Advanced models of Stirling engines may incorporate the effects of varying speed of sound with temperature and pressure to predict engine performance more accurately under different operating conditions. This can involve simulations that take into account the real gas behavior and non-linearities in the speed of sound.

Similarly, several other parameters significantly influence the performance and design of Stirling engines, in addition to the Beale number and speed of sound. Since Stirling machines operate primarily through heat transfer mechanisms, heat transfer formulas and correlations are crucial. These parameters are essential for evaluating the engine's efficiency, operational characteristics, and design optimization. Key parameters include:[25]

1. Reynolds Number

The Reynolds number in a Stirling engine is critical for analyzing the flow regime (laminar or turbulent) within the engine, especially in the heat exchangers and regenerator. It affects heat transfer rates and pressure drops, which in turn influence the engine's efficiency and performance.

$$Re = \frac{\rho \cdot v \cdot L}{\mu} \tag{59}$$

Where, ρ Density of the fluid, v velocity of the fluid, L characteristic length (such as hydraulic diameter), and μ dynamic viscosity of the fluid.

Impact: High Reynolds numbers indicate turbulent flow, which can enhance heat transfer but also increase friction and pressure losses. Optimizing the Reynolds number for different components of the Stirling engine can lead to improved efficiency.

2. Grashof Number

The Grashof number is a dimensionless quantity used in the analysis of natural convection flows within the engine, particularly around the heating and cooling sections. It indicates the ratio of buoyancy to viscous force in the fluid.

$$Gr = \frac{g \cdot \beta \cdot (T_s - T_\infty) \cdot L^3}{v^2} \tag{60}$$

Where, g acceleration due to gravity, β thermal expansion coefficient (1/t for ideal gases at constant pressure), T_s surface temperature, T_∞ ambient fluid temperature, L characteristic length, and v kinematic viscosity.

Impact: Understanding the Grashof number helps in designing the heat exchange surfaces to maximize heat transfer through natural convection, improving the engine's thermal efficiency.

3. Prandtl Number

The Prandtl number is a dimensionless number that relates the fluid's viscosity to its thermal conductivity. In Stirling engines, it affects the design and performance of the regenerator, a critical component for heat exchange between the compression and expansion spaces.

$$Pr = \frac{v}{\alpha} \tag{61}$$

Where, v kinematic viscosity, and α thermal diffusivity.

Impact: The Prandtl number influences the choice of working fluid and regenerator material by indicating the relative effectiveness of momentum and energy transport in the fluid.

4. Schmidt Number

For Stirling engines operating with gaseous working fluids where mass transfer (such as in leakages or during gas exchanges) might be a concern, the Schmidt number becomes relevant. It relates the fluid's viscosity to its diffusivity.

$$Sc = \frac{v}{D} \tag{62}$$

Where, v kinematic viscosity, and D mass diffusivity.

Impact: This parameter can influence the design considerations regarding seals and the choice of working fluids, aiming to minimize losses and optimize the mass transfer characteristics.

5. Mach Number

The Mach number, which is the ratio of the velocity of the working fluid to the speed of sound in that fluid, is crucial for understanding the compressibility effects in the engine, particularly for high-speed Stirling engines.

$$Ma = \frac{v}{a} \tag{63}$$

Where, v flow velocity, and a speed of sound in the medium.

Impact: It helps in assessing whether compressibility effects are significant and in designing the engine components to accommodate or mitigate these effects, thus affecting the engine's performance and efficiency.

6. Efficiency Parameters

Thermal Efficiency: Indicates the proportion of heat converted to work and is a direct measure of the engine's performance.

$$\eta_{th} = \frac{W_{net}}{Q_{in}} \tag{64}$$

Where, W_{net} - Net work output per cycle, and Q_{in} - Heat input per cycle.

Mechanical Efficiency: Reflects the losses due to friction and other mechanical factors in the engine.

$$\eta_{mech} = \frac{W_{output}}{W_{input}} \tag{65}$$

Where, W_{output} useful work output, and W_{input} total work input (or gross work output without losses).

7. Specific Power

Specific power is a measure of the engine's power output per unit mass or volume of the engine. It is crucial for evaluating the engine's performance in weight or space-sensitive applications.

$$Specific\ power\ = \frac{P}{m} \tag{66}$$

Where, P Power output, and m mass of the Stirling engine.

Impact: High specific power is desirable for portable or aerospace applications, influencing the choice of materials and design configurations to minimize weight while maximizing power output.

3.4.7 Overview of Energy Losses Methods on the System

Energy losses in an HP process, such as in reversed Stirling cycle HPs, significantly impact the system's overall efficiency and performance. This leads to reduced efficiency, increased

operational costs, more frequent maintenance, and a shortened lifespan of the HP. There are many losses in the Stirling machine, which can be categorized into two common types of energy losses in this HP as follows:[29]

1. Thermal Losses
    - Conduction losses
    - Cylinder heat transfers
    - Regenerator enthalpy loss
    - External radiation and convection
2. Mechanical losses (Thermodynamic losses)
    - mechanical friction
    - aerodynamic friction (fluid viscous losses)
    - gas spring hysteresis losses
    - seal leakage losses
    - heat transfer between gas and walls
    - mixing losses
    - appendix gap losses (shuttle heat transfer, gas enthalpy transfer & hysteresis heat transfer)
    - adiabatic working space loss

However, the following losses are of primary concern in practical applications due to their significant impact:

- Heat losses from the hot side to the cold side of the cylinder.
- Heat losses through the external surface.
- Energy losses in secondary circuits.
- Electrical energy losses.

Chapter 4 Methodology

4.1 Experimental Setup at IVAR

The HoegTemp HP installed at IVAR in Stavanger is used to generate steam, which facilitates the capture of CO_2 from the waste recycling plant. The entire setup used for my thesis date measurement and analysis.

This HP system can be divided into several main components for clarity, as outlined below. These classifications have been established to streamline the description and analysis of the system.

1. Hoeg Temp HP unit.
    - Stirling Machine (Engine) Unit
    - Electric Motor Unit
    - Stirling Machine Oil pumping unit
2. Cold water recirculation unit
3. Hot water recirculation unit
4. Steam Generator unit
5. Control panel unit
6. Refrigerant Storage tanks (Cylinders), Connecting tubing to HP and Portable Air Compressor.

4.1.1 Stirling Machine (Engine) Unit.

The Stirling machine, a typical model of an ideal gamma type Stirling engine, is composed of two distinct cylinder banks. Each of these cylinder banks integrates two separate pairs of working fluid circuits, facilitating the machine's overall thermodynamic efficiency. As shown in *Figure 17*, each cylinder bank is meticulously equipped with two comprehensive sets of heat exchanger units. These units play a crucial role in the thermal management and efficiency of the machine by transferring heat to and from the working fluids.

Within each cylinder bank, there are three dual-acting cylinders arranged in a specific configuration. The central dual-acting cylinder in this arrangement functions as the power piston for both fluid circuits contained within the bank. This power piston is responsible for

absorbing the thermal energy from cold side and transferring to hot side, thereby driving the machine's output.

Flanking the central power piston, the dual-acting cylinders positioned on either side operate as displacers. Each displacer is dedicated to one of the two separate fluid circuits, ensuring that the working fluids are appropriately displaced and cycled through the heat exchangers. The displacers are crucial for maintaining the continuous flow and pressure variations of the working fluids, which are necessary for the Stirling cycle's regenerative process.

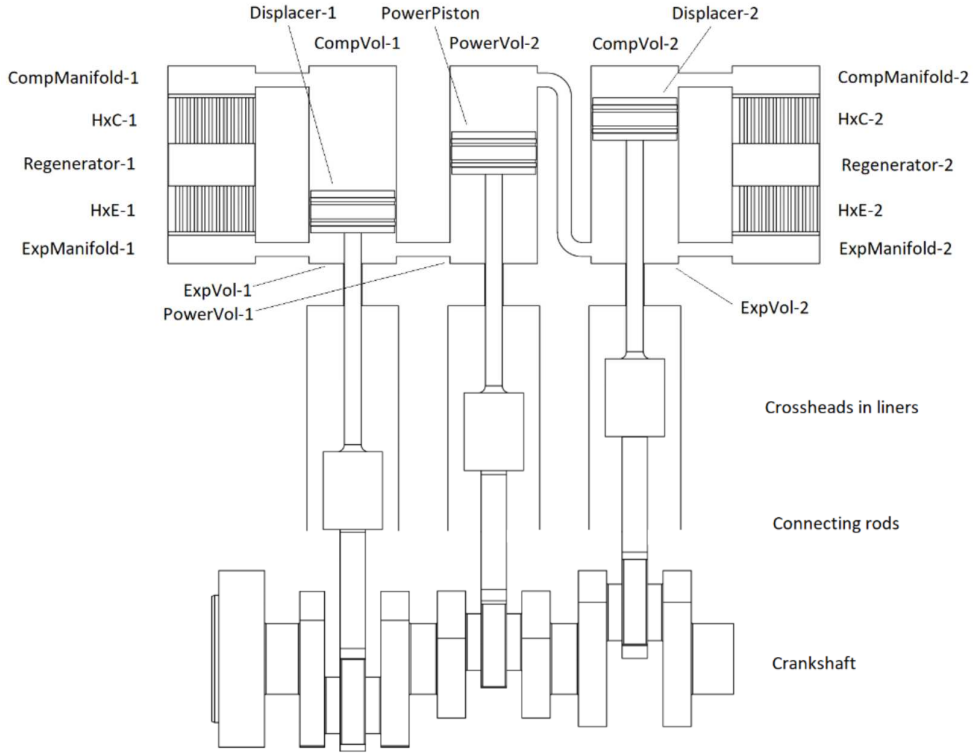

Figure 17 Conventional double-acting layout

This intricate arrangement allows for the simultaneous and efficient operation of the two working fluid circuits within each cylinder bank, optimizing the machine's performance and efficiency. The dual-acting nature of both the power piston and the displacers underscores the complexity and sophistication of the Stirling machine's design, contributing to its theoretical and practical significance in thermodynamic applications.

The Stirling machine cylinders' volume was not taken from the HoegTemp HP at IVAR; it was also sourced from previously developed models and a revised high-performance (HP) design provided by Enerin publications.[26]

Table 3 Volume Characteristics of the Stirling Machine HP at IVAR

Volume Section	**Volume/(cm^3)**
Expansion Swept Volume	7175
Compression Swept Volume	7175
Expansion Dead Volume	11274
Compression Dead Volume	11274
Regenerator Volume	9671

In the Stirling machine, a total of eight heat exchanger units are intricately connected to the two-cylinder banks. Each heat exchanger unit comprises three essential components: a cold-side heat exchanger, a regenerator, and a hot-side heat exchanger, as depicted in *Figure 18*. These components collaborate to facilitate the efficient transfer and regulation of thermal energy within the system, thereby enabling effective heating.

The cold-side heat exchanger is responsible for absorbing heat from the external environment, causing the working fluid to cool. This cooled fluid then passes through the regenerator, which serves a dual purpose: it temporarily stores thermal energy and enhances the overall efficiency of the thermal cycle by pre-cooling the working fluid on its way to the hot-side heat exchanger. The hot-side heat exchanger subsequently transfers this absorbed heat into the space to be heated, raising the temperature of the working fluid before it re-enters the cycle.

To streamline the integration with the secondary water circuit, each heat exchanger unit is designed with two heat exchangers connected in parallel. This parallel configuration simplifies the connection process, ensuring a smooth and efficient thermal exchange with the secondary circuit. The use of parallel connections also enhances the system's redundancy and reliability, allowing for continuous operation even if one of the heat exchangers requires maintenance.

Therefore, within each cylinder bank, these heat exchanger units are strategically placed on either side. This arrangement ensures balanced thermal management across the entire system, optimizing the performance and efficiency of the HP. The precise placement and configuration

of these units underscore the thoughtful engineering behind the design, aimed at maximizing the thermodynamic effectiveness of the HP.

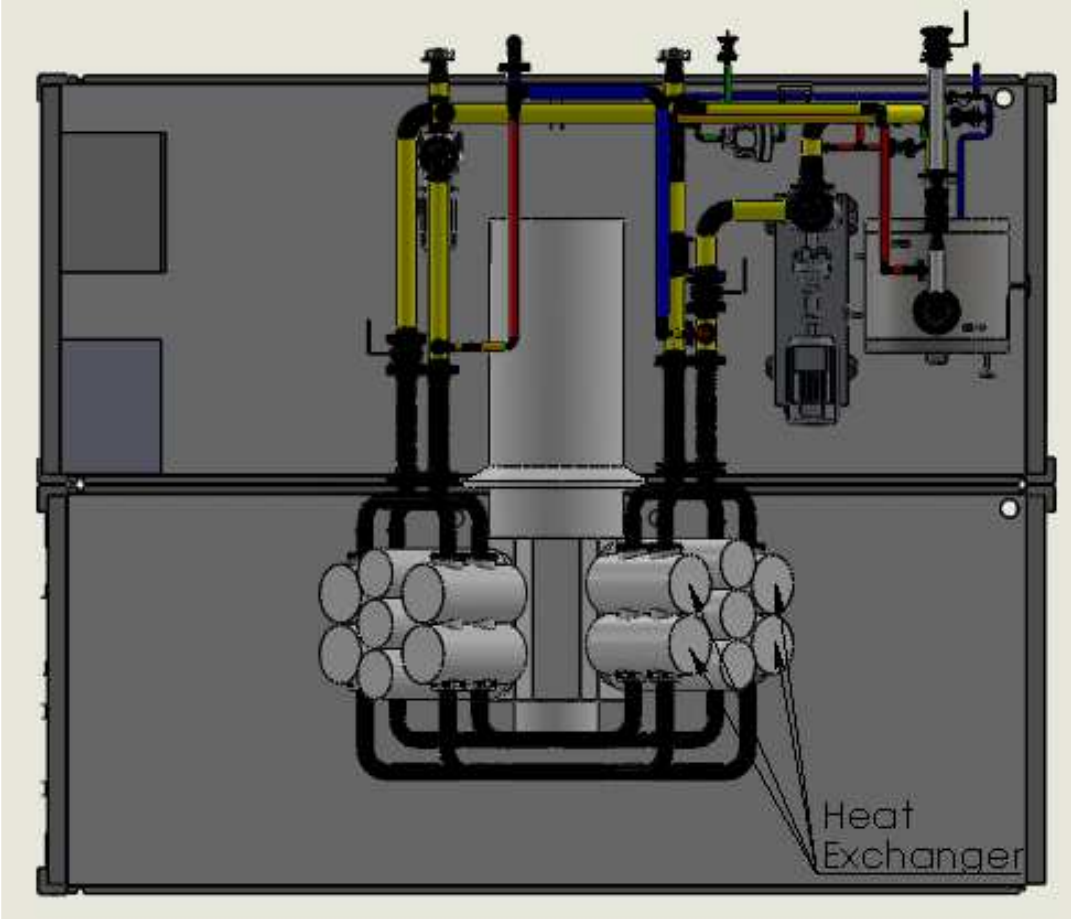

Figure 18 Top view of HoegTemp HP installation at IVAR

Similar to cylinder volume details, the design parameters for the heat exchanger and regenerator were sourced from previously developed models and a revised high-performance (HP) design provided by Enerin publications.[26] It is assumed that both heat exchangers (cold side and hot side) have identical dimensions for the purposes of this analysis. Currently, the HP system is operational, eliminating the possibility of conducting physical measurements.

Table 4 Heat Exchanger Physical Parameters

Heat Exchanger	Number of Tubes	Length/(m)	Tube Diameter/(m)
Hot side	704	0.248	0.0034
Cold side	704	0.248	0.0034

4.1.2 Electric Motor Unit

The electric motor coupled directly with the Stirling machine HP is a critical component to ensure efficient operation and optimal performance of the HP system. The electric motor model:3SIE355H8D and operates on a three-phase power supply with versatile voltage options of 400V or 690V at a frequency of 50Hz. It delivers a power output of 250 kW (340 HP) and is suitable for continuous operation (S1 duty). Key electrical characteristics include a nominal current of 488A at 400V and 282A at 690V, a synchronous speed of 742 rpm, and a nominal torque of 3218 Nm. The motor's torque ratios are also noteworthy, with a locked rotor torque to full load torque ratio of 1.3, a breakdown torque to full load torque ratio of 2.0, and a locked rotor current to full load current ratio of 6.0. These specifications ensure that the motor can handle the demanding conditions of continuous industrial operation.

Table 5 Electrical Motor Parameters at Different Voltages

Parameter	**400V**	**600V**
Nominal Current (In)	488A	282A
Synchronous Speed (n)	742 rpm	742 rpm
Nominal Torque (T)	3218 Nm	3218 Nm

The motor's performance characteristics are optimized for various load conditions, with efficiency and power factor values as follows:

Table 6 Electrical motor's performance characteristics

Load	**Efficiency**	**Power Factor**
50%	94.2%	0.63
75%	94.8%	0.74
100%	94.8%	0.78

Table 7 General data of electric motor

Feature	**Specification**
Efficiency Class	IE3
Sound Pressure Level	77 dB
Terminal Box Position	Top/Side
Starting Methods	DOL, Y/D, VSD
Insulation Class	F
Bearings (D-side/ND-side)	6322 C3
Cooling Method	IC411

Mounting Arrangements	IMB3, B35, V1
Weight (IMB3)	2440 kg
Moment of Inertia	12.9 kgm²
Housing Material	Cast iron
Degree of Protection	IP55
Direction of Rotation	CW/CCW
Painting	RAL5010
Ambient Temperature	Up to +40°C
Altitude	Up to 1000 meters
Relative Humidity	Up to 95%
Terminals	6
Temperature Sensors	2 x Pt100 in bearings, 6 x Pt100 in windings
Standards	IEC 60034-1

4.1.3 Stirling Machine Oil pumping unit

The integrated Stirling machine oil recirculation pumping unit described is a sophisticated system designed to maintain the optimal operating temperature and cleanliness of engine oil in Stirling machine. This system features a high-performance KSB HPK125-100-200 SGBS W oil pump coupled with a Siemens electric motor, enhancing its reliability and efficiency. The pump, boasts a flow rate of 116.48 m³/h, a total head of 12.0 meters, and operates at 1500 rpm, ensuring efficient fluid transfer and pressure maintenance for machines processes. The Siemens motor, part of the 1LE1501 series, provides a power rating of 1.5 kW (2 HP) and is designed to operate at various voltage and frequency combinations, further contributing to the system's robustness.

The oil recirculation unit is equipped with a heat exchanger, which plays a crucial role in cooling the engine oil. This heat exchanger is connected to a cold-water pipeline, ensuring efficient heat transfer and maintaining the oil at a safe operating temperature. The use of a heat exchanger is essential in preventing the oil from overheating, which can lead to reduced lubrication efficiency and potential damage to engine components. By integrating this cooling mechanism, the system ensures that the engine operates within the optimal temperature range, enhancing its performance and longevity. The materials used in the pump's construction, though not explicitly detailed on the nameplate, are typically high-grade metals, providing durability and reliability under continuous operation.

To further enhance the oil quality, the system incorporates a dual-stage filtration process. The primary oil filter is designed to remove large impurities and contaminants from the oil, protecting the subsequent components from excessive wear and tear. Following this, the secondary oil filter provides finer filtration, removing smaller particles and ensuring that the oil remains clean and free from contaminants that could affect the engine's performance. This two-stage filtration system is critical for maintaining high oil quality, reducing the risk of engine damage, and extending the service life of both the oil and the engine components.

4.1.4 Cold water recirculation unit

The cold water recirculation unit consists of 4-inch pipeline connections to the high-pressure circulation pump, flow meter, and temperature and pressure sensors. The insulated 3-inch diameter pipeline circulates fresh water from a reservoir through the water pump, ensuring efficient distribution of cold water throughout the Stirling machine heat exchangers and the designated system. This setup not only enhances the cooling efficiency but also maintains the desired temperature and pressure levels within the system. The pump is a robust unit, designed to handle significant volumes of water, and built for durability and reliability in demanding environments.

Figure 19 Cold Water Circulation Pump

This system features a high-performance TP 100-110/4 A-F-A-BQQE-JW3 water pump coupled with a Siemens electric motor, enhancing its reliability and efficiency. The water pump boasts a flow rate of 85.9 m^3/h, a total head of 8.7 meters, and operates at 1455 rpm. It has a maximum

operating pressure of 16 bar and can handle temperatures up to 120°C with an efficiency of 83.4%. This ensures efficient fluid transfer and pressure maintenance for machine processes. The pump is coupled with a three-phase Siemens electric motor, known for its high efficiency and reliability. The motor has a power rating of 3.0 kW, an operating voltage range between 400 V and 690 V with an efficiency of 87.7%, and a frequency of 50/60 Hz. This motor adheres to the IE3 energy efficiency class, ensuring reduced energy consumption and operational costs while delivering consistent performance.

4.1.5 Hot water recirculation unit

The hot water recirculation system is a closed-loop, pressurized system designed for efficient hot water circulation. It utilizes a 4-inch pipeline with insulation and includes critical components such as a high-pressure circulation pump, a flow meter, and temperature and pressure sensors. These elements work together to monitor and regulate the supply and return flow within the pipeline, ensuring optimal performance and safety.

In this system, one end of the pipeline passes through the Stirling machine heat exchangers, where it absorbs heat energy. This absorbed heat is then transferred to a steam generator located at the other end of the pipeline, where it is used to produce steam. The design of this system ensures that the heat energy collected is efficiently utilized for steam generation, making it a vital component in industrial applications requiring consistent and reliable heat and steam production.

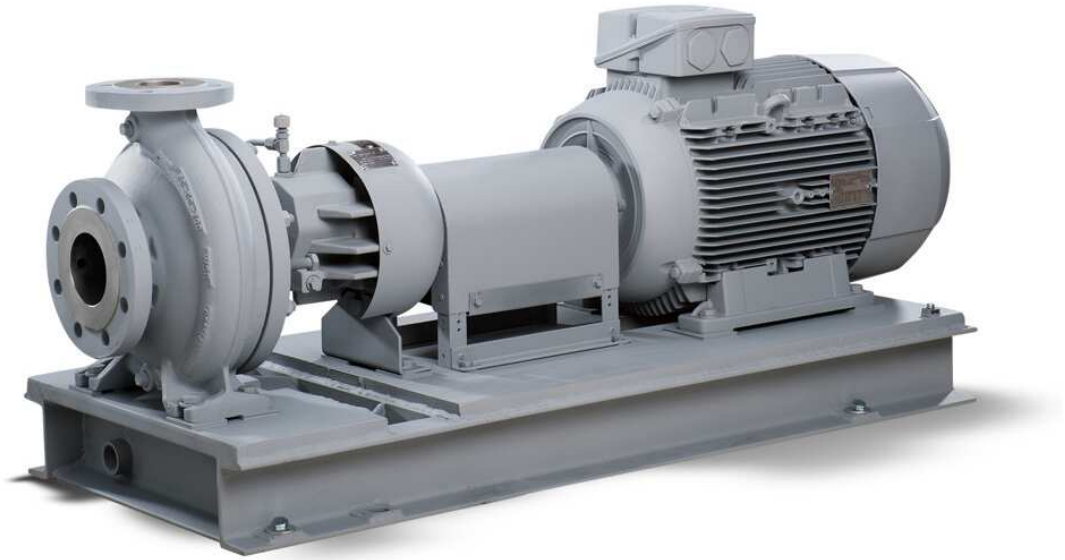

Figure 20 Hot Water Circulation Pump

This system features a high-performance HPKL125-100-200 SGBS W W01104 B heat transfer liquid (water) pump coupled with a KSB SuPremE® electric motor, enhancing its reliability and efficiency. The pump boasts a flow rate of 116.50 m^3/h, a total head of 12.0 meters, and operates at 1500 rpm. It has a maximum operating pressure of 22.5 bar and can handle temperatures up to 180°C with an efficiency of 76.4%. This ensures efficient fluid transfer and pressure maintenance for machine processes. The pump is coupled with a three-phase Siemens electric motor, known for its high efficiency and reliability. The motor has a power rating of 11.0 kW, an operating voltage 400 V with an efficiency of 93.5%, a frequency of 50 Hz and operates at 1500 rpm. This motor adheres to the IE5 energy efficiency class, ensuring reduced energy consumption and operational costs while delivering consistent performance.

4.1.6 Steam Generator

A plate and shell heat exchanger, functioning as a steam generator, is a highly efficient device designed to produce steam by utilizing heat transfer between a hot fluid and water. This type of heat exchanger comprises a series of plates and a surrounding shell, as illustrated in *Figure 21*. The plates are made from materials such as 1.4404/SA240-316L stainless steel, which provide excellent thermal conductivity and resistance to corrosion. The steam generator operates by channeling the hot fluid through the plates, transferring heat to the water within the shell, which subsequently vaporizes into steam. This method ensures uniform heat distribution and minimizes thermal stresses within the system, thereby enhancing the reliability and longevity of the equipment.

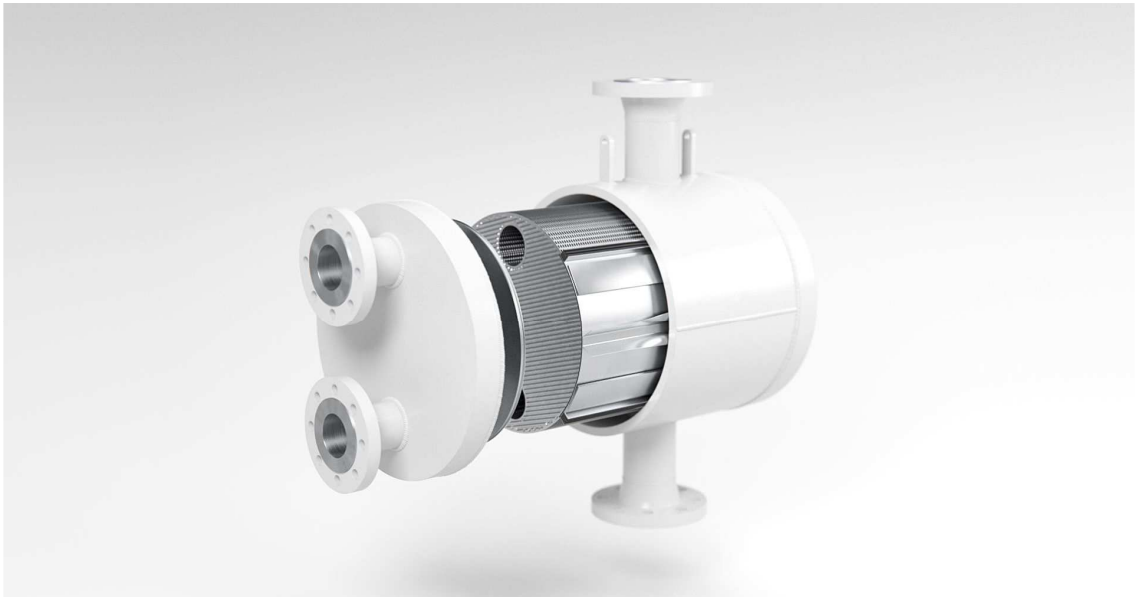

Figure 21 Steam Generator

The design parameters of the plate and shell heat exchanger are meticulously engineered to meet stringent performance and safety standards. For instance, the technical specifications indicate a design pressure range of 0 to 250 bar and an operating temperature between 70°C and 184.4°C, with a capacity of approximately 229.57 liters. The heat exchanger's construction follows the EN 13445-4 design code and complies with the PED 2014/68/EU and AD 2000 standards, ensuring it meets the highest quality and safety requirements. Additionally, the materials used, such as P355NL2 and P235GH steel for various components, provide robust structural integrity, while the helium vacuum and leakage tests guarantee the unit's operational reliability and efficiency. This comprehensive design approach makes the plate and shell heat exchanger an optimal solution for efficient and reliable steam generation in industrial applications.

The HP secondary hot water recirculation supply and return pipelines are connected to the cold side inlet and outlet of the steam generator, respectively. Similarly, the water inlet and steam outlet pipelines are connected to the hot side inlet and outlet of the steam generator, respectively. The water inlet is supplied with treated cold water, and the steam outlet pipeline is directly connected to the biogas facility for CO_2 capture. The unit is equipped with a circulation pump and a flow meter integrated with the steam generator. Additionally, it features pressure and temperature transmitters to monitor the supply and return conditions of the pipeline.

4.1.7 Control Panel

The Stirling machine HP is equipped with a sophisticated control system comprising two primary control panels.

The first control panel includes an electrical breaker that manages the main power supply to the key components of the system. This panel distributes power to the main electric motor, secondary water pumps (for both cold and hot circuits), the steam generator pump, and the oil pump. By centralizing the power distribution, this control panel ensures that all critical components receive a stable and reliable power supply, which is essential for the efficient operation of the HP.

The second control panel is a fully integrated control unit that manages the entire setup through an advanced computer interface. This panel is interconnected with a network of temperature sensors, pressure sensors, flow meters, pneumatic valve controls, and other critical monitoring

devices. The computer screen provides real-time data visualization and allows for precise control and adjustments of the system parameters. Additionally, this control panel can be operated remotely from the main facility in Oslo, enabling centralized monitoring and control of the HP's operation from a distant location. This remote capability enhances the flexibility and responsiveness of the system management, ensuring optimal performance, efficiency, and reliability even when direct on-site supervision is not possible. The ability to monitor and adjust various parameters remotely ensures that the Stirling machine HP can operate optimally under varying conditions, maintaining the desired temperature and pressure levels across the system.

4.1.8 Refrigerant Storage tanks (Cylinders), Connecting tubing to HP and Portable Compressor)

The Stirling Machine HP system features an advanced setup for refrigerant storage tanks and delivery, designed to ensure optimal performance and safety. The storage tanks(cylinders) are strategically positioned outside the main HP building, which reduces the risks associated with leaks and simplifies maintenance, refilling of cylinders and monitoring. These tanks are connected to the HP through standard-sized ¼ inches AIS316 tubing, facilitating efficient refrigerant transfer. This setup is essential for maintaining the desired thermal exchange processes within the Stirling cycle, thereby enhancing the overall efficiency and reliability of the HP system.

Central to this system is a pneumatic valve arrangement, controlled via a second control panel interface connected to a computer. This interface allows for precise regulation of the refrigerant flow, enabling the HP to adapt to varying thermal loads and operational demands. A small air compressor supports the pneumatic valve operation by providing the necessary compressed air to actuate the valves. This integration ensures reliable and responsive valve operation, allowing for quick adjustments in refrigerant flow as needed.

4.1.9 The Stirling Machine HP System: Starting Procedures & Important Guidance

Preparation:

- Check the System: Before starting the HP, ensure all components are properly installed and secured. This includes the displacer, power piston, regenerator, heat exchangers, and all connecting parts.

- Inspect for Leaks: Verify that the system is sealed and there are no leaks in the working fluid (Here used helium, hydrogen and Argon). Leaks can significantly reduce efficiency.
- Lubrication: Ensure that all moving parts are well-lubricated to reduce friction and wear.
- Cooling and Heating Sources: Confirm that the heat source (for the hot end) and the cooling source (for the cold end) are ready and operational. This could involve pre-heating the heat source and ensuring the cooling system (like a water circulation system) is functional.

Starting Procedure:

Step-1: The start operation of the secondary water circuit on the cold side of a Stirling machine HP involves begins by opening the pipeline valve and then activating the water pump to circulate treated water through the system. When the pump is activated, water flows from the reservoir into the heat exchanger, where it absorbs heat from the engine's cold side, thereby cooling it. The cooled water then circulates back through the pipes to the reservoir, completing the cycle. Throughout this process, sensors and the flow meter continuously monitor the temperature, pressure and flow rate to ensure efficient operation. This secondary water circuit effectively manages the thermal load, maintaining the desired low temperature on the cold side and ensuring optimal performance of the Stirling machine HP.

Step-2: The start operation of the secondary compressed water circuit in a Stirling machine's hot side begins by opening the pipeline valve and then activating the water pump, which initiates the circulation of compressed water through the system. As the pump starts, water circulates into the heat exchanger and the steam generator, where it absorbs heat from the machine's hot side. The heated water then circulates through a steam generator unit through pipeline and returns to the heat exchanger to complete the cycle. During this process, temperature and pressure sensors and the flow meter continuously monitor the system to ensure optimal operation. This circulation helps maintain the Stirling machine's thermal efficiency by effectively transferring the heat from the hot side and ensuring stable performance.

Step-3: Filled the Stirling machine with the gas (i.e. helium, nitrogen & argon) design pressure. Initially by ensuring the Stirling machine is turned off and cooled down. Prepare the gas cylinder with the appropriate regulator. Securely connect the gas cylinder to the engine's filling port. Open the purge valve to remove any air from the system, ensuring the purity of the

working gas. Slowly open the valve on the gas cylinder to start filling the Stirling machine, carefully monitoring the pressure gauges to reach the desired level. Once the appropriate pressure is achieved, close all valves and ensure they are tightly sealed to prevent any leaks. Conduct a thorough leak check using a detection solution or electronic leak detector. Finally, verify that all steps have been properly completed and that the machine is ready for operation.

Step-4: The oil recirculation pump in the Stirling machine is a crucial component responsible for the recirculation and cooling of the machine's crank system. When activated, it continuously circulates oil through the machine's lubrication system, ensuring that bearings, the crankshaft, and other moving components are adequately lubricated to minimize friction and wear. Additionally, the pump helps dissipate heat generated during operation, enhancing overall efficiency and longevity. By maintaining a consistent flow of oil, the recirculation pump plays a vital role in the smooth and reliable performance of the Stirling machine.

Step-5: The starting of Stirling machine by powering on the coupled motor and gradually increasing its speed to handle 50% of the load. During this phase, ensure and monitor that the oil recirculation pump is active to lubricate moving parts, and the secondary water circuits to manage thermal conditions. Allow the system to stabilize approximately 10 to 15 minutes at this intermediate load level, monitoring temperature, pressure, and lubrication parameters.

After achieving stability at 50% load, gradually increase the motor load to 75%. This involves adjusting the flow of working gas and enhancing the heat exchange processes. Allow the system to stabilize approximately 10 to 20 minutes at this load level, should be closely monitored for any signs of instability among the cylinder banks, and adjustments should be made as necessary to maintain optimal performance.

Once the system is stable at 75% load, further increase the load to 100%. This final phase requires precise control to ensure that the Stirling machine HP components can handle full operational capacity. Allow the system to stabilize approximately 10 to 20 minutes, continue to monitor all system parameters, including temperatures, pressures, and lubrication levels, to ensure safe and efficient operation.

Monitoring and Adjustments:

- Check Operating Parameters: Monitor temperature, pressure, and displacement characteristics to ensure they are within design limits. Adjust the heat input and displacement speeds as needed.

- Observe for Stability: Look for any signs of instability or unusual noise, which could indicate mechanical issues or misalignment.
- Fine-tuning: The input energy (heat) and the displacer's frequency to optimize performance. This might involve adjusting the phase angle between the displacer and the power piston.

Safety Checks:

- Safety Systems: Ensure all safety systems are functional. This includes overpressure valves, temperature sensors, and emergency shutdown mechanisms.
- Routine Checks: Regularly check and maintain the system to prevent any long-term issues from developing.

4.2 Data Collection and Analysis Methods

In the experimental setup, the methods used for data collection and analysis are important to ensuring the validity and reliability of the final results. The systematic approach adopted for gathering and interpreting data in this analysis is discussed further. By using advanced sensors and precision instruments, the data collection process captures critical parameters with high accuracy. The subsequent analysis employs both traditional statistical techniques and modern computational tools to derive meaningful insights from the raw data. This comprehensive approach facilitates a thorough understanding of the system's performance, allowing for the development of robust predictive models and the identification of key factors influencing efficiency and effectiveness. Through meticulous data collection and sophisticated analysis, the thesis aims to achieve a high degree of precision and reliability in its conclusions.

4.2.1 Data Collection

The data collection involves the use of various sensors and measurement instruments integrated into the experimental setup to monitor and record key parameters such as temperature, pressure, flow rates, and power consumption. High-precision thermocouples are used to measure the temperature at various points in the system, while pressure transducers monitor the pressure within the pump and heat exchanger. Flow meters are installed to measure the flow rate of both cold and hot secondary water circuit. Additionally, power analyzers are used to record the electric power consumption of the motor and pump unit.

To ensure accuracy and reliability, all sensors and instruments are calibrated before the start of the experiments. Data is recorded at regular intervals using a data acquisition system (DAQ), which is connected to a computer for real-time monitoring and storage. The DAQ system is configured to collect data at a high sampling rate to capture transient phenomena and provide detailed insights into the system's performance.

The experimental measured data:

The experiment was conducted under two different pressure conditions of the Stirling machine HP for all three refrigerants. The pressure set points were defined as one high pressure and one low pressure, as follows:

- High Pressure Set Point: The motor speed was maintained at approximately 600 RPM. Concurrently, the heat added to the HP was around 133 kW. Various parameters were measured under these conditions for all three refrigerants.
    - Test – 1: Helium gas at high pressure
    - Test – 3: Argon gas at high pressure
    - Test – 5: Nitrogen gas at high pressure
- Low Pressure Set Point: The motor speed was maintained at approximately 600 RPM. Concurrently, the heat added to the HP was around 100 kW. Various parameters were measured under these conditions for all three refrigerants.
    - Test – 2: Helium gas at low pressure
    - Test – 4: Argon gas at low pressure
    - Test – 6: Nitrogen gas at low pressure

There are six sets of test measurements were recorded for each refrigerant at both pressures set points; however, for display purposes, only one measurement for each case for all three gases is shown in Table 8.

Table 8 Measurements of Experimental Data at IVAR

Test	Q_{in} /(kW)	Li /(kW)	N /(rpm)	P_{mean} /(bar)	Th_{in} /(°C)	Th_{out} /(°C)	m_{hot} /(kg/s)
1.	132.94	91.80	600.01	4.506	134.60	136.49	16.81
2.	100.66	70.22	600.72	3.605	134.19	135.68	16.14
3.	133.03	92.54	600.00	3.515	134.58	136.45	16.90
4.	96.14	64.69	550.12	2.801	133.83	135.19	16.92
5.	132.82	90.56	600.00	4.483	134.59	136.45	16.97
6.	100.58	69.33	600.00	3.595	133.96	135.45	16.15

Where, Qin = Heat added to the HP, Li = Motor power consumption, N = Motor rotational speed, P_{mean} = Working mean pressure of HP, Th_{in} = Hot water circulation inlet temperature, Th_{out} = Hot water circulation outlet temperature & m_{hot} = Hot water circulation flow rate.

To review the measurements, the series of measurements is enclosed in Appendices. The HP was operated using helium. For ease of understanding, please refer to the P&ID diagram shown in *Figure 27*.

4.2.2 Data Analysis

Based on the measurements obtained from the HP system, MATLAB simulations were conducted to generate results for comparing theoretical and practical values. However, direct comparisons are not possible due to the inability to measure the internal pressure and temperature of the Stirling machine.

Accordingly, multiple simulations were conducted to compare the results for each series of measurements.

1st Simulation

- The initial MATLAB simulation was performed to determine the cold side temperature of the high-pressure side (TL) by utilizing heat transfer measurements obtained from cold water circulation through a heat exchanger
- The aforementioned simulation was extended to determine the hot side temperature of the high-pressure side (TH) by utilizing heat transfer measurements obtained from hot water circulation through a heat exchanger.
- The simulation - 1 concluded with the determination of the COP for each measurement, followed by plotting COP versus TL and COP versus TH.

2nd Simulation

The second MATLAB simulation was performed to evaluate the performance of each cycle series based on the results of the initial simulation. This analysis specifically focuses on high-pressure and low-pressure cycles. The analysis was based on the following mathematical formulations:

- Scenario 1: When TL, TH, & Li are known then P_{mean} can be determined. The P-V diagram can then be plotted accordingly.

- Scenario 2: When TL, TH, & P_{mean} are known then Li can be determined. The P-V diagram can be plotted accordingly.

3rd Simulation

The third MATLAB simulation uses the calculated TL values from the first simulation, along with the remaining measurements (i.e., Pmean, Li, and N) to determine the TH. Once TH is determined, the P-V diagram can be plotted accordingly. The P-V diagram can be plotted for two scenarios similar to Result 2.

- Scenario 3: When TL, TH, & Li are known then P_{mean} can be determined. The P-V diagram can then be plotted accordingly.
- Scenario 4: When TL, TH, & P_{mean} are known then Li can be determined. The P-V diagram can be plotted accordingly.

4th Simulation

The fourth MATLAB simulation uses only high-pressure condition measurements on He, N_2, and Ar gases, such as TL, Pmean, Li, and N to determine TH. Accordingly, plot the P-V diagram. This analysis focuses on investigating how Stirling machine geometry influences the COP of the cycle.

- Scenario 5: Changing the phase angle of the machine (45°, 90°, 135°, and 180°).
- Scenario 6: Increasing the Stirling machine's swept volume by 10%, 20%, and 30%.
- Scenario 7: Increasing the Stirling machine's regenerator volume by 10%, 20%, and 30%.
- Scenario 8: Increasing the Stirling machine's dead volume by 10%, 20%, and 30%.

5th Simulation

The fifth simulation investigates the impact of higher compression on system performance. This simulation uses high-pressure condition measurements on He, N_2, and Ar gases. The mean pressure is increased by 10%, 20%, and 30%, while TL, Li, and N remain the same to determine TH. Subsequently, the P-V diagram is plotted.

4.3 Justification and explanation of chosen model parameters

4.3.1 Phase Angle

The phase angle in a Stirling engine plays a crucial role in determining its efficiency and performance. It refers to the angular relationship between the piston's position (power piston & displacer piston) and the corresponding pressure and volume within the engine's working space. This phase angle is vital for optimizing the engine's thermodynamic cycle, as it influences the timing of key events, such as the intake and expulsion of working fluid, compression, and expansion. Properly controlling the phase angle ensures that these processes are synchronized to maximize power output and minimize energy losses, ultimately leading to improved overall efficiency. it a fundamental parameter in the design and volume variation of compression and expansion due to phase angle. The variations in compression and expansion volumes of the IVAR Stirling machine for different phase angles are shown in *Figure 22*.

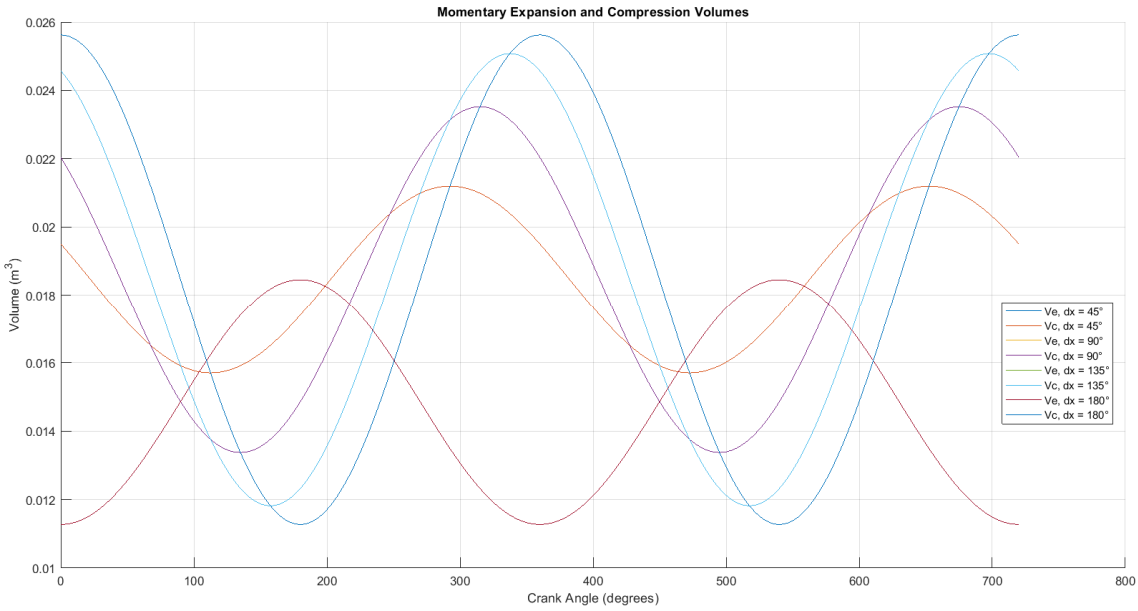

Figure 22 Volume Variation of Compression and Expansion at Different Phase Angles

According to the design and development of the IVAR Stirling machine HP, with consideration of geometry and other design parameters, the optimal phase angle for the machine configuration is 90 degrees, and its volume variations are shown in *Figure 23.*

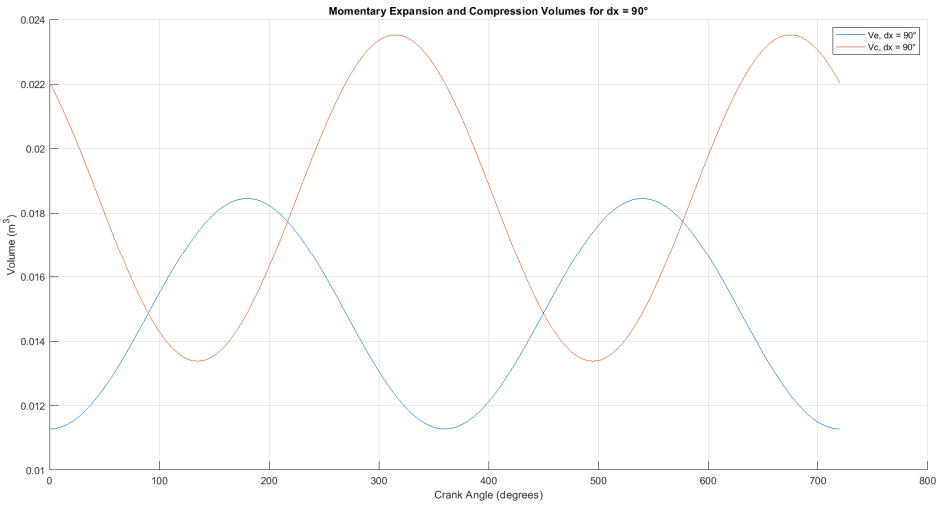

Figure 23 Volume Variation of Compression and Expansion at 90 Degree Phase Angles

4.3.2 Thermodynamic Properties of Helium, Argon, Nitrogen, and Water in HP Simulation

The thermodynamic properties of helium, argon, nitrogen, and water were critically analyzed and incorporated into the simulation to ensure a precise depiction of their behaviors under varying operational conditions within the Stirling HP system. Helium, argon, and nitrogen were chosen as refrigerants due to their unique thermophysical characteristics, which significantly influence the efficiency and performance of the HP. Additionally, water properties were meticulously integrated to accurately model the heat exchange processes within the secondary circulation loops on both the hot and cold sides of the system. By employing these specific thermodynamic properties, the simulation aims to optimize the overall performance of the Stirling machine HP, offering valuable insights into the efficiency, feasibility, and comparative benefits of utilizing different refrigerants alongside water-based secondary circulation systems. These property values were taken from the REFPROP software.

Table 9 The Properties of Circulating Water on the Cold Side

T /(°C)	P /(bar)	ρ /(kg/m^3)	μ /(Pa.s)	K /(W/m.K)	Cv /(kJ/kg.K)	Cp /(kJ/kg.K)	Cp/Cv
28.6	1	996.06	0.00082482	0.61225	4.1230	4.1801	1.0138

Table 10 The Properties of Recirculating Water on the Hot Side

T /(°C)	P /(bar)	ρ /(kg/m^3)	μ /(Pa.s)	K /(W/m.K)	Cv /(kJ/kg.K)	Cp /(kJ/kg.K)	Cp/Cv
135.1	4.5	930.52	0.00021961	0.68296	3.5924	4.2715	1.1890

Where, T = temperature, P = Pressure, ρ = density, μ = dynamic viscosity, K = thermal conductivity, C_V = Specific Heat at Constant Volume, C_P=Specific Heat at Constant Pressure, & C_P/C_V = Ratio of Specific Heats or Gamma(γ).

Table 11 The Flow Rates and Sizes of Secondary Water Circulation Pipelines

Secondary water circulation	Pipe size (ID)/ m	Flow rate/ (kg/s)
Cold water	0.1047496	13.5
Hot water	0.1047496	16.5

On the test day at the testing facility, the average temperature of the cold water supply was 28.6°C.

4.3.3 Assessment of instrumentation accuracy and limitations

The Stirling machine HP operates as a fully closed system. Due to the system's design and the internal working pressures and temperatures, it is not possible to directly measure the internal pressure and temperature within the compression and expansion cylinders, as well as the cold and hot sides of the heat exchanger. However, a mitigation method involves measuring the surface temperature by inserting a probe into the cylinder to a safe depth for temperature measurement. The thermocouple installation on the compression cylinder is shown in *Figure 24*.

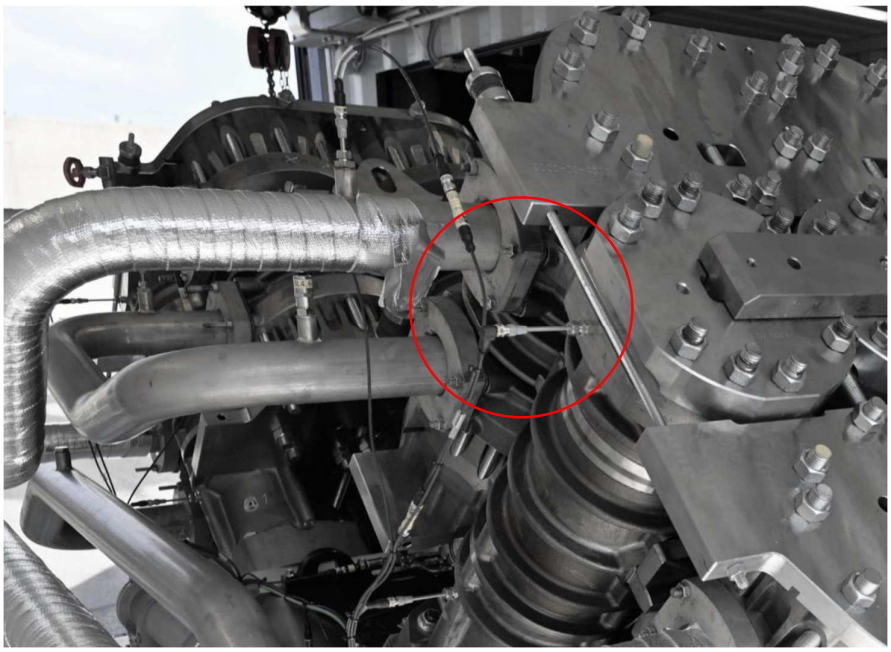

Figure 24 The Thermocouple Installation on the Compression Cylinder

The measurements of the system temperatures and pressures at the specified locations, as shown in *Figure 25*, were recorded using transmitters. These transmitters operate continuously, recording data 24 hours a day, 7 days a week. However, this continuous operation can lead to inaccuracies in the pressure and temperature records of the HP system. These types of errors can be minimized, and in some cases, overcome by following certain procedures, which are discussed in the recommendations in Chapter 0.

4.4 Simplified simulation model for the HP system

In the course of this thesis, the simulation of a Stirling machine HP was originally intended to be modeled in its entirety using MATLAB. However, due to the inherent complexity and the numerous variables involved in accurately representing the full setup, it became evident that a direct and comprehensive modeling approach would be exceedingly complex and computationally demanding. To mitigate these challenges and ensure the feasibility of the simulation, a decision was made to adopt a simplified model of the Stirling machine HP. This simplified model retains the core physical principles and essential dynamics of the original setup while reducing the computational overhead and complexity. By focusing on the fundamental aspects, this approach allows for a more manageable and efficient simulation process, facilitating a clearer analysis and understanding of the HP's performance characteristics within the MATLAB environment.

Enerin As uses the Sage simulation tool for research and development. Sage, a simulation program developed by David Gedeon and first launched in 1995, offers a robust platform for modeling and optimizing Stirling processes. This makes it highly relevant for the study of reversed Stirling cycle HPs. Its unique classified three-structure design for model components facilitates an in-depth understanding and detailed analysis of Stirling engines. At the top level, the parent components provide a comprehensive overview of the engine's integration, offering a macroscopic perspective on its functioning.

In academic work, computational simulations commonly utilize tools such as MATLAB or Scilab. Additionally, process simulation tools like Nexsys (a Rust-based equation-solving program), pyENL (Python "Ecuaciones No Lineales"), and EES (Engineering Equation Solver) are viable options. These applications provide comprehensive libraries containing thermodynamic data for various fluids, an advantage over MATLAB or Scilab, where thermodynamic properties must be input manually. These properties can be found in the REFPROP thermodynamic database tool. Developing a simulation program from scratch is a

difficult task that requires extensive model verification. Conversely, using existing simulation programs and adapting them to a specific system is more straightforward and likely includes models already validated in terms of thermodynamic principles and transient behavior.

The complex thermodynamic cycles of Stirling machine HPs pose a challenge for detailed analysis and optimization. Simplified models are essential to enable designers to effectively design, analyze, and optimize these systems. This thesis presents a simplified model developed in MATLAB, a widely-used engineering simulation tool. The model is based on a set of assumptions and simplifications derived from Schmidt's Theory, as discussed in Schmidt Analysis Chapter 3.3. It models key aspects of the Stirling cycle, including compression, expansion, regenerative heating, and cooling, using a series of algebraic and differential equations. The simplifications for the model include assuming ideal gas behavior, perfect regeneration, and isothermal compression and expansion processes. The MATLAB simulation environment is utilized for its robust numerical solvers and its ease of integration with various input parameters and boundary conditions. The model allows for adjustments in key design parameters, such as temperature ratios, volume ratios, dead volume, and phase angle, enabling exploration of their impacts on system performance.

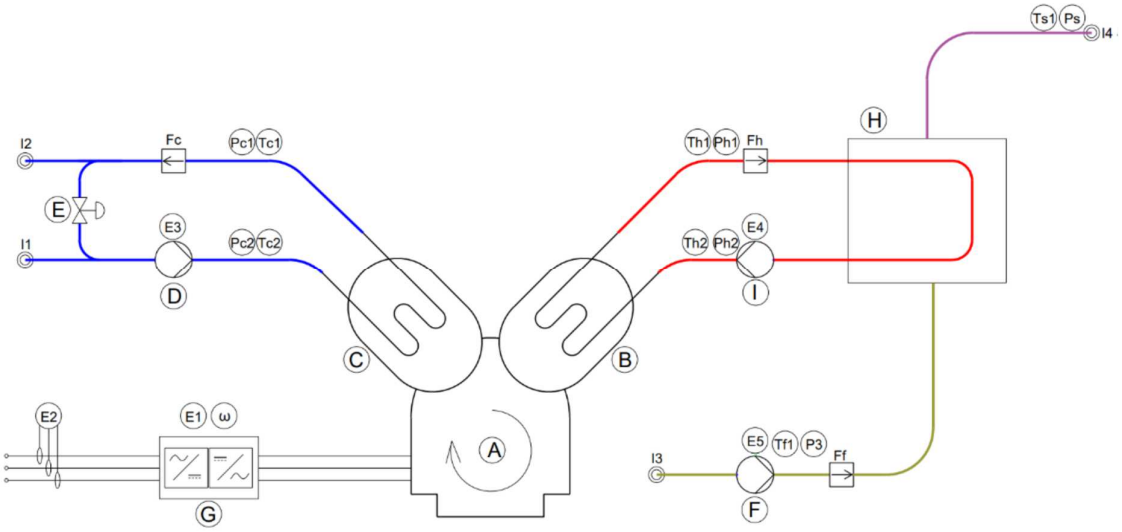

Figure 25 Simplified Approach of the HoegTemp HP

Based on the simplified diagram shown in *Figure 25*, measurements were taken, and calculations were carried out using a simulation model in MATLAB.

- A-Stirling machine HP
- B-Hot side heat exchanger
- C-Cold side heat exchanger
- C-Cold side circulation pump
- E-Bypass control valve
- F-Water-Steam line pump
- G-Three phase electric motor coupled with HP
- H-Steam generator
- I-Hot side circulation pump

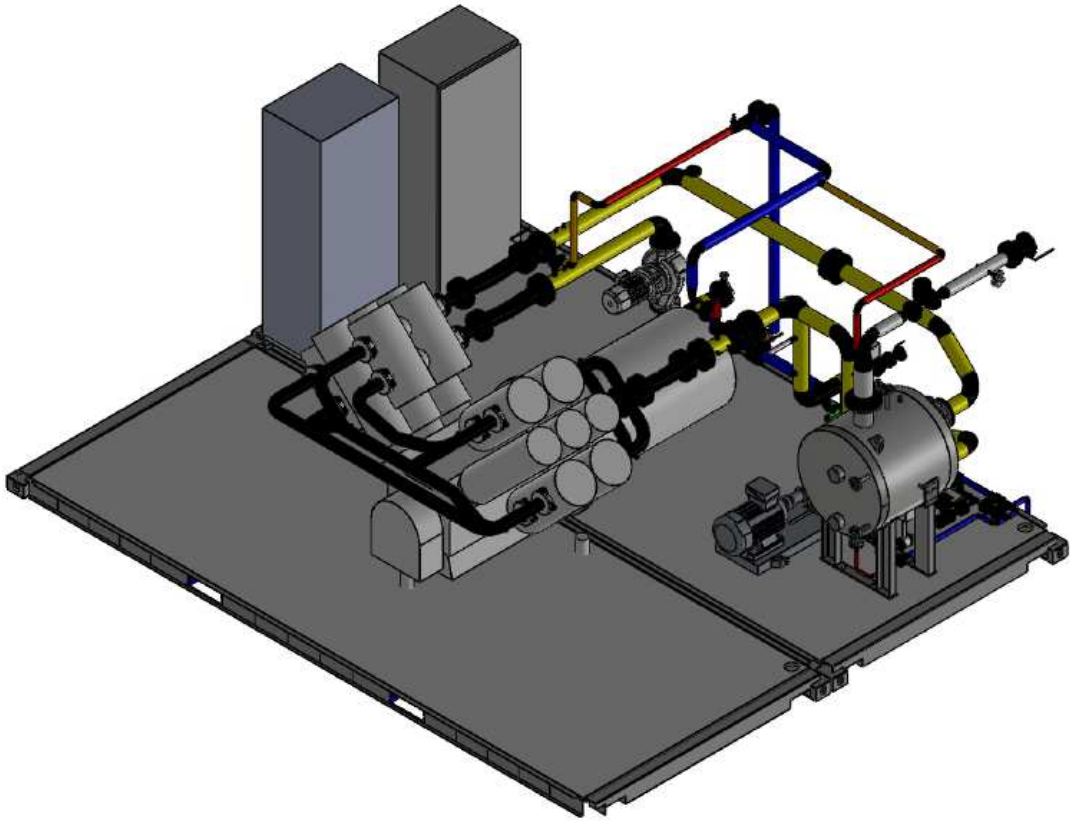

Figure 26 3D representation of HoegTemp HP installation at IVAR

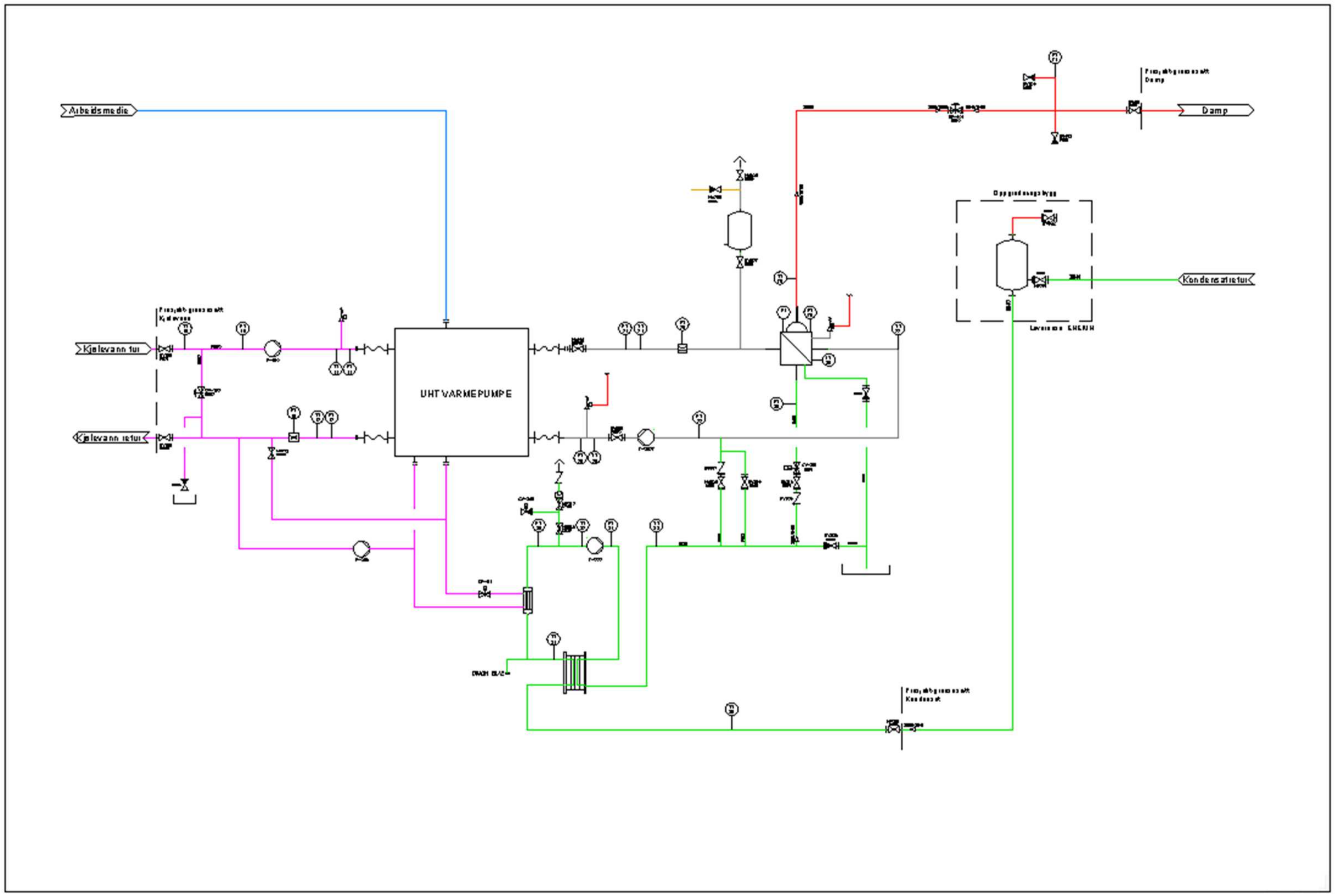

Figure 27 P&ID of HoegTemp installation with steam generating unit at IVAR

Chapter 5 Results

5.1 Comparison of Theoretical and Experimental Data

5.1.1 Results – 1

Based on simulation-1, TL, TH, and COP of the HP were calculated for all six sets of measurements, and the variation of COP with TL and TH was plotted separately for all three gases.

Table 12 Simulation – 1; Results for TL, TH, and COP of the HP

Test	P /(bar)	Li /(kW)	TL /(°C)	TH /(°C)	COP
1.	4.506	91.80	25.10	143.25	3.52
2.	3.605	70.22	25.95	140.96	3.60
3.	3.515	92.54	25.10	143.15	3.53
4.	2.801	64.69	26.07	140.06	3.62
5.	4.483	90.56	25.10	143.12	3.53
6.	3.595	69.33	25.95	140.73	3.61

Where, P – Mean pressure, Li - Power consumption, N - Motor speed, TL - HP cold side temperature, TH - HP hot side temperature, & COP – Coefficient of performance.

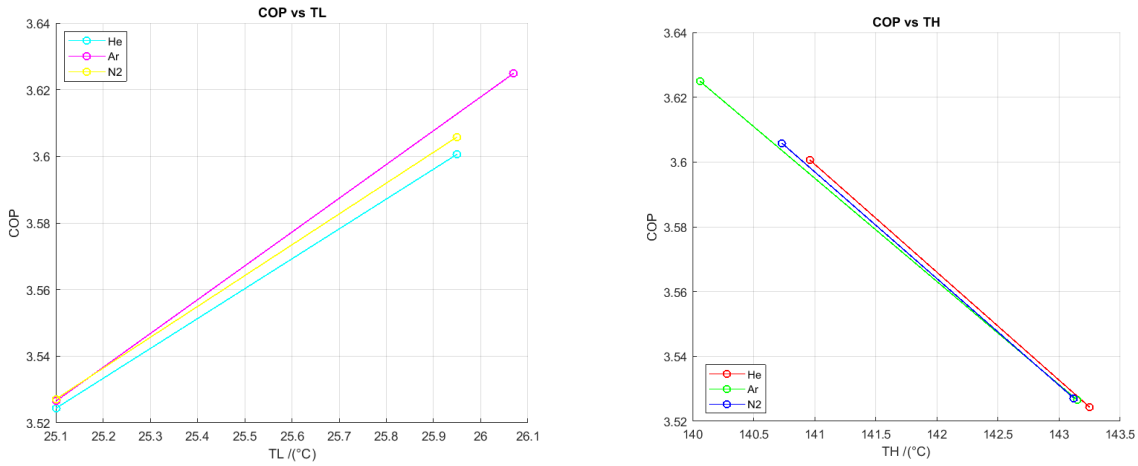

Figure 28 COP vs TL(Left), COP vs TH(Right) for 1st Simulation Results

Results – 2

Based on the resutls - 1, there are two possibilities for the Pressure-Volume diagram for each cycle:

1. If TL, TH, & Li are known then Pmean can be determined.

2. If TL, TH, & Pmean are known then Li can be determined.

Scenario 1: If P_{mean} is unknown, it was calculated through simulation – 2 scenario - 1 for all sets of measurements and tabulated below. Accordingly, the P-V diagram was plotted.

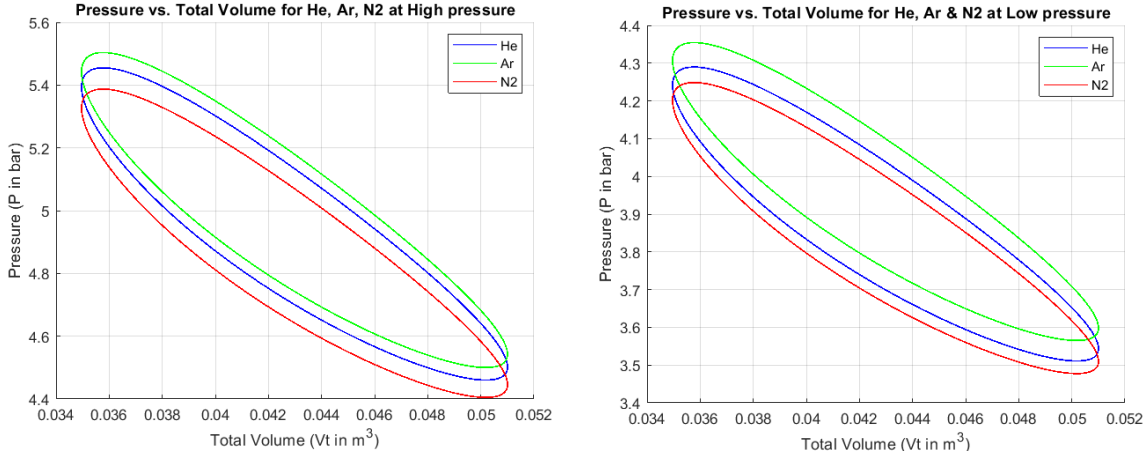

Figure 29 P-V Diagram for simulation – 2 scenario - 1, high pressure (left) & low pressure(right)

Table 13 Simulation-2 Results for Mean Pressure under Test Conditions

Test	TL /(°C)	TH /(°C)	Li /(kW)	P /(bar)
1.	25.10	143.25	91.80	4.93
2.	25.95	140.96	70.22	3.88
3.	25.10	143.15	92.54	4.98
4.	26.07	140.06	64.69	3.94
5.	25.10	143.12	90.56	4.87
6.	25.95	140.73	69.33	3.84

Where, TL - HP cold side temperature, TH - HP hot side temperature, Li - Power consumption. & P – Mean pressure.

Scenario 2: If Li unknown, it was calculated through simulation – 2 scenario - 2 for all sets of measurements and tabulated below. Accordingly, the P-V diagram was plotted.

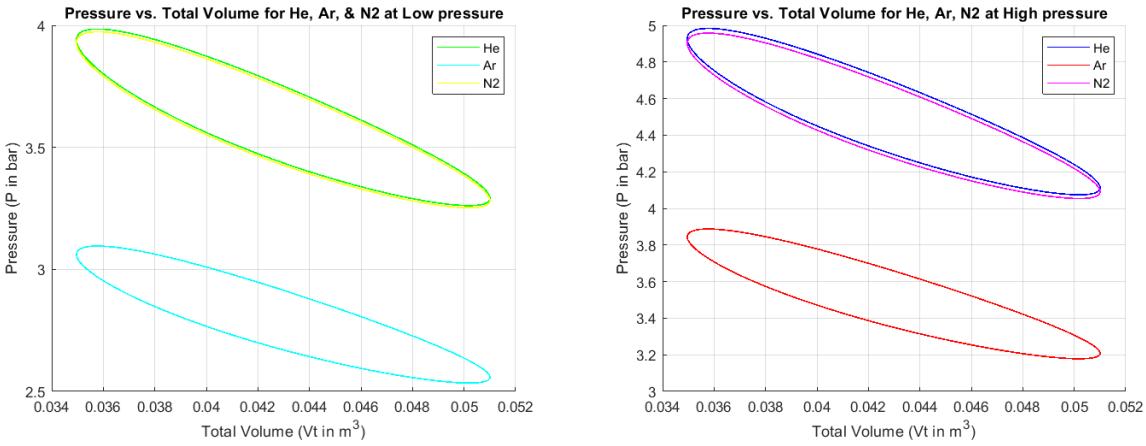

Figure 30 P-V Diagram for simulation – 2 scenario - 2, high pressure (right) & low pressure(left)

Table 14 Simulation-2 Results for Motor Power under Test Conditions

Test	TL /(°C)	TH /(°C)	P /(bar)	Li /(kW)
1.	25.10	143.25	4.51	83.86
2.	25.95	140.96	3.60	65.23
3.	25.10	143.15	3.52	65.36
4.	26.07	140.06	2.80	45.99
5.	25.10	143.12	4.48	83.34
6.	25.95	140.73	3.60	64.84

Where, TL - HP cold side temperature, TH - HP hot side temperature, P – Mean pressure, & Li - Power consumption.

5.1.2 Results – 3

The third results were tabulated from simulation – 3, TH, and COP of the HP were calculated for all six sets of measurements, and the variation of COP with TL and TH was plotted separately for all three gases.

Table 15 Simulation-3 Results for TH & COP under Test Conditions

Test	P /(bar)	Li /(kW)	N /(rpm)	TL /(°C)	TH /(°C)	COP
1.	4.506	91.80	600.01	25.10	154.62	3.30
2.	3.605	70.22	600.72	25.95	149.90	3.41
3.	3.515	92.54	600.00	25.10	193.46	2.77
4.	2.801	64.69	550.12	26.07	187.48	2.85
5.	4.483	90.56	600.00	25.10	153.51	3.32
6.	3.595	69.33	600.00	25.95	148.80	3.43

Where, P – Pressure, Li - Power consumption, N - Motor speed, TL - HP cold side temperature, TH - HP hot side temperature, & COP – Coefficient of performance.

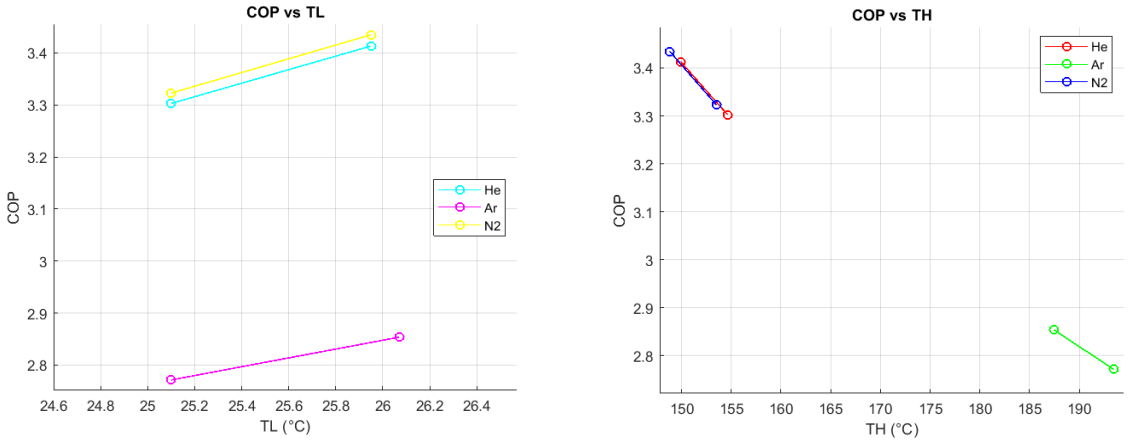

Figure 31 COP vs TL(Left), COP vs TH(Right) for 3rd Simulation Results

Results – 4

From Results - 3, there are two possibilities for the Pressure-Volume diagram for each cycle, similar to Results - 2.

Scenario 3: If P_{mean} is unknown, it was calculated through simulation – 3 scenario - 3 for all sets of measurements and tabulated below. Accordingly, the P-V diagram was plotted.

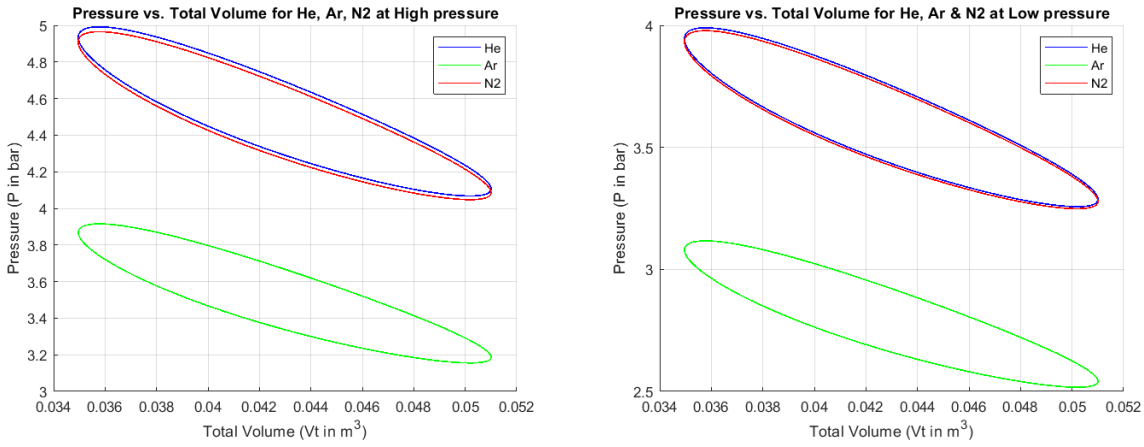

Figure 32 P-V Diagram for simulation – 3 scenario - 3, high pressure (right) & low pressure(left)

Table 16 Simulation-3 Results for Mean Pressure under Test Conditions

Test	TL /(°C)	TH /(°C)	Li /(kW)	P /(bar)
1.	25.10	154.62	91.80	4.51
2.	25.95	149.90	70.22	3.61
3.	25.10	193.46	92.54	3.52
4.	26.07	187.48	64.69	2.80
5.	25.10	153.51	90.56	4.48
6.	25.95	148.80	69.33	3.60

Where, TL - HP cold side temperature, TH - HP hot side temperature, Li - Power consumption. & P – Mean pressure.

Scenario 4: If Li unknown, it was calculated through simulation – 3 scenario - 4 for all sets of measurements and tabulated below. Accordingly, the P-V diagram was plotted.

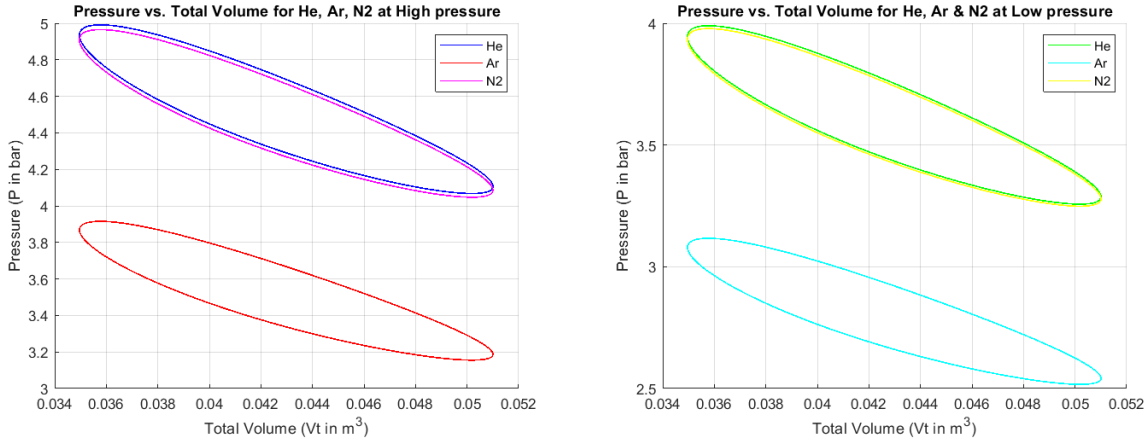

Figure 33 P-V Diagram for simulation – 3 scenario - 4, high pressure (right) & low pressure(left)

Table 17 Simulation-3 Results for Motor Power under Test Conditions

Test	TL /(°C)	TH /(°C)	P /(bar)	Li /(kW)
1.	25.10	154.62	4.51	91.80
2.	25.95	149.90	3.60	70.22
3.	25.10	193.46	3.52	92.54
4.	26.07	187.48	2.80	64.69
5.	25.10	153.51	4.48	90.56
6.	25.95	148.80	3.60	69.33

Where, TL - HP cold side temperature, TH - HP hot side temperature, P – Mean pressure, & Li - Power consumption.

5.1.3 Results – 5

The HP TH deviations compared all six sets of measurements from Results – 1 & Results – 3 and tabulated below,

Table 18 TH Deviations between Results - 1 and Results - 3

Test	TH_1 /(°C)	TH_2 /(°C)	TH difference /(°C)	TH deviation /(%)
1	143.25	154.62	11.70	7.9
2	140.96	149.90	08.94	6.3
3	143.15	193.46	50.31	35.1
4	140.06	187.48	47.42	33.9
5	143.12	153.51	10.39	7.3
6	140.73	148.80	08.07	5.7

Where, TH- HP hot side temperature, TH_1- HP hot side temperature from results-1 & TH_2- HP hot side temperature from results-3.

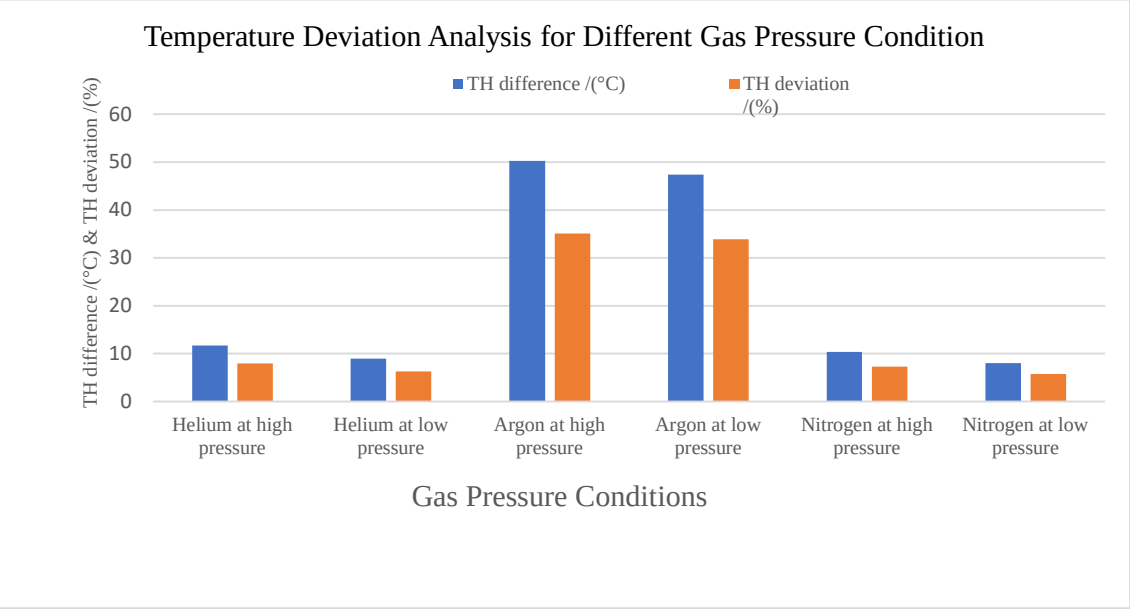

Figure 34 Temperature Deviation Analysis for Different Gas Pressure Condition

5.2 Effects of Working Fluid Properties on Cycle Performance.

The HoegTemp HP at IVAR is set to operate from -10°C to a high temperature of up to 200°C for testing on a pilot installation. Although it is capable of reaching up to 250°C, the system will not be operated at this higher temperature until testing is complete. Additionally, the design mean pressure of this HP is 5 bar. Due to this, working fluid properties influence analyses limit to, temperature between -10°C to 200°C and Pressure 1 to 10 bar.

The analysis involves examining the variation of gas properties at constant pressures ranging from 1 to 10 bar in 1-bar increments, across a temperature range from -10°C to 200°C. Similarly, the properties are analyzed at constant temperatures ranging from -10°C to 200°C in 10°C increments. This dual approach ensures a comprehensive understanding of how the thermodynamic and transport properties of the gases vary under different thermal and pressure conditions.

The initial phase of the analysis focuses on the fundamental thermodynamic properties: Density, Specific Heat at Constant Volume (Cv), Specific Heat at Constant Pressure (Cp), and the Cp/Cv ratio. These properties provide a critical baseline understanding of gas behavior under varying temperature and pressure conditions. Density is a primary property that directly influences other thermodynamic properties and serves as a fundamental parameter for understanding gas behavior. Cv and Cp are essential in determining the amount of energy required to raise the temperature of a gas at constant volume and constant pressure, respectively. These specific heats are vital for calculating the internal energy and enthalpy changes in thermodynamic processes. The ratio of Cp to Cv, known as the gamma (γ), is crucial for understanding the efficiency of thermodynamic cycles and the behavior of gases during adiabatic processes. By analyzing these properties first, we establish a foundational understanding of the thermodynamic characteristics of Helium, Nitrogen, and Argon, which is essential for interpreting subsequent analyses.

The variations in the density of He, N_2, and Ar with pressure at different temperatures are shown in *Figure 35.*

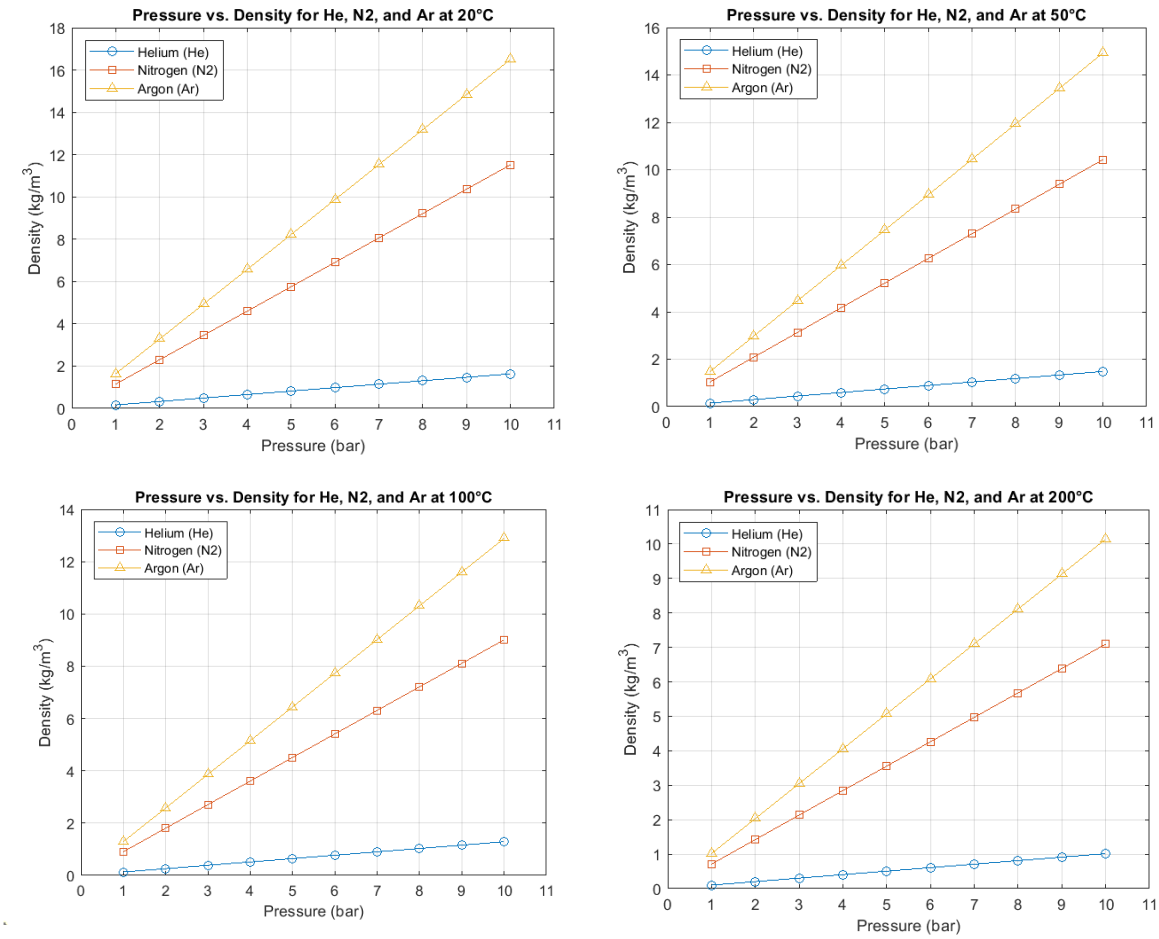

Figure 35 Pressure vs Density for He, N_2 & Ar, at 20°C(Left top), at 50°C(Right top), at 100°C(Left bottom), & at 200°C(Right bottom)

The variations trend of He, N_2, and Ar densities with temperature under specified pressure conditions are shown in *Figure 36 & Figure 37*

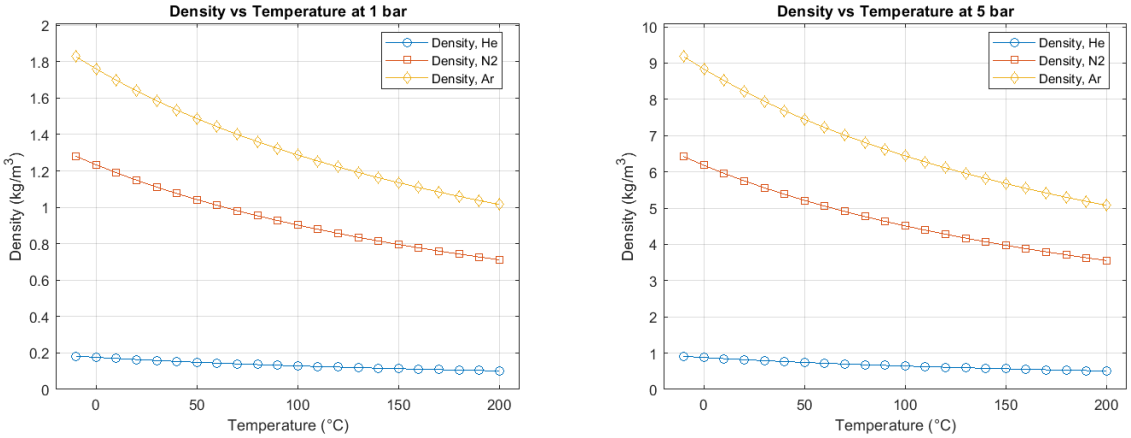

Figure 36 Temperature vs Density for He, N_2 & Ar, at 1 bar(Left) & 5 bar(Right)

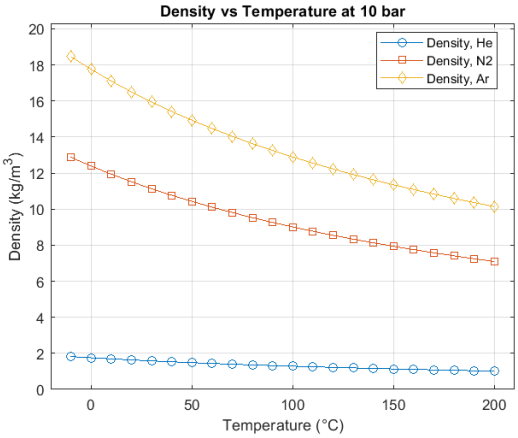

Figure 37 Temperature vs Density for He, N_2 & Ar, at 10 bar

The variations in the specific heat capacity at constant volume (C_V) of He, N_2, and Ar with pressure at different temperatures are shown in *Figure 38*.

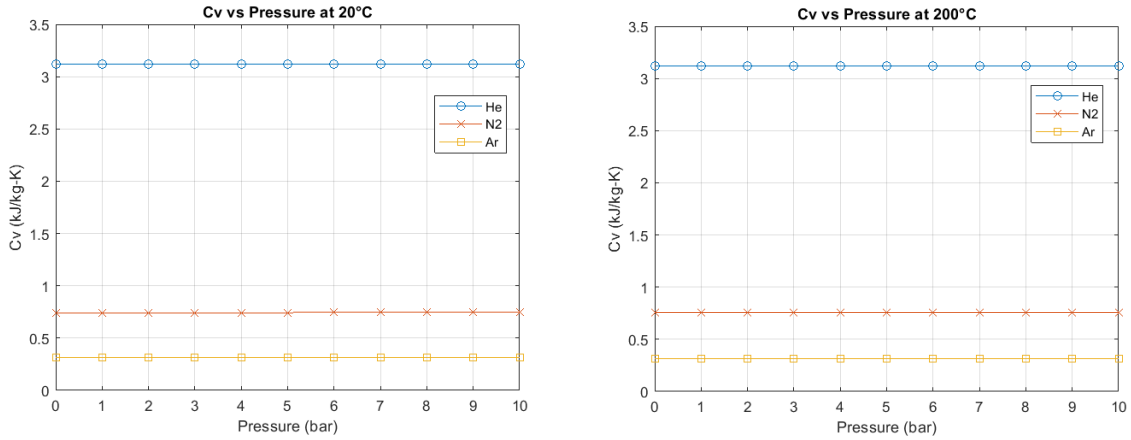

Figure 38 Pressure vs C_V for He, N_2 & Ar, at 20°C(Left) & 200°C(Right)

The variations in the specific heat capacities at constant volume (Cv) of He, N_2, and Ar with temperature under specified pressure conditions are shown in *Figure 39*.

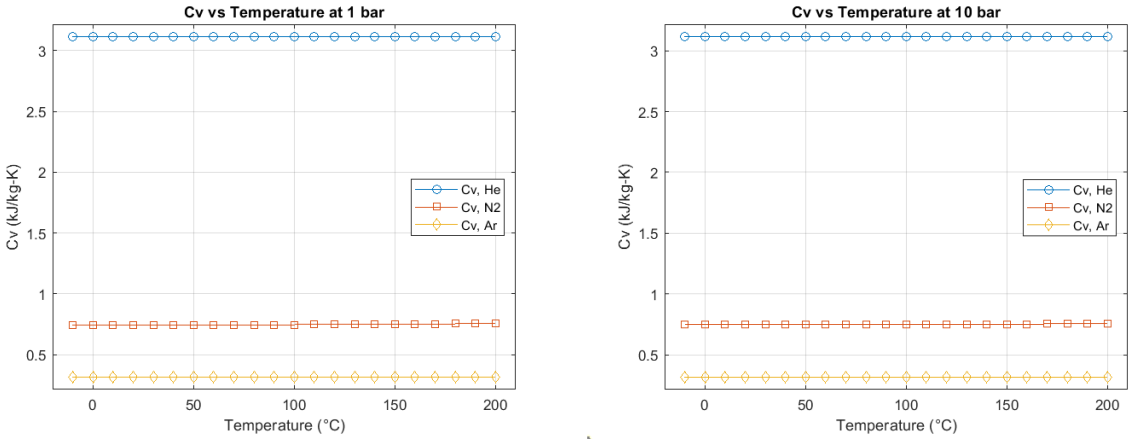

Figure 39 Temperature vs C_V for He, N_2 & Ar, at 1 bar(Left) & 10 bar(Right)

The variations in the specific heat capacity at constant pressure (C_P) of He, N_2, and Ar with pressure at different temperatures are shown in *Figure 40*.

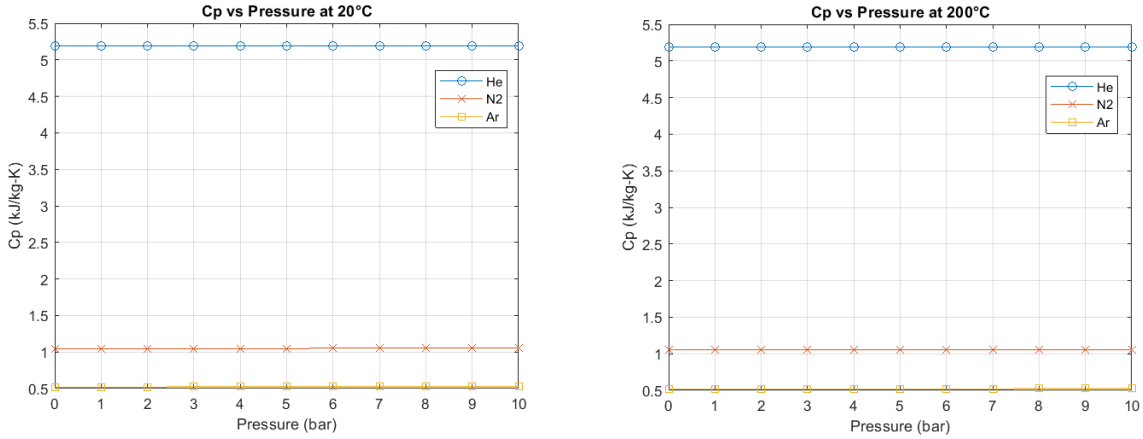

Figure 40 Pressure vs C_P for He, N_2 & Ar at 20°C(Left) & 200°C(Right)

The variations in the specific heat capacity at constant pressure (Cp) of He, N_2, and Ar with temperature under specified pressure conditions are shown in *Figure 41*.

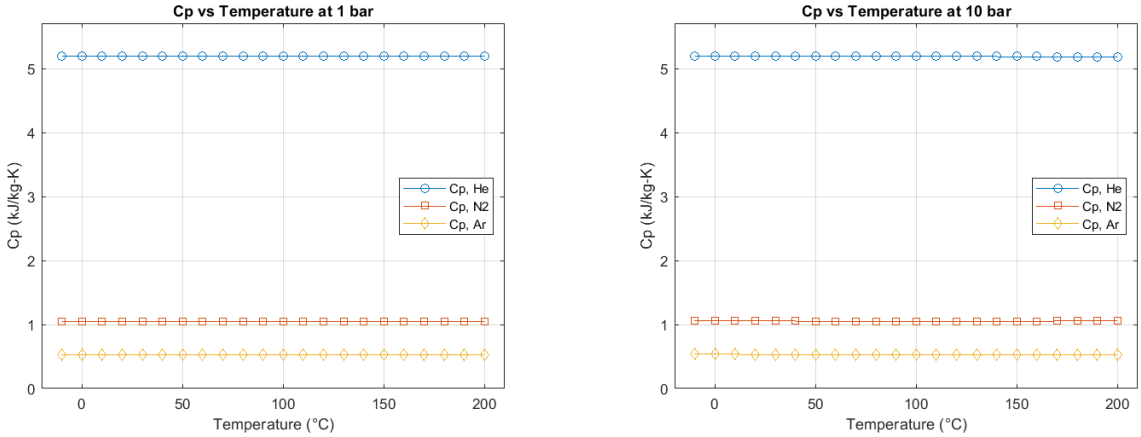

Figure 41 Temperature vs C_P for He, N_2 & Ar at 1 bar(Left) & 10 bar(Right)

The variations in the Cp/Cv of He, N_2, and Ar with pressure at different temperatures are shown in *Figure 42 &* Figure 43.

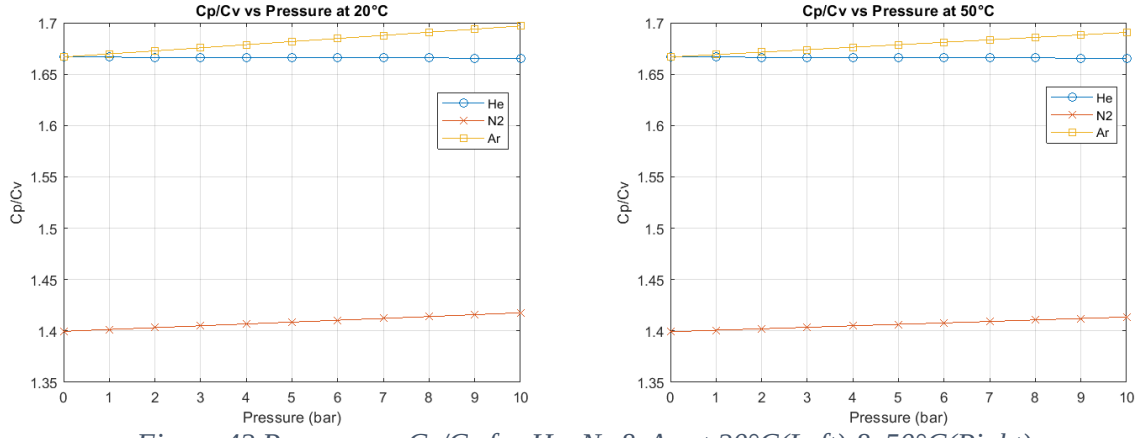

Figure 42 Pressure vs C_P/C_V for He, N_2 & Ar at 20°C(Left) & 50°C(Right)

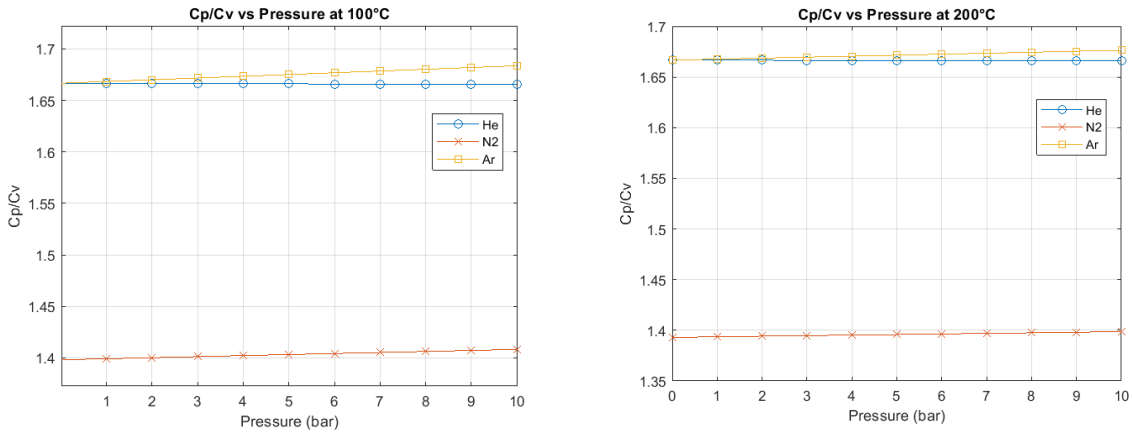

Figure 43 Pressure vs C_P/C_V for He, N_2 & Ar at 100°C(Left) & 200°C(Right)

The variations in the Cp/Cv of He, N_2, and Ar with temperature under specified pressure conditions are shown in *Figure 44*.

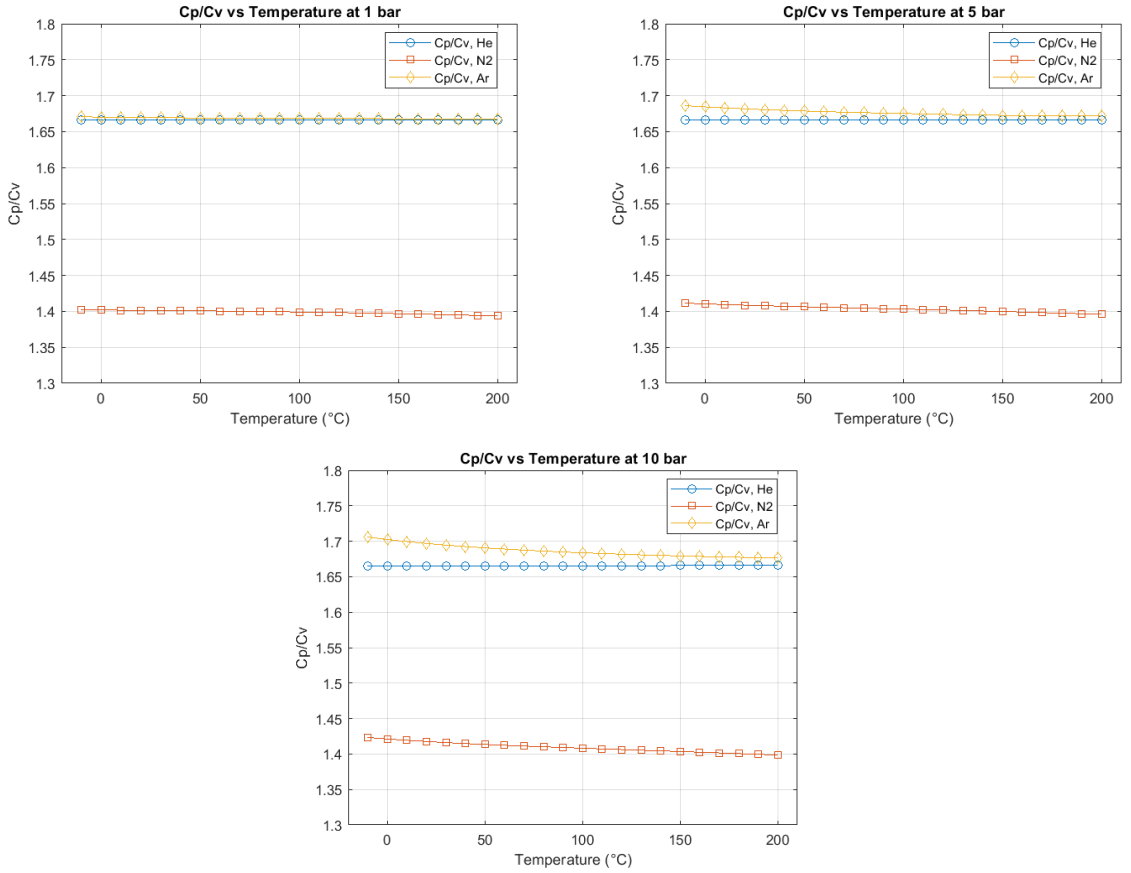

Figure 44 Temperature vs C_P/C_V for He, N_2 & Ar at 1 bar(Top left), 5 bar(Top right) & 10 bar(Bottom)

Following the analysis of fundamental thermodynamic properties, the next step is to examine the sound speed in the gases. Sound speed, which is influenced by the thermodynamic properties of the gas, provides a crucial link between these properties and the acoustical characteristics of the gases. It is determined by both the density and Cp/Cv ratio and offers insights into how quickly pressure waves propagate through the medium. Understanding the sound speed in Helium, Nitrogen, and Argon under varying temperature and pressure conditions is essential for applications involving acoustic wave propagation, such as in thermodynamic cycles and material science. The subsequent analysis of thermal conductivity and viscosity investigates into the heat and momentum transfer capabilities of the gases. Thermal conductivity measures a gas's ability to conduct heat, which is vital for applications in heat exchanger design and thermal management systems. Viscosity, on the other hand, indicates the internal friction within the gas, affecting fluid flow and aerodynamic properties. Together, these properties are crucial for comprehending how energy and momentum are transferred within the gases. By sequentially analyzing these properties, gives clear picture of how Helium, Nitrogen, and Argon behave under different thermal and mechanical conditions, bridging the gap between static thermodynamic properties and dynamic transport phenomena.

The variations in the sound speed of He, N_2, and Ar with pressure at different temperature level are shown in *Figure 45 & Figure 46.*

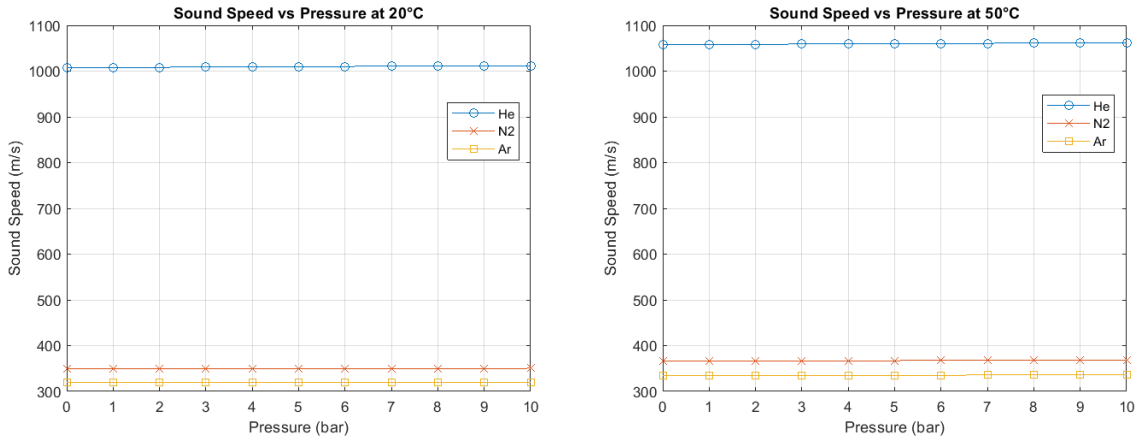

Figure 45 Pressure vs Sound speed for He, N_2 & Ar, at 20°C(Left) & 50°C(Right)

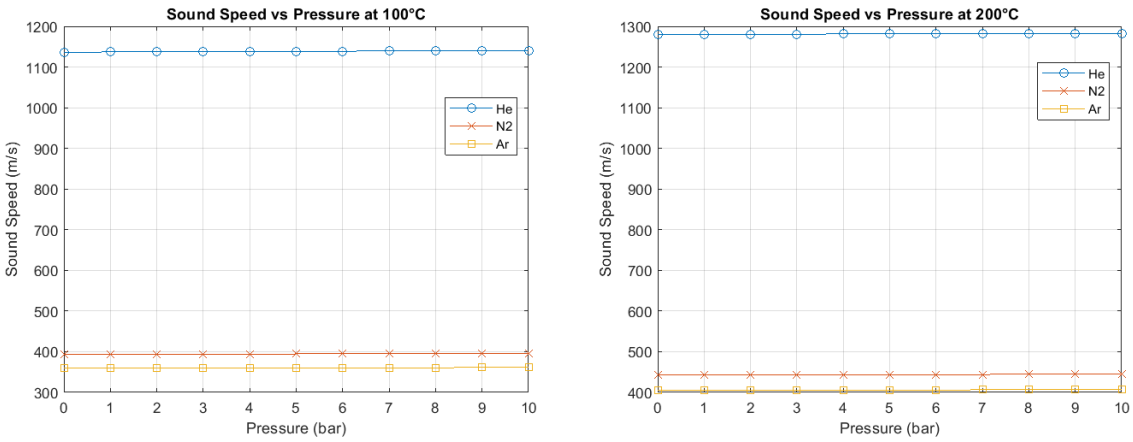

Figure 46 Pressure vs Sound speed for He, N_2 & Ar, at 100°C(Left) & 200°C(Right)

The variations in the sound speed of He, N_2, and Ar with temperature under specified pressure conditions are shown in *Figure 47*.

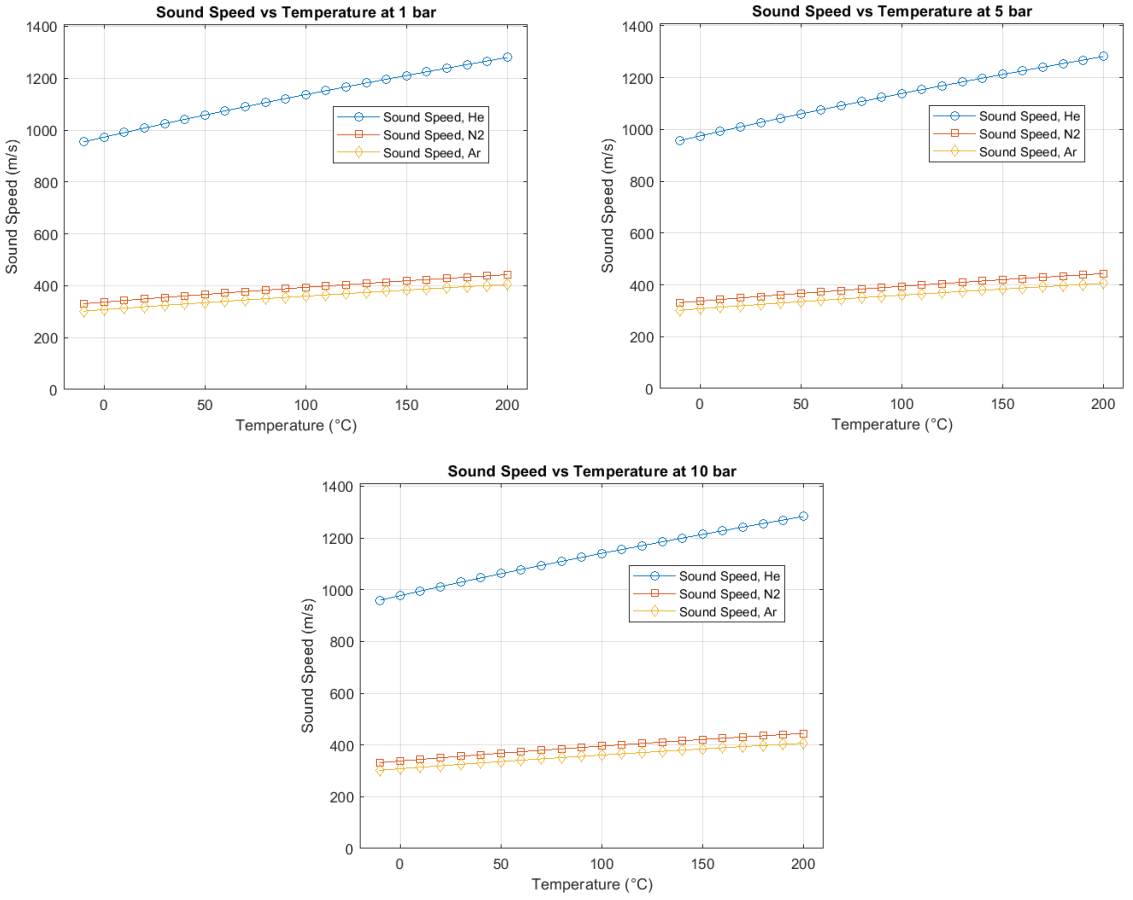

Figure 47 Temperature vs Sound speed for He, N_2 & Ar, at 1 bar(Top left), 5 bar(Top right) & 10 bar(Bottom)

The variations in the thermal conductivity of He, N_2, and Ar with pressure at different temperature level are shown in *Figure 48*.

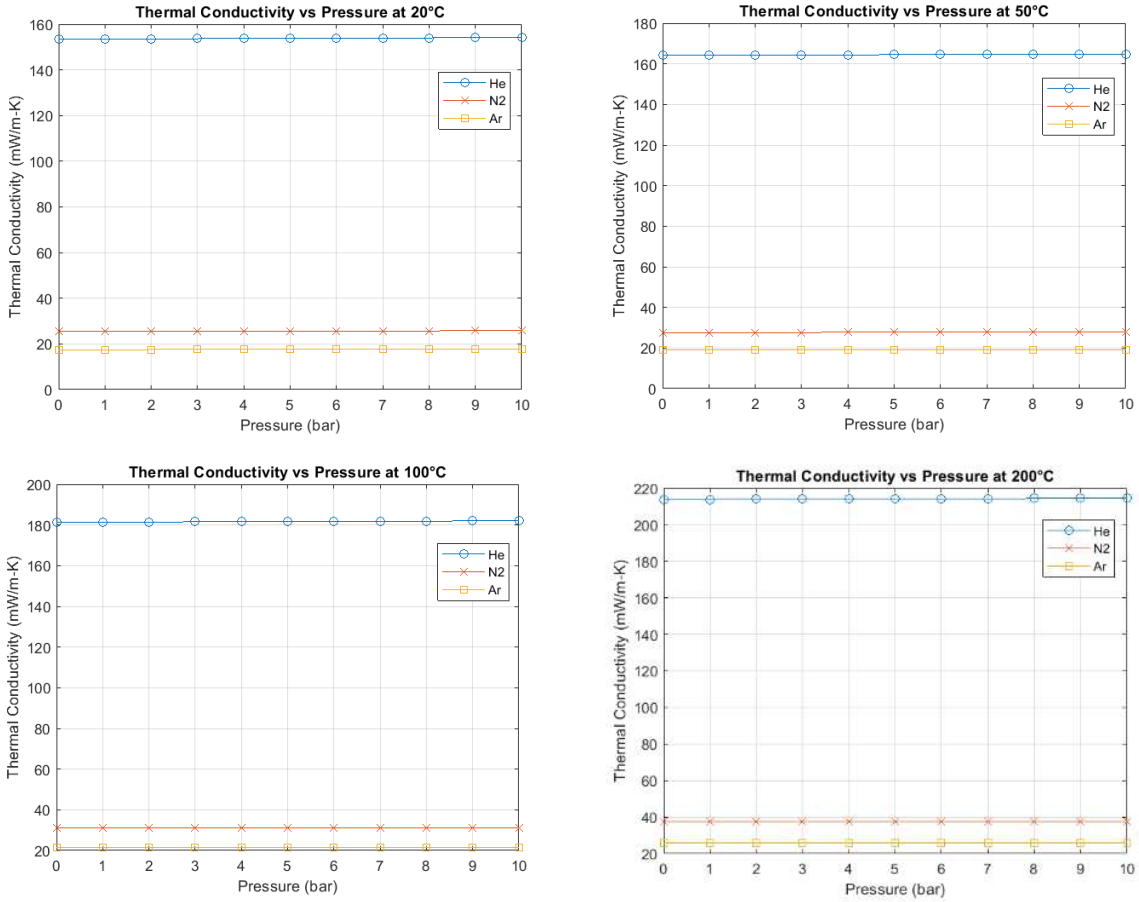

Figure 48 Pressure vs Thermal conductivity for He, N_2 & Ar at 20°C(Top left), 50°C(Top right), 100°C(Bottom left) & 200°C(Bottom right)

The variations in the thermal conductivity of He, N_2, and Ar with temperature under specified pressure conditions are shown in *Figure 49 & Figure 50.*

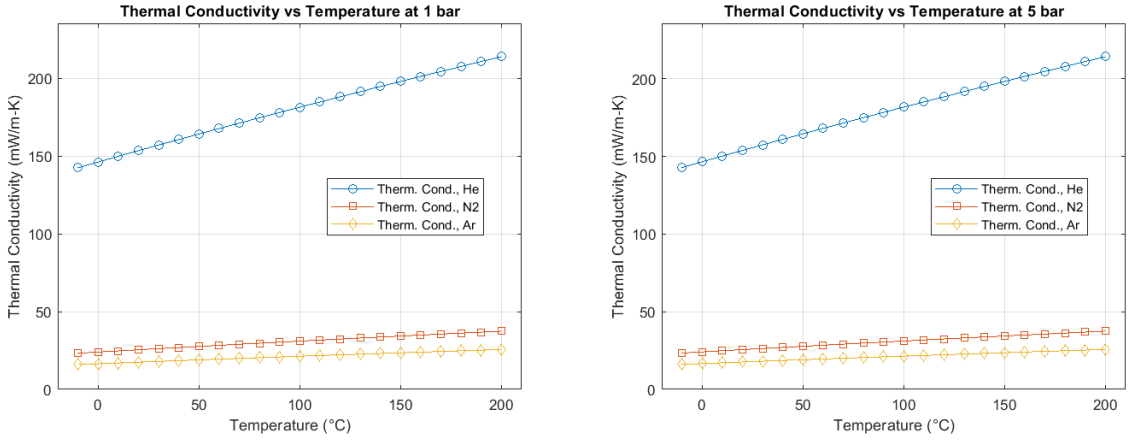

Figure 49 Temperature vs Thermal conductivity for He, N_2 & Ar at 1 bar(Left) & 5 bar(Right)

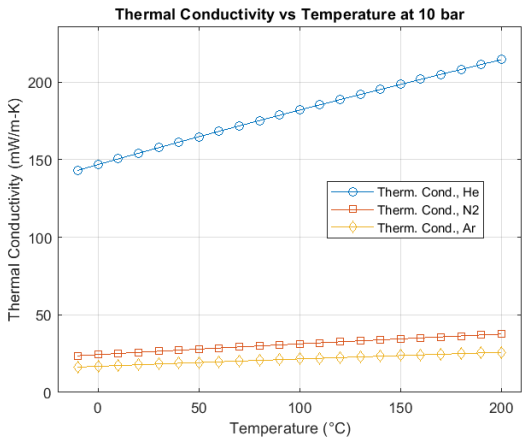

Figure 50 Temperature vs Thermal conductivity for He, N_2 & Ar at 10 bar

The variations in the viscosity of He, N_2, and Ar with pressure at different temperature level are shown in *Figure 51*.

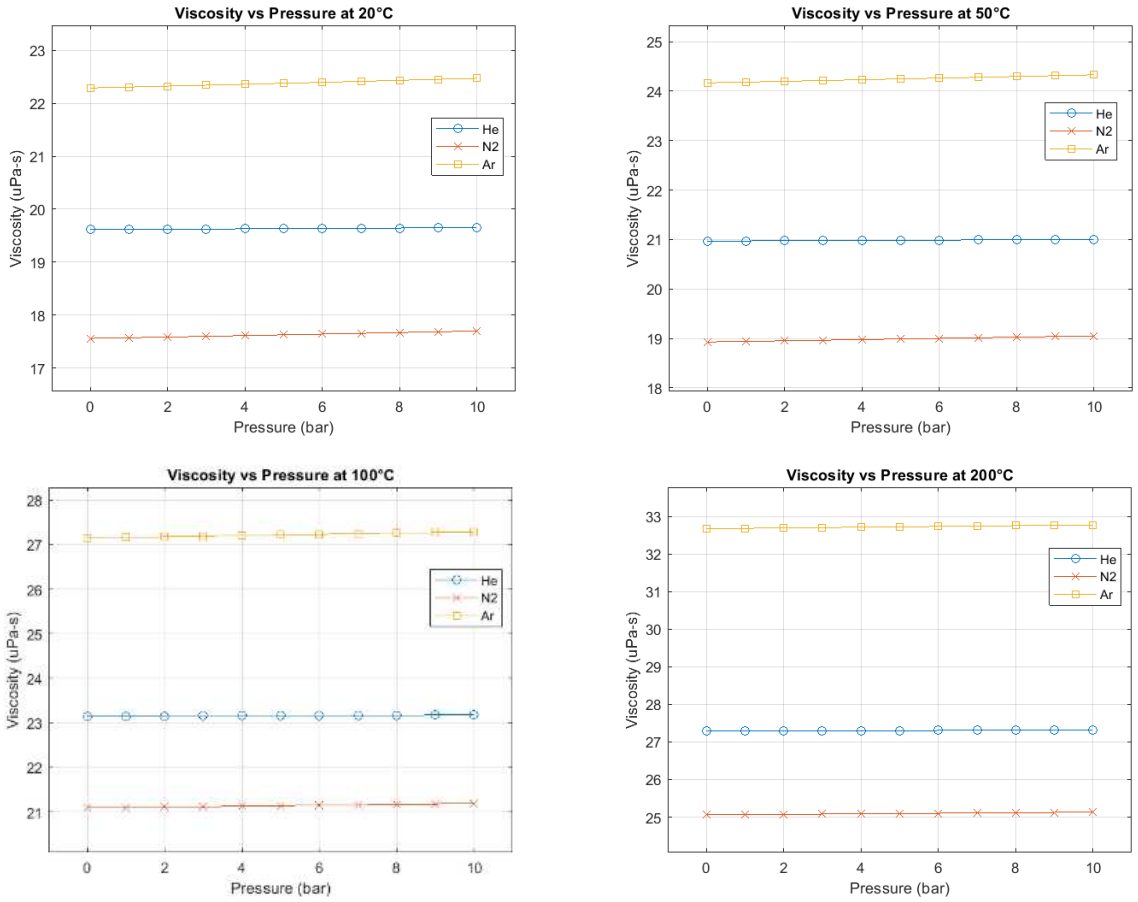

Figure 51 Pressure vs Viscosity for He, N_2 & Ar at 20°C(Top left), 50°C(Top right), 100°C(Bottom right) & 200°C(Bottom right)

The variations in the viscosity of He, N_2, and Ar with temperature under specified pressure conditions are shown in *Figure 52*.

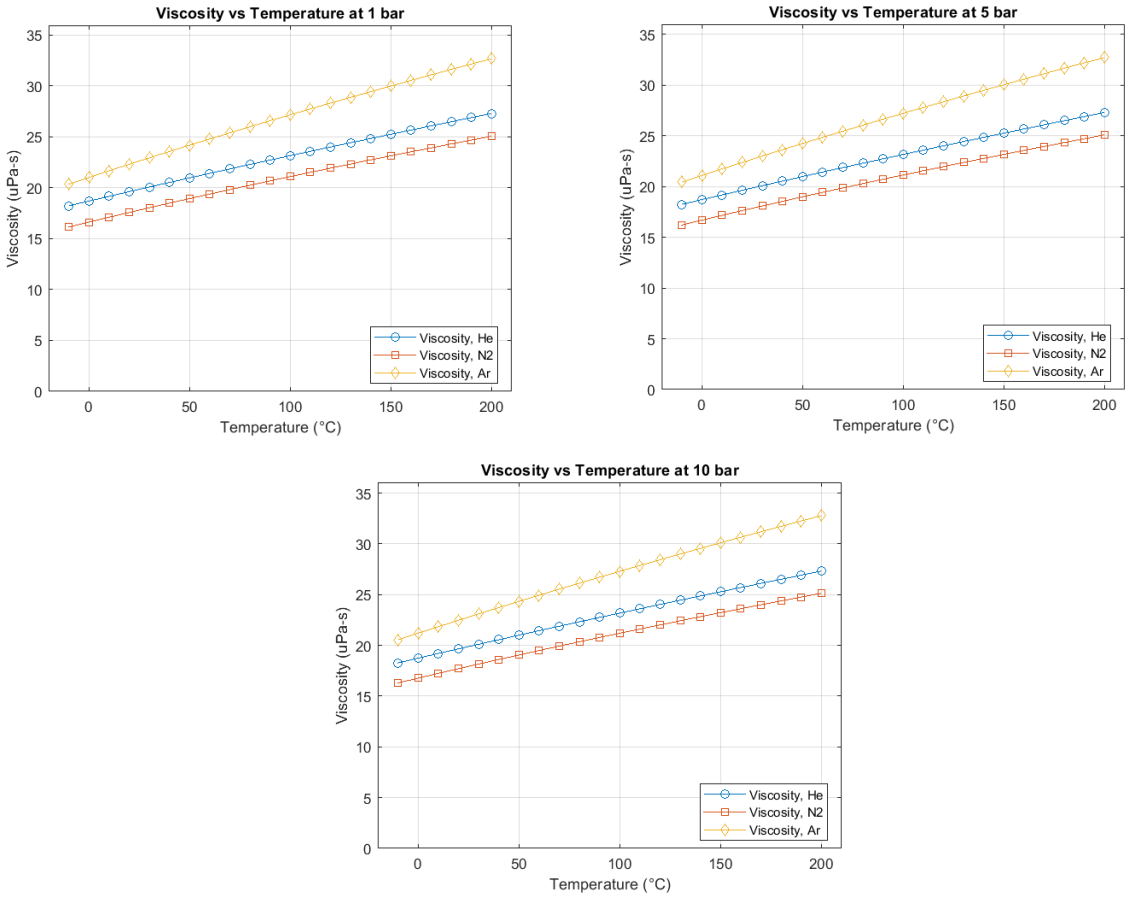

Figure 52 Temperature vs Viscosity for He, N_2 at 1 bar(Top left), 5 bar(Top right) & 10 bar(Bottom)

5.3 Influence of Machine Geometry on Efficiency

In the design of Stirling machine geometry, several parameters play a pivotal role. These include the swept volumes of both the compression and expansion spaces, the dead volumes in the compression and expansion spaces, the regenerator volume, and the heat exchanger volume (which is considered part of the dead volume). Additionally, the phase angle is a crucial factor.

5.3.1 Analysis of different phase angle

Based on the simulation - 4 scenario – 5, there are 4 phase angles 45°,90°,135°, & 180° analyses tabulated,

Table 19 Calculated TH & COP for phase Angle: 45 degrees

Gas	Pmean /(bar)	Li /(kW)	N /(RPM)	TL /(°C)	TH /(°C)	COP
Helium	4.51	91.8	600.01	25.1	464.09	1.68
Argon	3.52	92.54	600	25.1	-	-
Nitrogen	4.48	90.56	600	25.1	458.47	1.69

Table 20 Calculated TH & COP for phase Angle: 90 degrees

Gas	Pmean /(bar)	Li /(kW)	N /(RPM)	TL /(°C)	TH /(°C)	COP
Helium	4.51	91.8	600.01	25.1	154.62	3.3
Argon	3.52	92.54	600	25.1	193.46	2.77
Nitrogen	4.48	90.56	600	25.1	153.51	3.32

Table 21 Calculated TH & COP for phase Angle: 135 degrees

Gas	Pmean /(bar)	Li /(kW)	N /(RPM)	TL /(°C)	TH /(°C)	COP
Helium	4.51	91.8	600.01	25.1	122.65	4.06
Argon	3.52	92.54	600	25.1	147.62	3.43
Nitrogen	4.48	90.56	600	25.1	121.91	4.08

At a phase angle of 180 degrees, no real values for TH were found for any of the three gases. Consequently, it was not possible to calculate the COP for this phase angle.

According to the above results, the P-V diagram was plotted to analyze the variations at each phase angle.

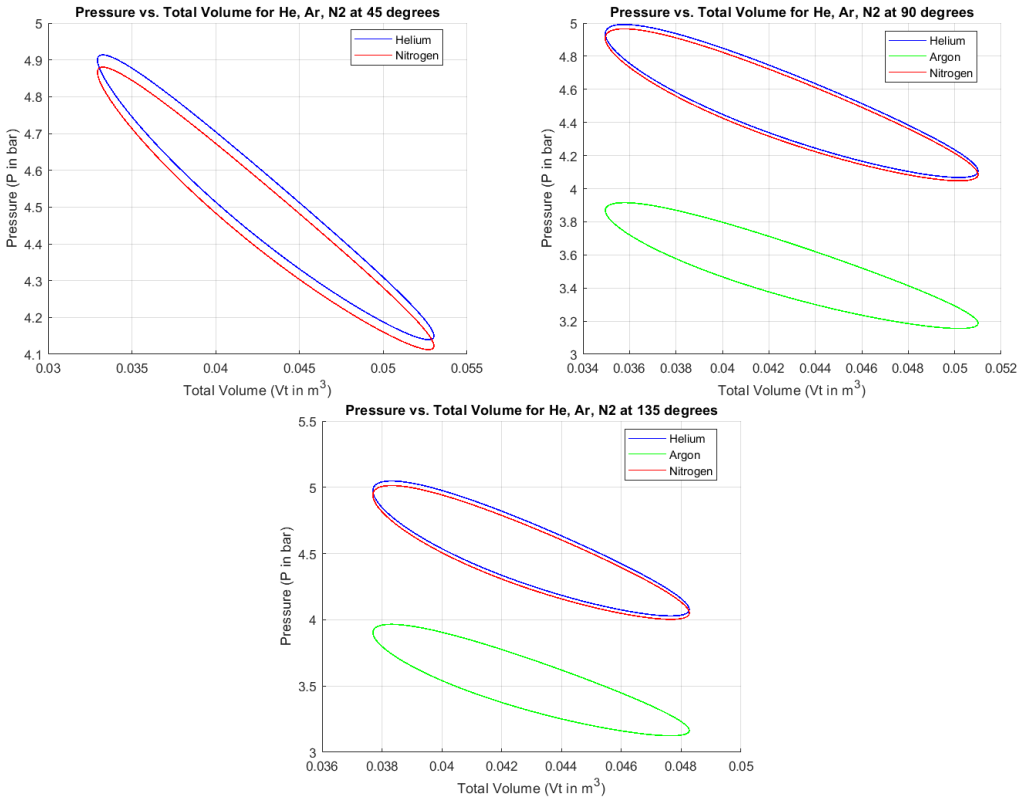

Figure 53 P-V diagram for He, N_2 & Ar at different Phase Angles(45°,90° & 135°)

5.3.2 Analysis of different swept volumes

Based on simulation - 4, scenario - 6, the swept volume was increased by 0%, 10%, 20%, and 30%, and the results were tabulated.

Table 22 The TH & COP values at initial swept volume

Gas	Pmean /(bar)	Li /(kW)	N /(RPM)	TL /(°C)	TH /(°C)	COP
Helium	4.51	91.8	600.01	25.1	154.62	3.3
Argon	3.52	92.54	600.00	25.1	193.46	2.77
Nitrogen	4.48	90.56	600.00	25.1	153.51	3.32

Table 23 The TH & COP values at Swept Volume Increase of 10%

Gas	Pmean /(bar)	Li /(kW)	N /(RPM)	TL /(°C)	TH /(°C)	COP
Helium	4.51	91.8	600.01	25.1	134.63	3.7231
Argon	3.52	92.54	600.00	25.1	167.28	3.0977
Nitrogen	4.48	90.56	600.00	25.1	133.69	3.7465

Table 24 The TH & COP values at Swept Volume Increase of 20%

Gas	Pmean /(bar)	Li /(kW)	N /(RPM)	TL /(°C)	TH /(°C)	COP
Helium	4.51	91.8	600.01	25.1	119.25	4.1678
Argon	3.52	92.54	600.00	25.1	147.23	3.442
Nitrogen	4.48	90.56	600.00	25.1	118.45	4.1951

Table 25 The TH & COP values at Swept Volume Increase of 30%

Gas	Pmean /(bar)	Li /(kW)	N /(RPM)	TL /(°C)	TH /(°C)	COP
Helium	4.51	91.8	600.01	25.1	107.14	4.6355
Argon	3.52	92.54	600.00	25.1	131.47	3.8038
Nitrogen	4.48	90.56	600.00	25.1	106.44	4.6668

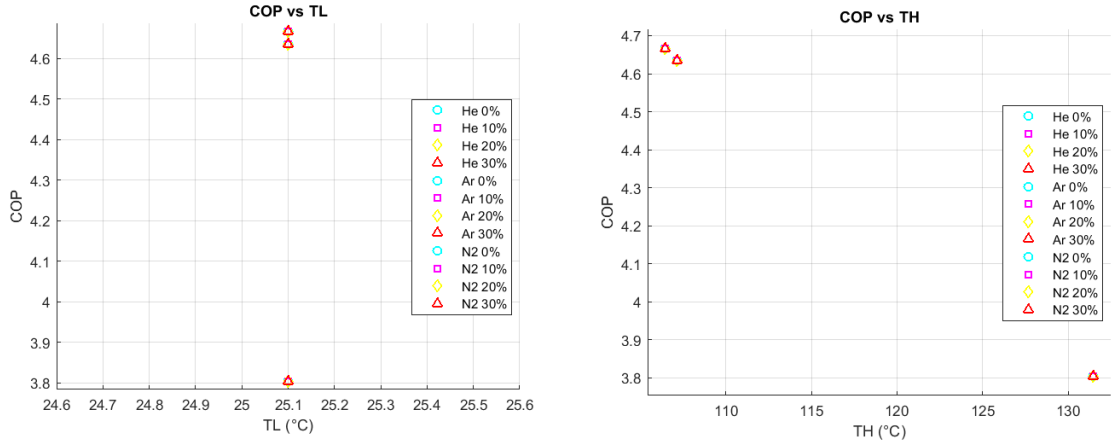

Figure 54 The COP vs TL(Left) & COP vs TH(Right) at different Swept Volumes (0%, 10%, 20% & 30%)

5.3.3 Analysis of different dead volumes

Based on simulation - 4, scenario - 7, the dead volume was increased by 0%, 10%, 20%, and 30%, and the results were tabulated

Table 26 The TH & COP values at initial dead volume

Gas	Pmean /(bar)	Li /(kW)	N /(RPM)	TL /(°C)	TH /(°C)	COP
Helium	4.51	91.8	600.01	25.1	154.62	3.30
Argon	3.52	92.54	600	25.1	193.46	2.77
Nitrogen	4.48	90.56	600	25.1	153.51	3.32

Table 27 The TH & COP values at Dead Volume Increase of 10%

Gas	Pmean /(bar)	Li /(kW)	N /(RPM)	TL /(°C)	TH /(°C)	COP
Helium	4.51	91.8	600.01	25.1	161.53	3.19
Argon	3.52	92.54	600	25.1	202.56	2.68
Nitrogen	4.48	90.56	600	25.1	160.36	3.21

Table 28 The TH & COP values at Dead Volume Increase of 20%

Gas	Pmean /(bar)	Li /(kW)	N /(RPM)	TL /(°C)	TH /(°C)	COP
Helium	4.51	91.8	600.01	25.1	168.45	3.08
Argon	3.52	92.54	600	25.1	211.71	2.60
Nitrogen	4.48	90.56	600	25.1	167.22	3.10

Table 29 The TH & COP values at Dead Volume Increase of 30%

Gas	Pmean /(bar)	Li /(kW)	N /(RPM)	TL /(°C)	TH /(°C)	COP
Helium	4.51	91.8	600.01	25.1	175.40	2.98
Argon	3.52	92.54	600	25.1	220.91	2.52
Nitrogen	4.48	90.56	600	25.1	174.10	3.00

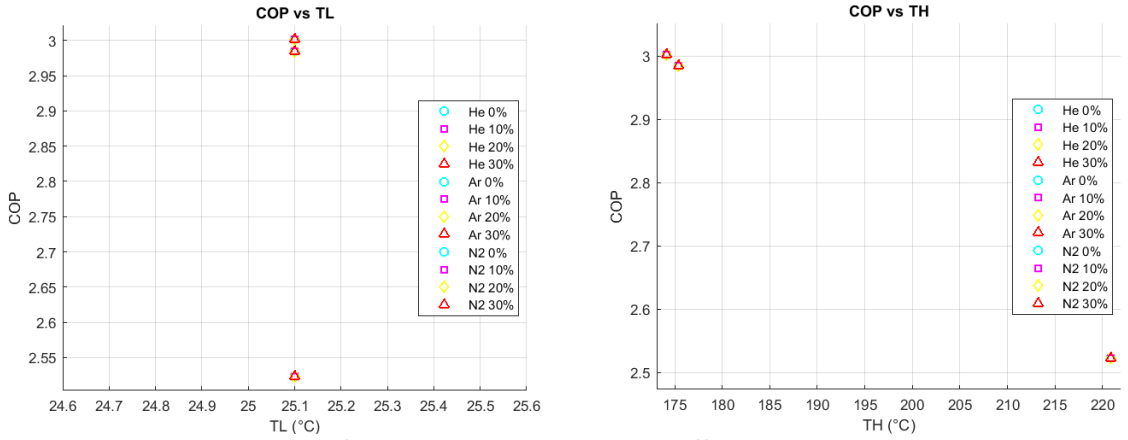

Figure 55 The COP vs TL(Left) & COP vs TH(Right) at different Dead Volumes (0%, 10%, 20% & 30%)

5.3.4 Analysis of different Regenerator volumes

Based on simulation - 4, scenario - 8, the regenerator volume was increased by 0%, 10%, 20%, and 30%, and the results were tabulated.

Table 30 The TH & COP values at initial Regenerator volume

Gas	Pmean /(bar)	Li /(kW)	N /(RPM)	TL /(°C)	TH /(°C)	COP
Helium	4.51	91.8	600.01	25.1	154.62	3.30
Argon	3.52	92.54	600	25.1	193.46	2.77
Nitrogen	4.48	90.56	600	25.1	153.51	3.32

Table 31 The TH & COP values at Regenerator Volume Increase of 10%

Gas	Pmean /(bar)	Li /(kW)	N /(RPM)	TL /(°C)	TH /(°C)	COP
Helium	4.51	91.8	600.01	25.1	157.49	3.25
Argon	3.52	92.54	600	25.1	197.16	2.73
Nitrogen	4.48	90.56	600	25.1	156.35	3.27

Table 32 The TH & COP values at Regenerator Volume Increase of 20%

Gas	Pmean /(bar)	Li /(kW)	N /(RPM)	TL /(°C)	TH /(°C)	COP
Helium	4.51	91.8	600.01	25.1	160.34	3.21
Argon	3.52	92.54	600	25.1	200.86	2.70
Nitrogen	4.48	90.56	600	25.1	159.19	3.22

Table 33 The TH & COP values at Regenerator Volume Increase of 30%

Gas	Pmean /(bar)	Li /(kW)	N /(RPM)	TL /(°C)	TH /(°C)	COP
Helium	4.51	91.8	600.01	25.1	163.20	3.16
Argon	3.52	92.54	600	25.1	204.55	2.66
Nitrogen	4.48	90.56	600	25.1	162.02	3.18

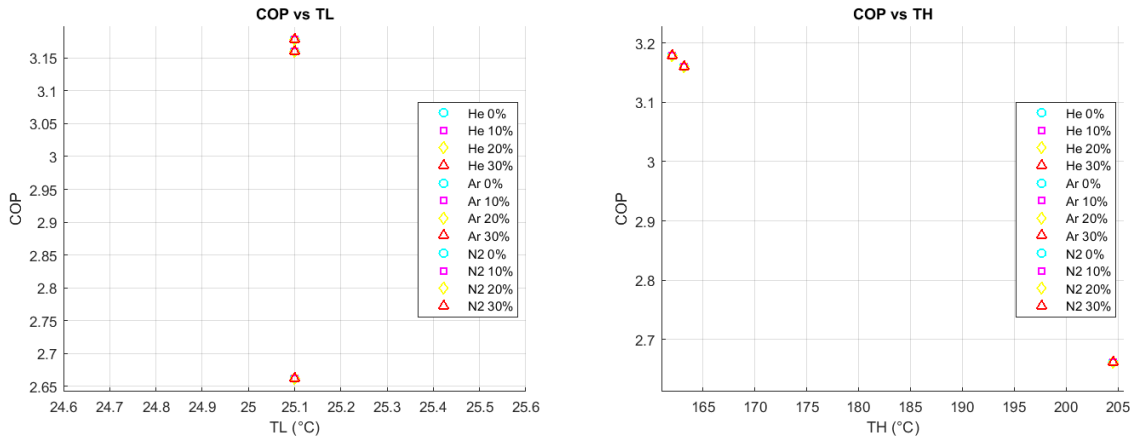

Figure 56 The COP vs TL(Left) & COP vs TH(Right) at different Regenerator Volumes (0%, 10%, 20% & 30%)

5.4 Impact of Higher Compression on System Performance

The results of Simulation 5 are tabulated to show the impact of each 10% increase in Pmean on TH and COP separately.

Table 34 The TH & COP values at measured Pmean values.

Gas	Pmean /(bar)	Li /(kW)	N /(RPM)	TL /(°C)	TH /(°C)	COP
Helium	4.51	91.8	600.01	25.1	154.62	3.3
Argon	3.52	92.54	600.00	25.1	193.46	2.77
Nitrogen	4.48	90.56	600.00	25.1	153.51	3.32

Table 35 The TH & COP values at Pmean increase: 10%.

Gas	Pmean /(bar)	Li /(kW)	N /(RPM)	TL /(°C)	TH /(°C)	COP
Helium	4.96	91.8	600.01	25.1	142.67	3.54
Argon	3.87	92.54	600.00	25.1	177.77	2.95
Nitrogen	4.93	90.56	600.00	25.1	141.66	3.56

Table 36 The TH & COP values at Pmean increases of 20%.

Gas	Pmean /(bar)	Li /(kW)	N /(RPM)	TL /(°C)	TH /(°C)	COP
Helium	5.41	91.8	600.01	25.1	132.74	3.77
Argon	4.22	92.54	600.00	25.1	164.78	3.14
Nitrogen	5.38	90.56	600.00	25.1	131.82	3.79

Table 37 The TH & COP values at Pmean increases of 30%.

Gas	Pmean (bar)	Li /(kW)	N /(RPM)	TL /(°C)	TH /(°C)	COP
Helium	5.86	91.8	600.01	25.1	124.37	4.00
Argon	4.57	92.54	600.00	25.1	153.84	3.32
Nitrogen	5.83	90.56	600.00	25.1	123.52	4.03

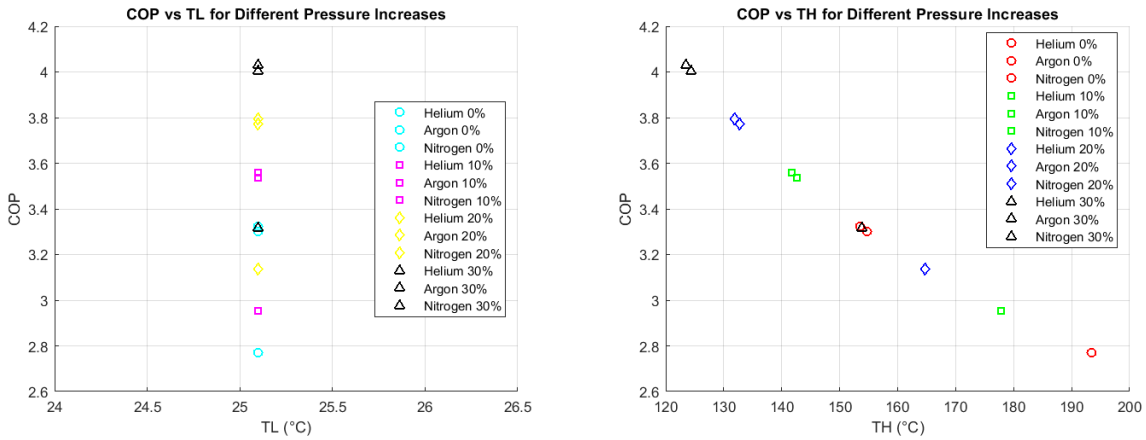

Figure 57 The COP vs TL(Left) & COP vs TH(Right) at different Mean pressures (0%, 10%, 20% & 30%)

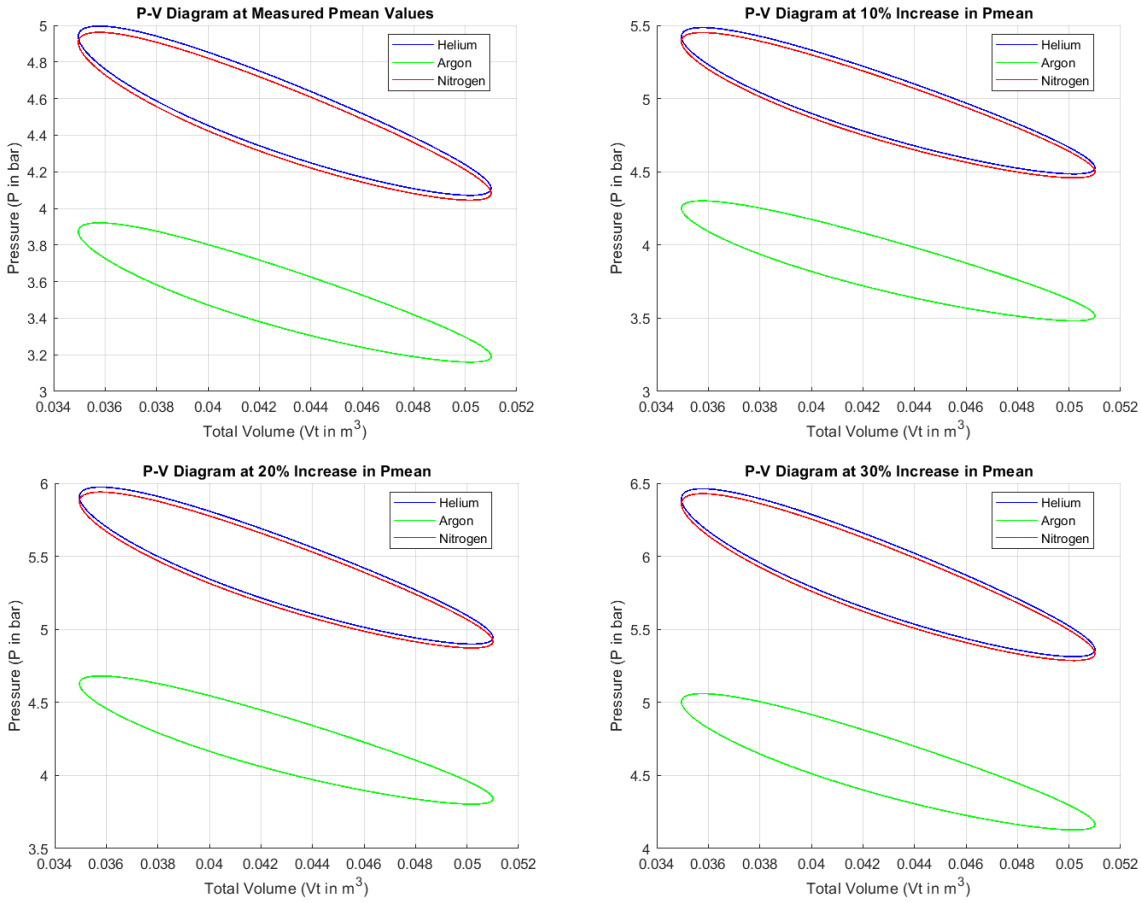

Figure 58 The P-V Diagram for He, Ar, N_2 at Initial Pmean(Top left), 10% increase of Pmean(Top right), 20% Increase of Pmean(Bottom left) & 30% increase of Pmean(Bottom right)

Chapter 6 Discussion

6.1 Analysis of Working Fluids in Stirling Cycle Performance

The working fluid properties analysis, starts with fluid density variations with pressure & temperature, the density of He, N_2, and Ar behaviors with pressure at different temperature levels as shown in *Figure 35*, it is evident that the density of all three gases increases linearly with pressure at each of the specified temperatures (20°C, 50°C, 100°C, and 200°C). He gas consistently exhibits the lowest density values across all pressures, followed by N_2, with Ar having the highest density values. This trend is consistent at all the examined temperatures, indicating that the molecular weights of the gases significantly influence their densities.

At a constant temperature of 20°C, the density of He, N_2, and Ar increases as pressure rises from 1 bar to 10 bar. This behavior is similarly observed at 50°C, 100°C, and 200°C, with the density increase being more pronounced at higher pressures. However, the impact of temperature on density is also evident, as higher temperatures lead to slightly lower densities for the same pressure. This is due to the increased kinetic energy of gas molecules at higher temperatures, causing them to occupy a larger volume. Despite these variations, the relative order of densities remains unchanged, with He having the lowest and Ar the highest density, reinforcing the influence of molecular mass on gas density.

Similarly, the density of He, N_2, and Ar behavior with temperature under specified pressure conditions as shown in *Figure 36 & Figure 37*, it is evident that the density of all three gases decreases with increasing temperature at each of the specified pressures (1 bar, 5 bar, and 10 bar). This inverse relationship between temperature and density is due to the expansion of gas molecules as temperature rises, leading to a decrease in density.

At a constant pressure of 1 bar, the density of He, N_2, and Ar decreases as temperature increases from -10°C to 200°C. This trend is consistent at 5 bar and 10 bar, with the rate of decrease being more pronounced at higher pressures. Despite the varying rates of density decrease with temperature, the relative order of densities remains unchanged, with He exhibiting the lowest density, followed by N_2, and Ar having the highest density. This consistent ranking is attributed to the molecular masses of the gases, where helium, being the lightest, has the lowest density and argon, being the heaviest, has the highest density. The observed trends highlight the influence of both temperature and pressure on gas density, aligning with the fundamental principles of gas behavior.

The specific heat capacity at constant volume (Cv) of He, N_2, and Ar variation trends with pressure at different level temperatures as shown in *Figure 38*, that Cv remains relatively constant across the range of pressures studied for each gas. He consistently shows the highest Cv values, followed by N_2, with Ar exhibiting the lowest Cv values. This stability of Cv with varying pressure at fixed temperatures indicates that the specific heat capacity at constant volume for these gases is not significantly affected by changes in pressure, reaffirming their ideal gas behavior under the studied conditions. Similarly, the variations in Cv with temperature under specified pressure conditions *(Figure 39),* shows similar to the pressure variations, the specific heat capacities for He, N_2, and Ar remain relatively stable across the temperature range from 0°C to 200°C. The data again confirm that helium has the highest Cv, followed by N_2 and Ar. This invariance of Cv with temperature under constant pressure conditions suggests that the internal energy contributions per unit mass for these gases are predominantly influenced by their molecular properties rather than external conditions such as pressure and temperature within the examined range.

The specific heat capacity ratio (Cp/Cv) or gamma of He, N_2, and Ar with pressure at different temperatures as shown in *Figure 42 & Figure 43,* All three gases exhibit minimal change with increasing pressure across the temperature range. This indicates that the gamma is relatively insensitive to pressure changes for these gases within the studied temperature range. Helium consistently shows a Cp/Cv ratio around 1.66, which is slightly higher than that of nitrogen and argon, reflecting its monoatomic nature compared to the diatomic nitrogen and the heavier monoatomic argon. Similarly, in the *Figure 44* reveal that the Cp/Cv ratios of He, N_2, and Ar are relatively stable across the temperature range, with only slight variations. The stability of the Cp/Cv ratio with respect to temperature suggests that the internal energy distribution within the molecules remains fairly constant despite changes in thermal energy. This behavior is characteristic of ideal gases, where the specific heat capacities are functions of temperature and molecular structure, rather than pressure. Overall, the data affirm that for helium, nitrogen, and argon, the Cp/Cv ratio remains nearly constant across a wide range of temperatures and pressures, reinforcing their ideal gas behavior under the studied conditions.

The variations in the sound speed of He, N_2, and Ar with pressure at different temperature levels are shown in *Figure 45 & Figure 46*, that the sound speed in helium is significantly higher than in nitrogen and argon across all pressures and temperatures. This difference is attributed to the lower molar mass of helium, which allows sound waves to propagate more quickly. Additionally, the sound speed in all three gases exhibits a relatively constant trend with

increasing pressure at a given temperature, indicating that pressure has a minimal effect on the sound speed of these gases within the examined range.

Under the specified pressure conditions, the variations in sound speed with temperature are depicted in *Figure 47*. As temperature increases, the sound speed in helium, nitrogen, and argon all show an upward trend. This behavior is consistent with the kinetic theory of gases, where higher temperatures increase the kinetic energy of gas molecules, thus enhancing the propagation speed of sound waves. Helium, with its lower molecular weight, shows the most pronounced increase in sound speed with temperature, followed by nitrogen and argon.

The variations in the thermal conductivity of He, N_2, and Ar with pressure at different temperature levels are depicted in *Figure 48*. The thermal conductivity of He remains significantly higher than that of N_2 and Ar across the examined pressure range, showing minimal changes with increasing pressure. In contrast, N_2 and Ar exhibit relatively lower thermal conductivity values, which also remain largely unaffected by pressure variations. The thermal conductivity of He, N_2, and Ar shows consistency with the theoretical expectations where the lightest gas (He) possesses the highest thermal conductivity due to its smaller atomic size and higher speed of sound, facilitating more efficient energy transfer.

Under specified pressure conditions, the thermal conductivity of He, N_2, and Ar varies with temperature as shown in *Figure 49 & Figure 50*. Helium shows a noticeable increase in thermal conductivity with rising temperature, maintaining its superior thermal performance compared to N_2 and Ar. This trend aligns with the kinetic theory of gases, where thermal conductivity increases with temperature due to enhanced molecular motion and energy exchange. Nitrogen and argon, while exhibiting lower thermal conductivity than helium, also show slight increases with temperature, indicating that molecular agitation contributes to thermal transport even in heavier gases. The consistent behavior across different pressures and temperatures reinforces the reliability of the data and supports its relevance in practical applications involving these gases.

The variations in the viscosity of He, N_2, and Ar with pressure at different temperatures are depicted in *Figure 51*, that the viscosity of each gas remains relatively stable across the pressure range of 0 to 10 bar at all temperature levels studied (20°C, 50°C, 100°C, and 200°C). Helium exhibits the lowest viscosity, while argon shows the highest viscosity, with nitrogen in between. The slight increase in viscosity with increasing pressure is more noticeable in argon than in helium and nitrogen, indicating that argon's intermolecular interactions may be more sensitive

to pressure changes. Overall, the minimal variation suggests that pressure has a negligible effect on the viscosity of these gases within the examined range, aligning with the behavior expected for ideal gases.

The viscosity of He, N_2, and Ar as a function of temperature at specified pressures (1 bar, 5 bar, and 10 bar). Viscosity increases with temperature for all gases as illustrates in *Figure 52*, which is consistent with the kinetic theory of gases where higher temperatures lead to increased molecular collisions, thereby increasing resistance to flow. At a constant pressure, argon consistently exhibits the highest viscosity followed by nitrogen and helium, respectively. The rate of increase in viscosity with temperature appears uniform across different pressures, suggesting that temperature is a more significant factor affecting viscosity than pressure for these gases. This uniformity underscores the dominant influence of thermal energy over intermolecular forces in determining the viscosity of these gases.

6.2 Evaluation of Simplified Model Predictions

The initial phase of the analysis involved conducting a simplified MATLAB simulation of the HP model, utilizing the data collected from empirical measurements. During the measurement process at the IVAR facility, it was observed that Ar exhibited an anomalous response in HP performance compared to He and N_2. Nevertheless, these empirical measurements were subjected to further analysis using the simplified MATLAB simulation model to understand the underlying dynamics.

Based on the result – 1, the *Figure 28(Right)* illustrate COP versus TH indicates a negative correlation between TH and COP for all three gases. As TH increases from approximately 140°C to 143°C, the COP decreases. This trend is consistent across He, Ar, and N_2, suggesting that higher hot side temperatures lead to reduced efficiency of the HP. This could be attributed to the increased energy requirements to maintain higher TH levels. Helium, Argon, and Nitrogen exhibit similar slopes, indicating comparable performance characteristics under varying TH conditions.

Conversely, the *Figure 28(Left)* demonstrates a positive correlation between the COP and the TL for all three gases. As TL increases from approximately 25.1°C to 26.1°C, the COP correspondingly improves, indicating that higher cold side temperatures enhance the performance of the HP. This enhancement is most pronounced for argon, followed by helium

and nitrogen, suggesting that argon may be more effective in improving the HP's efficiency at elevated TL levels.

The tabulated data form *Table 12* clearly indicate that the COP values range from 3.52 to 3.62 across various test conditions. Both pressure and power consumption exhibit significant variability, which in turn influences the COP. These findings suggest that optimizing both the TH and the low side temperature TL can lead to substantial improvements in the COP of the HP. Specifically, lower TH and higher TL are advantageous for achieving enhanced performance. Among the gases tested, Ar demonstrates a marginally superior improvement in COP with increasing TL compared to He and N_2, indicating its potential as an effective candidate for enhancing HP efficiency under specific operating conditions.

The Results – 2 represent the two scenarios (1 & 2). In the scenario - 1 (*Figure 29)* the high-pressure plot, pressures range from approximately 4.4 bar to 5.6 bar, and volumes from 0.034 m^3 to 0.052 m^3. The distinct elliptical curves for He, Ar, and N_2 indicate cyclic pressure-volume relationships, representing the work done by the system during a complete cycle, directly linked to the net power supplied by the motor. Helium, due to its small atomic radius, shows minimal volume changes, whereas nitrogen, being diatomic, displays the largest volume range. This suggests that helium is more compressible compared to nitrogen. These patterns align with the intermolecular forces and physical properties of the gases under high-pressure conditions. In the low-pressure plot, the pressure ranges from about 3.5 bar to 4.4 bar, with the same volume ranges. Helium again shows the most compact curve, suggesting minimal volume changes with pressure fluctuations, while nitrogen's curve occupies the highest volume range, indicating the least compressibility. These observations are consistent with the intrinsic properties of these gases. The similarity in volume range across different pressure conditions implies that these gases maintain their physical constraints regardless of pressure variations.

The Helium curve has the smallest enclosed area among the three gases, suggesting that under high pressure, the motor supplies the least power to compress and expand helium due to its higher compressibility and lower atomic mass. In contrast, the Argon curve encloses a larger area than helium, indicating that more power is required by the motor to compress and expand argon. Argon’s larger atomic size compared to helium contributes to this increased power requirement. The Nitrogen curve encloses the largest area, suggesting that the motor supplies the most power for nitrogen under high-pressure conditions. Nitrogen’s diatomic nature and

higher molecular weight mean it is less compressible, requiring more energy for the same volume change compared to helium and argon.

When comparing the calculated mean pressure in Scenario 1(*Table 13*) from simulation - 2 and the measured mean pressure, it is evident that the calculated mean pressure is higher. This discrepancy is due to the fact that losses in the HP system were not considered.

Table 38 Comparison of Measured and Calculated Mean Pressure in Scenario 1

Test	P /(bar)	P_{S1} /(bar)	Deviation %
1.	4.51	4.93	9.31
2.	3.60	3.88	7.78
3.	3.52	4.98	41.48
4.	2.80	3.94	40.71
5.	4.48	4.87	8.71
6.	3.60	3.84	6.67

Where, P – Mean pressure measured value, P_{S1}-Calculated mean pressure from scenario 1.

The Scenario -2 from the results – 2, (*Figure 30*) The high-pressure conditions, with pressures ranging from approximately 3.0 bar to 5.0 bar, the helium curve, which encloses the smallest area, indicates that the motor supplies the least power to helium due to its higher compressibility and lower atomic mass. Conversely, the nitrogen curve, which encloses the largest area, suggests that the motor supplies the most power to nitrogen, reflecting its lower compressibility and higher molecular weight.

In low-pressure conditions, with pressures ranging from approximately 2.5 bar to 4.0 bar, similar trends are observed. Helium again shows the smallest enclosed area, indicating minimal power requirements for compression and expansion. Argon occupies a middle position, requiring more power than helium but less than nitrogen. Nitrogen's curve, with the largest area, signifies the highest power requirement from the motor under low-pressure conditions, consistent with its physical properties. These observations reinforce the patterns seen in high-pressure conditions and highlight the gases' intrinsic properties.

Both the low-pressure and high-pressure plots show the Ar curve positioned below the He and N_2 curves. This indicates that argon has less compression and expansion pressure compared to nitrogen & helium. This consistent positioning across different pressure conditions highlights the predictable nature of argon's behavior in response to pressure changes.

When comparing the calculated motor power in Scenario 2 *(Table 14)* to the measured motor power, it is evident that the calculated motor power is smaller. This discrepancy is due to the

fact that in Scenario 1, the measured motor power involved higher mean pressure. Consequently, the measured pressure requires less motor power.

Table 39 Comparison of Measured and Calculated Motor Power in Scenario 2

Test	Li /(kW)	Li_{S2} /(kW)	Deviation %
1.	91.80	83.86	8.65
2.	70.22	65.23	7.11
3.	92.54	65.36	29.37
4.	64.69	45.99	28.91
5.	90.56	83.34	7.97
6.	69.33	64.84	6.48

Where, Li – Motor power measured value, Li_{S2}-Calculated motor power from scenario 2.

The Results - 3 from Simulation 3 involved calculating the TH and COP of the HP for six sets of measurements. These calculations were conducted using the Schmidt theory equations.

The *Figure 31* COP vs TL plot, it is observed that for all three gases, the COP increases with an increase in TL. Helium and nitrogen exhibit higher COP values compared to argon across the tested temperature range. This trend is consistent with the intrinsic properties of the gases, where helium, with its lower molecular weight and higher thermal conductivity, shows superior performance.

In the COP vs TH plot, a decrease in COP with increasing TH is noted for all gases. Helium and nitrogen again demonstrate higher COP values relative to argon. This inverse relationship indicates that the efficiency of the HP reduces at higher hot side temperatures, which could be attributed to increased thermal losses and reduced temperature differentials across the system.

The tabulated results in *Table 15* show that the pressure and motor power consumption vary significantly across the tests, affecting the COP values. Higher pressures generally correlate with higher power consumption and lower COP, emphasizing the importance of optimizing operating conditions for improved performance.

The consistent positioning of the gases in the plots reflects their predictable thermodynamic behavior under varying temperatures. Helium's superior COP in both TL and TH plots underscores its efficiency in HP applications, whereas argon, with its moderate performance, occupies an intermediate position. Nitrogen, though similar to helium in performance, shows slightly lower COP values due to its higher molecular weight and lower thermal conductivity.

The Results - 4 is similar to Result - 2 there are two scenarios found to perform P – V plots based on the outcome on result 3. However, it was found in both scenario P – V plot show the

same result. In the high-pressure plot *(Figure 32 & Figure 33)*, with pressures ranging from approximately 3.0 bar to 5.0 bar, the helium and nitrogen curves closely align, suggesting similar volumes and pressures for these gases under high-pressure conditions. However, the helium curve encloses a slightly smaller area, indicating that helium requires less power for compression and expansion due to its higher compressibility and lower atomic mass. In contrast, the argon (Ar) curve is positioned below the helium and nitrogen curves, signifying that argon occupies a larger volume for a given pressure, requiring more power than helium but less than nitrogen. This positioning reflects argon's intermediate compressibility and molecular weight compared to the other gases.

In the low-pressure plot *(Figure 32 & Figure 33)*, with pressures ranging from approximately 2.5 bar to 4.0 bar, similar trends are observed. Helium and nitrogen again show closely aligned curves, with helium enclosing a smaller area, indicating lower power requirements for the compression and expansion cycles. Argon, once more, occupies a larger volume for the same pressure range, positioned below the helium and nitrogen curves. This consistent pattern across both high and low-pressure conditions highlights the predictable nature of argon's behavior due to its atomic size and molecular weight.

The distinct separation of the argon curve from the helium and nitrogen curves in both pressure scenarios underscores the importance of gas selection based on their thermodynamic properties. Helium, with its high compressibility and low atomic mass, demonstrates superior efficiency in compression and expansion processes, making it an ideal candidate for applications where minimal power consumption is crucial. Argon's moderate performance reflects its balanced properties, while nitrogen, with its lower compressibility and higher molecular weight, requires the most power, as evidenced by the largest enclosed areas in the P-V diagrams.

The Results – 5 show the deviations of TH from Results -1 which calculated through heat exchanger and hot water circulation heat transfer with Results – 3 through the Schmidt analysis of HP. The comprehensive analysis of temperature deviations under two different gas pressure conditions of He, N_2 & Ar showed in *Table 18*. Notably, Tests 3 and 4 from Ar exhibit the highest TH differences (50.31°C and 47.42°C) and deviations (35.1% and 33.9%), indicating significant variability. In contrast, He and N_2 show relatively smaller differences, with N_2 at low pressure condition having the lowest TH difference (8.07°C) and deviation (5.7%). As earlies said Ar show abnormal results with this Stirling machine HP. This due to the Stirling

machine design configurations. In general, Stirling machine designed for the particular application with particular gas. HP designed for He, that is the reason this abnormal representation of Ar gas. It can clearly displayed in *Figure 34* through bar chat. Helium and Nitrogen exhibit more stable behavior with lower TH differences and deviations, suggesting less sensitivity to pressure changes. These observations indicate that Argon is more sensitive to pressure changes, potentially impacting temperature control processes, while Helium and Nitrogen provide more stable performance under varying pressures.

The comprehensive analysis of temperature deviations under two different gas pressure conditions for He, N_2, and Ar reveals significant insights. Notably, Ar exhibit the highest TH differences (50.31°C and 47.42°C) and deviations (35.1% and 33.9%), indicating substantial variability. In contrast, He and N_2 show relatively smaller differences, with N_2 at low pressure having the lowest TH difference (8.07°C) and deviation (5.7%). These abnormal results for Ar in the Stirling machine's HP are due to its design configuration. Generally, Stirling machines are designed for specific applications with particular gases. The HoegTemp HP is designed for He, which explains the abnormal representation of Ar gas. This is clearly displayed in *Figure 34* through the bar chart.

He and N_2 exhibit more stable behavior with lower TH differences and deviations, suggesting less sensitivity to pressure changes. These observations indicate that Argon is more sensitive to pressure changes, potentially impacting temperature control processes, while Helium and Nitrogen provide more stable performance under varying pressures. This analysis is crucial for optimizing systems where temperature stability is vital, and it highlights the importance of selecting appropriate gases for specific Stirling machine configurations.

The impact of machine geometry on the HP performance analysis starts with phase angles. Based on the results of simulation 4, scenario 5, the analysis reveals significant variations in the calculated TH and COP for helium, argon, and nitrogen gases. At a phase angle of 45 degrees, helium and nitrogen exhibit COP values of 1.68 and 1.69, respectively, whereas argon does not provide a realistic COP due to the lack of a valid TH value. This discrepancy suggests that argon may not perform efficiently under this specific phase angle, potentially leading to inaccurate or unfeasible operational conditions.

At a phase angle of 90 degrees, all three gases show feasible COP values, with helium demonstrating the highest COP at 3.3, followed by nitrogen and argon at 3.32 and 2.77,

respectively. This indicates that the system is most efficient for helium and nitrogen at this phase angle. For a phase angle of 135 degrees, helium again shows the highest COP at 4.06, with nitrogen closely following at 4.08, and argon at 3.43. However, at 180 degrees, no real values for TH were found, preventing COP calculation for any gas. This suggests that the system may encounter limitations or operational challenges at this specific phase angle, making it impractical for efficient performance.

The P-V diagrams for He, Ne, and Ar at phase angles of 45, 90, and 135 degrees in *Figure 53* provide valuable insights into the thermodynamic behavior of these gases under varying conditions. At a phase angle of 45 degrees, both He & Ne exhibit similar curve loops with slight deviations. As the phase angle changes from 45 to 90 and then to 135 degrees, the Pmax for He & Ne increases, while the Pmin decreases. In contrast, Ar shows a decrease in Pmax and an increase in Pmin at 135 degrees. These trends are clearly visualized in the P-V diagrams, highlighting the influence of phase angles on the operational performance of each gas within the heat pump system

The simulation – 4 scenario 6 results in *Table 22, Table 23, Table 24 &*

Table 25 illustrate the impact of increasing swept volume on the TH and COP of He, Ar, and N_2. As the swept volume increased to 10%, 20%, and 30%, there was a notable decrease in TH and a corresponding increase in COP for all three gases. For instance, at a 30% increase in swept volume, He's TH decreased to 107.14°C, and its COP improved to 4.64. Similarly, N_2's TH decreased to 106.44°C, and its COP increased to 4.67.

These trends indicate that increasing the swept volume enhances the efficiency of the Stirling engine, as evidenced by the higher COP values and lower TH values for all gases. This improvement is more pronounced in He and N_2, which exhibit higher COP values across all swept volume increments compared to Ar. The lower TH values suggest a more effective heat transfer process, contributing to the increased efficiency. The consistency of these results across different gases highlights the robustness of the Stirling engine's performance improvements with increased swept volume. However, Increasing the swept volume alone does not yield a positive impact on system optimization due to the observed decline in temperature lift.

The simulation – 4 scenario 7 results in *Table 26, Table 27, Table 28 & Table 29* illustrate the effects of varying dead volumes on TH and COP of He, Ar, and N_2. As the dead volume increases to 10%, 20%, and 30%, the TH values rise for all three gases, while the COP values generally decrease. For instance, at a 30% increase in dead volume, He's TH increases to 175.40°C, and its COP decreases to 2.98. Similarly, Ar's TH increases to 220.91°C, and its COP decreases to 2.51.

These trends suggest that increasing the dead volume negatively impacts the efficiency of the Stirling engine, as evidenced by the decreasing COP values and rising TH values. The increase in TH indicates that more heat is retained in the system, which reduces the efficiency of the heat pump process. The consistency of these results across different gases underscores the critical role of dead volume in determining the engine's performance.

The simulation – 4 scenario 8 results in *Table 30, Table 31, Table 32 & Table 33* present the results of analyzing the impact of varying regenerator volumes on TH & COP. As the regenerator volume is increased to 10%, 20%, and 30%, there is a general trend of increasing TH values and decreasing COP values across all gases. For instance, at a 30% increase in regenerator volume, He's TH increases to 163.20°C, and its COP decreases to 3.16. Similarly, Ar's TH increases to 204.55°C, and its COP decreases to 2.66.

These results indicate that increasing the regenerator volume negatively impacts the efficiency of the Stirling engine. The rising TH values suggest that more heat is retained within the system, which reduces the efficiency of the heat pump process as reflected by the decreasing COP values. He, Ar, and N_2 all exhibit similar trends, with He and N_2 maintaining relatively higher COP values compared to Ar across all tested regenerator volume increases. The consistency of these trends across different gases highlights the significant role of regenerator volume in influencing the performance of the Stirling engine.

6.3 Insights from Higher Compression Tests

The results presented in the *Table 34, Table 35, Table 36 & Table 37* illustrate the mean pressure increases impacts the TH and COP of He, Ar, and N_2. For He, as increases from its measured value to 30% higher, consistently decreases from 154.62°C to 124.37°C. This inverse relationship between Pmean and TH suggests that higher pressures facilitate a lower TH, likely enhancing the cooling effect. Concurrently, the COP for helium improves from 3.30 to 3.74, indicating better performance efficiency at elevated pressures.

Argon exhibits a similar pattern where TH decreases with rising Pmean, though the decline is less steep compared to helium. At the measured pressure, TH is 193.46°C, and it falls to 151.56°C at a 30% increase in Pmean. The COP for argon also increases from 2.77 to 3.31 across the same pressure range. This trend suggests that while argon benefits from higher pressures, the efficiency gains are somewhat less obvious than those for helium. However, the consistent improvement in COP with increased pressure underscores the positive impact on system performance.

Nitrogen follows a similar trend to helium and argon, with TH decreasing from 153.51°C at measured Pmean to 123.52°C at a 30% increase. The COP for nitrogen shows a steady rise from 3.32 to 3.75 over the same pressure range. Overall, the results indicate that increasing Pmean enhances the thermodynamic efficiency across all three gases, with helium showing the most significant improvement, followed by nitrogen and argon. These findings highlight the importance of optimizing Pmean to achieve better performance, making higher pressures a beneficial strategy for improving the effectiveness of thermodynamic systems using these gases. Increasing the charge pressure alone does not yield a positive impact on system optimization due to the observed decline in temperature lift. Therefore, it is recommended to increase the motor power consumption simultaneously when raising the charge pressure to achieve a higher temperature lift while also enhancing the COP.

The P-V diagrams illustrate in *Figure 58* the behavior of He, Ar, and N_2 under varying Pmean conditions, including the measured values and increments of 10%, 20%, and 30%. At the measured Pmean, He and N_2 exhibit similar P-V loops, indicating comparable thermodynamic performance, whereas Ar shows a distinct, lower-pressure loop. As Pmean increases, all gases experience elevated peak pressures in their P-V loops. Helium and Nitrogen continue to show similar behavior, with their loops shifting to higher pressures more significantly than Argon's loop. This trend is consistent across the 10%, 20%, and 30% increments, highlighting that He and N_2 benefit more from increased Pmean in terms of pressure elevation. Ar, although improved, consistently exhibits lower pressure values compared to He and N_2. These findings suggest that while increasing Pmean enhances the pressure characteristics and overall performance of all gases, He and N_2 show more pronounced improvements, emphasizing the need to optimize Pmean for better thermodynamic efficiency, especially when using He and N_2.

Chapter 7 Conclusion and Recommendations

7.1 Key Findings

The HoegTemp HTHP, developement is an innovative solution designed for industrial applications requiring heat at elevated temperatures. This HP designed and operates on the Stirling cycle, utilizing helium (R-704) as a working medium, which offers several environmental benefits, including being non-toxic, non-flammable, and having zero ozone depletion potential (ODP) and global warming potential (GWP). The HoegTemp can generate heat up to 200°C from sources as low as -10°C, with a high coefficient of performance (COP), making it more efficient than traditional vapor compression HPs for temperature ratios above 1.3 K/K.

One of the key features of the HoegTemp HP is its adaptability and robustness across a wide range of temperatures, operating efficiently in both heating and cooling modes. The system's design includes external source and sink circuits, allowing it to handle varying heat loads without temperature limits related to boiling points or condensing. This flexibility is further enhanced by the use of a patented piston rod seal and a clean-sheet design, which is based on over 30,000 hours of industrial operating experience.

The HoegTemp's performance was evaluated through a series of pilot installations and extensive testing at various industrial sites. For instance, at the IVAR biogas facility, the HP was integrated into the CO_2 capture process, demonstrating significant efficiency improvements. The experimental setup allowed for comprehensive performance mapping under controlled source temperatures between 5°C and 45°C, and sink temperatures between 140°C and 190°C. The results indicated an expected COP higher than vapor compression cycles, particularly beneficial for applications with temperature ratios above 1.3 K/K.

In terms of economic impact, the HoegTemp HP presents substantial energy savings and cost benefits. It has achieved energy consumption reductions of 50-70% compared to fossil fuel-based systems. The technology promises a high return on investment, depending on the application.

Looking forward, the commercial scalability of the HoegTemp HP is promising. Plans include further pilot installations in various industrial sectors, such as pharmaceuticals and food

processing, with an aim to expand its use globally. Continued research and development are also planned to explore higher temperature applications and improve overall system efficiency.

In conclusion, the HoegTemp HTHP represents a significant advancement in industrial heating technology, offering high efficiency, adaptability, and substantial environmental and economic benefits. Its successful pilot implementations and favorable performance metrics position it as a leading solution for high-temperature industrial heating needs.

7.2 Practical Implications of the Study

The results of this thesis provide a clear pathway for industries utilizing HoegTemp HTHP systems to achieve significant efficiency improvements. By optimizing the cold side (TL) and hot side (TH) temperatures and selecting appropriate gases, especially depend on the applications, industries can reduce their energy consumption, leading to lower operational costs. For instance, the working fluid properties analysis indicates that using Helium as the working fluid can enhance the COP at higher cold side temperatures, making it a preferred choice in specific industrial processes.

Implementing the optimized conditions identified in this study can substantially reduce the carbon footprint of industrial HTHP systems. Improved efficiency translates to less energy required for the same output, thereby decreasing greenhouse gas emissions. This aligns with global sustainability goals and supports industries in meeting environmental regulations. Additionally, it helps reduce global warming by utilizing surplus heat from various industries as a source for HoegTemp HTHP.

The potential cost savings from reduced energy consumption with the HoegTemp HTHP are significant. Industries can achieve a faster return on investment through lower operational costs. Additionally, the adoption of advanced HP designs based on this study’s findings can drive technological innovation and create new market opportunities

This thesis outcome can give some inputs energy policy makers in crafting regulations that promote the adoption of efficient HTHP systems. By incorporating these optimized conditions into industry standards, which can ensure that best practices are widely implemented, leading to broader energy efficiency gains.

7.3 Limitations and Future Research Directions

7.3.1 Limitations

In this thesis analysis, we primarily use first-order analysis to evaluate the Stirling engine. However, there are several limitations in collecting accurate data for simulation and calculation:

Data Collection Limitations: Obtaining precise data for simulation is challenging due to constraints in accessing comprehensive information about the Stirling engine's internal dimensions and related technical details. This is because manufacturers often keep such information confidential for competitive and economic reasons.

HoegTemp HP System Development: Although the HoegTemp HP system is available for commercial use in various industries, it remains in the research and development stage. This limits the availability of standardized data and reliable performance metrics, impacting the accuracy of our analysis.

Measurement Constraints: Measuring the internal temperatures and pressures within the compression and expansion cylinders of the Stirling engine is not feasible with the current design configuration due to safety concerns. Instead, we rely on cylinder surface temperature measurements for basic calculations. Additionally, secondary water circuit heat transfer calculations are used to approximate internal temperatures.

First-Order Analysis Limitations: Given that this analysis is based on first-order principles, it does not account for mechanical and thermal energy losses in detail. This limits our ability to perform a comprehensive analysis of the engine's efficiency and performance under real-world conditions.

Safety Considerations: Safety protocols restrict the direct measurement of high-pressure and high-temperature parameters within the engine. These restrictions necessitate indirect methods for estimating the operational characteristics, which may introduce some degree of approximation error.

Timeline Constraints: The entire analysis and results generation process is allocated a strict timeline of 20 weeks including holidays. This period includes all stages of research, data collection, simulation, and analysis, which places significant pressure on the accuracy and depth of the study.

Facility Visit for Measurements: Only one visit to the facility was conducted to take necessary measurements, spanning a duration of three days. This limited time frame for on-site data collection further constrains the comprehensiveness of the data, as it allows for only a snapshot of the engine's operational parameters rather than a continuous monitoring process.

Electronic Sensors and Transducers: All measurements were taken using electronic sensors and transducers. The engine operates continuously 24 hours a day, 7 days a week, which affects the precision of the measured values. Over time, the response time of sensors can increase, particularly for small temperature or pressure changes, due to the effects of continuous operation. This gradual degradation in sensor performance can introduce inaccuracies in the data collected, impacting the overall reliability of the analysis.

These limitations highlight the need for further research and more advanced analytical techniques to achieve a more precise and detailed understanding of Stirling engine performance.

7.3.2 Recommendation to overcome the limitations

There are some recommended procedures that can help minimize or overcome these limitations:

Enhanced Data Collection Methods:

- Collaborate with engine manufacturers to gain access to more detailed technical information under non-disclosure agreements (NDAs). This could provide more accurate data for simulations and calculations.
- Utilize advanced diagnostic tools and techniques to gather more comprehensive data during the facility visit, such as high-resolution imaging and detailed acoustic measurements.

Development and Standardization of HoegTemp HP System:

- Engage in ongoing research and development to standardize the HoegTemp HP system. Partnering with industrial stakeholders can facilitate access to standardized performance metrics and enhance data reliability.
- Conduct periodic reviews and updates of the system's specifications based on the latest research and industrial feedback.

Improved Measurement Techniques:

- Implement redundant measurement systems to cross-verify data and ensure accuracy. This could involve using multiple sensors for critical parameters and comparing their readings.
- Develop and employ non-invasive measurement techniques that can safely provide data on internal temperatures and pressures, such as infrared thermography or advanced computational modeling.

Advanced Analysis Methods:

- Integrate higher-order analysis methods to account for mechanical and thermal energy losses. Utilizing computational fluid dynamics (CFD) and finite element analysis (FEA) can provide a more detailed understanding of these losses.
- Conduct sensitivity analyses to identify and prioritize the most critical factors affecting engine performance, allowing for more focused and effective optimization efforts.

Safety Protocol Enhancements:

- Explore the use of advanced sensing technologies and data collection systems to safely measure high-pressure and high-temperature parameters.
- Design and implement safer engine configurations that allow for more accessible and accurate measurements without compromising operator safety.

Extended Timeline and Facility Access:

- Advocate for an extended timeline for the analysis and results generation process, allowing for more thorough research and data collection. Additional time can facilitate multiple visits to the facility for ongoing monitoring and data validation.
- Negotiate with the facility management to arrange for extended or repeated access for data collection, ensuring a more comprehensive dataset.

Sensor Maintenance and Calibration:

- Implement a regular maintenance and calibration schedule for all electronic sensors and transducers to ensure their accuracy and responsiveness. This can help mitigate the effects of continuous operation on sensor performance.
- Use high-quality, industrial-grade sensors designed for long-term continuous operation to reduce the likelihood of performance degradation.

Supplementary Data Sources:

- Supplement on-site measurements with data from similar Stirling engines operating under comparable conditions. This can help validate the collected data and provide a broader context for the analysis.
- Utilize historical performance data and case studies from academic and industrial research to fill in gaps and corroborate findings.

By implementing these recommendations, the limitations encountered in this thesis analysis can be minimized or overcome, leading to a more accurate and comprehensive evaluation of the Stirling engine's performance.

7.3.3 Future Research Directions

Comprehensive Data Collection:

- Conduct extended longitudinal studies to gather more comprehensive data over longer periods. This would involve multiple visits to facilities and continuous monitoring to capture a wide range of operating conditions and engine behaviors.
- Collaborate with multiple facilities to compare data across different Stirling engine models and configurations, creating a robust dataset for more generalized conclusions.

Enhanced Analytical Models:

- Develop higher-order analytical models that incorporate mechanical and thermal energy losses. Utilize computational fluid dynamics (CFD) and finite element analysis (FEA) to achieve more detailed simulations and better understand the factors affecting engine efficiency. This is crucial due to the complex heat transfer processes occurring within the engine.
- Implement machine learning algorithms to analyze large datasets and identify patterns or anomalies that could indicate potential areas for improvement in engine design and operation.

Design Optimization:

- Explore advanced design optimization techniques using multi-objective optimization algorithms to balance various performance metrics such as efficiency, power output, and durability. Consider the trade-offs between different design parameters to achieve optimal performance.

- Investigate modular design approaches that allow for easier customization and scalability of Stirling engines for different applications and power requirements.

Material Science Innovations:

- Investigate new materials and coatings that can improve the thermal and mechanical properties of Stirling engine components. Focus on materials that can withstand high temperatures and pressures while maintaining durability and efficiency.
- Study the effects of different material combinations on engine performance and longevity, aiming to optimize the balance between cost and performance.

Safety Enhancements:

- Develop safer engine configurations that facilitate easier and more accurate measurements of internal parameters without compromising operator safety. Focus on design modifications that allow for better accessibility and monitoring.
- Study the impact of different safety protocols and automated monitoring systems on the overall safety and reliability of Stirling engine operations.

Economic and Environmental Impact:

- Conduct comprehensive life-cycle assessments (LCA) to evaluate the economic and environmental impacts of Stirling engines. Analyze the total cost of ownership, including maintenance, energy consumption, and environmental benefits compared to alternative technologies.
- Investigate the potential for integrating Stirling engines with renewable energy sources, such as solar or biomass, to enhance their sustainability and reduce carbon footprint.

Industry Collaboration and Standardization:

- Foster closer collaboration between academic researchers, industry stakeholders, and regulatory bodies to develop standardized testing and reporting protocols. This would facilitate more consistent and comparable data across different studies and applications.
- Participate in industry consortia and working groups to share knowledge, best practices, and technological advancements, driving the overall progress of Stirling engine technology.

7.4 Concluding Remarks

Conclusions from the Analysis of Working Fluids in Stirling Cycle Performance:

The density of He, N_2, and Ar increases linearly with pressure across various temperatures, with He having the lowest density and Ar the highest. Temperature increases lead to a decrease in gas density for all three gases at constant pressure, with He showing the most significant density changes due to its lower molecular weight.

Cv remains relatively constant across different pressures for each gas, with He having the highest Cv and Ar the lowest, indicating that Cv is not significantly affected by pressure changes. Similar stability in Cv is observed with temperature variations, reinforcing the ideal gas behavior of He, N_2, and Ar under the studied conditions.

The Cp/Cv ratio shows minimal change with increasing pressure and temperature, with He consistently having a higher ratio due to its monoatomic nature compared to diatomic N_2 and monoatomic Ar.

The speed of sound is significantly higher in He across all pressures and temperatures, attributed to its lower molar mass. He exhibits the highest thermal conductivity, which increases with temperature, aligning with kinetic theory expectations.

Viscosity remains relatively stable across the pressure range for all three gases, with slight increases observed at higher pressures, especially for Ar. Temperature increases lead to higher viscosity for all gases, with Ar showing the highest viscosity and He the lowest, consistent with kinetic theory.

Evaluation of Simplified Model Predictions:

A negative correlation between TH and COP was observed, with higher TH leading to reduced HP efficiency. A positive correlation between TL and COP was found, indicating that higher TL enhances HP performance.

The tabulated data suggests that optimizing both TH and TL can significantly improve COP, with Ar showing potential for better efficiency at higher TL due to its abnormal behavior.

Further analysis explored the effects of varying swept volume, dead volume, and regenerator volume on the thermal performance and efficiency of the Stirling engine. Increasing the swept volume led to a decrease in TH and an improvement in COP, demonstrating enhanced engine efficiency. This effect was most pronounced in He and N_2. On the other hand, increasing the

dead volume and regenerator volume generally resulted in higher TH values and lower COP values, indicating a decrease in engine efficiency due to the retention of more heat within the system. These findings underscore the critical role of optimizing geometrical parameters such as swept volume, dead volume, and regenerator volume to achieve optimal performance.

The study also examined the impact of varying mean pressures on the engine's performance. It was observed that increasing the mean pressure consistently improved the COP for all gases, with He showing the most significant enhancement. This suggests that higher pressures facilitate better thermodynamic efficiency. However, it is important to balance this with the need for increased motor power consumption to achieve a higher temperature lift and maintain overall system optimization. The comprehensive analysis highlights the importance of selecting appropriate working gases and optimizing key engine parameters to enhance the efficiency and effectiveness of Stirling engines.

Recommendations for Optimization:

Gas Selection and Performance:

- Helium, due to its lower density, higher thermal conductivity, and superior COP under various conditions, is recommended for applications requiring high efficiency and minimal power consumption.
- Argon, while showing moderate performance, should be further investigated for specific configurations where its properties might offer advantages.

Optimizing Operating Conditions:

- Focus on optimizing TH and TL for improved COP, with lower TH and higher TL proving beneficial. However, this requires deep investigation due to the decreasing temperature lift
- Investigate the combined impact of increased Pmean and motor power consumption to achieve better temperature lift and system efficiency.

Experimental Validation:

- Conduct extended experimental studies with varying phase angles and operating conditions to validate simulation results and refine predictive models.

- Conduct extended experimental studies with varying swept volumes, dead volumes, regenerator volumes, and operating conditions to validate the simulation results and the developed predictive model
- Perform detailed analysis of motor power requirements and P-V characteristics to better understand the impact of different gases and pressures on engine performance.

By implementing these recommendations, research can achieve significant advancements in Stirling engine technology and its applications.

References

[1]. Robert, D. B., Marina, A., Zühlsdorf, B., Arpagaus, C., Bantle, M., Wik, V., Elmegaard, B., Corberan, J. M., & Benson, J. (2020). *Strengthening Industrial Heat Pump Innovation : Decarbonizing Industrial Heat*. https://hdl.handle.net/11250/2764774

[2]. D.G. Thombare, S.K. Verma, *Technological development in the Stirling cycle engines*, Renewable and Sustainable Energy Reviews, Volume 12, Issue 1, 2008, Pages 1-38, ISSN 1364-0321, https://doi.org/10.1016/j.rser.2006.07.001.

[3]. Suyitno, Suyitno & Juwana, Wibawa & Dwi, Oky & Hanggara, Putra & Sutarmo, & Huda, Sholiehul & Hissen, Ahmed. (2013). Effects of Working Fluids on the Performance of Stirling Engine. http://dx.doi.org/10.13140/2.1.2365.3125.

[4]. Salih, S. A., Aljashaami, B. A., Qasim, M. A., Mola, A. H., Shcheklein, S. E., & Dubinin, A. M. (2023). The Influence of Working Fluid on Stirling Engine Performance. In *Proceedings of the 2023 5th International Youth Conference on Radio Electronics, Electrical and Power Engineering, REEPE 2023: book* (pp. 1-5). Institute of Electrical and Electronics Engineers Inc. https://doi.org/10.1109/REEPE57272.2023.10086916

[5]. Bachelier, C. (2009). *Stirling engines: A technology overview*. Pratt School of Engineering, Smarthome Program, Duke University, Durham, North Carolina & Department of Energy Technology, Royal Institute of Technology, Stockholm, Sweden.

[6]. Walker, G., & Senft, J, (2012). Free Piston Stirling Engines (Softcover reprint of the original 1st Edition 1985, Vol. 12). Springer.

[7]. Finkelstein, T., & Organ, A. J. (2001). Air engines. ASME Press.

[8]. Sun J, Wang Y, Qin Y, Wang G, Liu R, Yang Y. A Review of Super-High-Temperature Heat Pumps over 100 °C. Energies. 2023; 16(12):4591. https://doi.org/10.3390/en16124591

[9]. Høeg, A., Løver, K., Asphjell, T.-A., & Lümmen, N. (2023). Performance of a new ultra-high temperature industrial heat pump. In Proceedings of the 14th IEA Heat Pump Conference (Paper No. 430). Chicago, USA.

https://heatpumpingtechnologies.org/publications/paper-no-430-performance-of-a-new-ultra-high-temperature-industrial-heat-pump-14th-iea-heat-pump-conference-chicago-usa/

[10]. Wolf, S., Lambauer, J., Blesl, M., Fahl, U., & Voß, A. (2012). Industrial heat pumps in Germany: Potentials, technological development and market barriers.

[11]. Michel D. Obrist, Ramachandran Kannan, Russell McKenna, Thomas J. Schmidt, Tom Kober, High-temperature heat pumps in climate pathways for selected industry sectors in Switzerland, Energy Policy, Volume 173, 2023, https://doi.org/10.1016/j.enpol.2022.113383.

[12]. Dobre, C. G., Grosu, L., Dobrovicescu, A., Chisiu, G., & Constantin, M. (2021). Stirling refrigerating machine modeling using Schmidt and finite physical dimensions thermodynamic models: A comparison with experiments. Entropy, 23(3), 368. https://doi.org/10.3390/e23030368

[13]. Getie, M., Lanzetta, F., Bégot, S., Admasu, B., & Hassen, A. (2020). Reversed regenerative Stirling cycle machine for refrigeration application: A review. International Journal of Refrigeration, 118, 173-187. https://doi.org/10.1016/j.ijrefrig.2020.06.007

[14]. Khan U, Zevenhoven R, Stougie L, Tveit T-M. Prediction of Stirling-Cycle-Based Heat Pump Performance and Environmental Footprint with Exergy Analysis and LCA. *Energies*. 2021; 14(24):8478. https://doi.org/10.3390/en14248

[15]. Yao, Xuyichen. (2023). Stirling engines: Advancements, applications, and environmental benefits. Theoretical and Natural Science. 25. 186-191. http://dx.doi.org/10.54254/2753-8818/25/20240963

[16]. Musmar, S. A., & Tlili, I. (2015). Numerical investigation of working fluid effect on Stirling engine performance. International Journal of Thermal & Environmental Engineering, 10(1), 31-36. https://doi.org/10.5383/ijtee.10.01.005

[17]. Costante M. Invernizzi, Stirling engines using working fluids with strong real gas effects, Applied Thermal Engineering, Volume 30, Issue 13, 2010, Pages 1703-1710, ISSN 1359-4311, https://doi.org/10.1016/j.applthermaleng.2010.03.029

[18]. Hachem H, Gheith R, Aloui F. Theoretical investigations of Stirling engine performances for different filling gas properties. *Int J Energy Res*. 2022; 46(14): 20462-20479. doi:10.1002/er.7875

[19]. Guarato, A. Z., Moura, C. M., Bernardes, M. S., & Malheiros, F. C. (2017, December). An experimental thermal analysis of an engine based on Stirling cycle model alpha. Paper presented at the 24th ABCM International Congress of Mechanical Engineering (COBEM 2017), Curitiba, PR, Brazil. Retrieved from https://www.researchgate.net/publication/321058872

[20]. Perozziello C, Grosu L, Vaglieco BM. Free-Piston Stirling Engine Technologies and Models: A Review. *Energies*. 2021; 14(21):7009. https://doi.org/10.3390/en14217009

[21]. Shichong Dong, Guoqing Shen, Mobei Xu, Shiping Zhang, Liansuo An, The effect of working fluid on the performance of a large-scale thermoacoustic Stirling engine, Energy, Volume 181, 2019, Pages 378-386, ISSN 0360-5442, https://doi.org/10.1016/j.energy.2019.05.142.

[22]. Muluken Z. Getie, François Lanzetta, Sylvie Bégot, Bimrew T. Admassu, Abdulkadir A. Hassen, Reversed regenerative Stirling cycle machine for refrigeration application: A review, International Journal of Refrigeration, Volume 118, 2020, Pages 173-187, ISSN 0140-7007, https://doi.org/10.1016/j.ijrefrig.2020.06.007.

[23]. Haywood, D., Raine, J. K., & Gschwendtner, M. A. (2002). Stirling-cycle heat-pumps and refrigerators – a realistic alternative? Proceedings of the International HVAC&R Conference, 2002. University of Canterbury, New Zealand. Retrieved from https://hdl.handle.net/10292/4942

[24]. Hirata, K. (n.d.). Schmidt theory for Stirling engines. National Maritime Research Institute. http://www.bekkoame.ne.jp/~khirata/academic/schmidt/schmidt.htm

[25]. Çengel, Y. A. (2007). Heat and mass transfer : a practical approach (3rd ed., pp. XXIV, 901). McGraw-Hill.

[26]. Høeg, A., & Tveit, T.-M. (2018). Process design for a 4 x 10.6 litre low-temperature Stirling engine. In Proceedings of the 17th International Stirling Engine Conference (pp. 1-15). ISEC International Stirling Engine Committee.

[27]. Høeg, A., & Tveit, T.-M. (2021). Low to very high temperature thermal energy recycling – 3 case studies. In *Proceedings of the 20th International Stirling Engine Conference (ISEC 2021)*.

[28]. Isshiki, N, Terada, F, and Tsukahara, S. Analysis of various internal losses in Stirling engines. United States: N. p., 1984. Web.

[29]. Alfarawi, S., AL-Dadah, R., & Mahmoud, S. (2024). Performance evaluation of gamma-type Stirling engine using combined Schmidt and mechanical loss model. *European Journal of Sustainable Development Research*, *8*(1), em0240. https://doi.org/10.29333/ejosdr/13888

[30]. Beale, W. T., "Free-piston Stirling engines - some model tests and simulations," SAE Technical Paper, 1969. Available at: SAE Technical Paper.

Appendices

Declaration of AI aids and -tools

Data Analysis Code and Models

Details of Experimental Setup with Component Datasheets

Additional Tables and Figures